ISTANBUL TECHNICAL UNIVERSITY ★ GRADUATE SCHOOL OF SCIENCE ENGINEERING AND TECHNOLOGY

PERFORMANCE MONITORING OF CLOSED CONTROL LOOPS

M.Sc. THESIS

Gizem KUŞOĞLU

Department of Chemical Engineering

Chemical Engineering Programme

May 2015

ISTANBUL TECHNICAL UNIVERSITY ★ GRADUATE SCHOOL OF SCIENCE ENGINEERING AND TECHNOLOGY

PERFORMANCE MONITORING OF CLOSED CONTROL LOOPS

M.Sc. THESIS

Gizem KUŞOĞLU
(506121015)

Department of Chemical Engineering

Chemical Engineering Programme

Thesis Advisor: Assoc.Prof. Dr. Devrim Barış KAYMAK

May 2015

İSTANBUL TEKNİK ÜNİVERSİTESİ ★ FEN BİLİMLERİ ENSTİTÜSÜ

KAPALI KONTROL DÖNGÜLERİNDE PERFORMANS İZLENME

YÜKSEK LİSANS TEZİ

Gizem KUŞOĞLU
(506121015)

İkimya Mühendisliği Anabilim Dalı

Kimya Mühendisliği Programı

Tez Danışmanı: Doç. Dr. Devrim Barış KAYMAK

Mayıs 2015

Gizem KUŞOĞLU, a M.Sc. student of ITU Graduate School of Science Engineering and Technology 506121015 successfully defended the thesis entitled **"PERFORMANCE MONITORING OF CLOSED CONTROL LOOPS"**, which he/she prepared after fulfilling the requirements specified in the associated legislations, before the jury whose signatures are below.

Thesis Advisor :	**Assoc.Prof. Dr. Devrim Barış KAYMAK** Istanbul Technical University	.....
Jury Members :	**Prof. Dr. Dursun Ali ŞAŞMAZ** Istanbul Technical University	.....
	Assoc. Prof. Dr. Mehmet Kemal GÜLLÜ Kocaeli University	.....
		.....

Date of Submission : **4 May 2015**
Date of Defense : **29 May 2015**

To my family,

FOREWORD

First of all, I am also thankful to my advisor for his support and for providing necessary guidance.

I would like to thank director of Research and Development(R&D) department, is always willing to support me about this new topic.

I am also greatful to the engineers in Tüpraş -İzmit Refinery Cooperation for their contribution to this study. I have investigated the control system and also control loop with them and they enable me to collect some data from SISO refinery control loops which are problematic ones.

Finally, I would like to express my thanks to my family, my mother, my sister and my father. They are always supporting me for everything.

This work has been supported by the 2228-TÜBİTAK(Scientific and Technological Research Council of Turkey)Programme.

May 2015

Gizem KUŞOĞLU
(Chemical Engineer)

TABLE OF CONTENTS

Page

ABBREVIATIONS

ACF : Auto-Covariance Function
AI : Area Index
APC : Advanced Process Control
ARMA : Auto-regressive Moving Average
CC : Cascade Control
CE : Control Error
CLPM : Control Loop Performance Monitoring
CPI : Controller Performance Index
CV : Controlled Variable
EHPI : Extended Horizon Performance Index
FB : Feed-back
FBC : Feed-back Control
FCOR : Filtering and Correlation
FF : Feed-forward
FFC : Feed-forward control
FFT : Fast Fourier Transform
FOPTD : First Order Plus Time Delay
IAE : Integral of the Absolute Value of the Error
IMC : Internal Model Control
ISE : Integral of the Squared Error
ITAE : Integral of the Time-weighted Absolute Error
ITNAE : Integral of the Multiplied Absolute Error
MA : Moving Average
MIMO : Multi-input Multi-output
MISO : Multi-input Single-output
MPC : Model Predictive Control
MV : Minimum Variance
MVC : Minimum Variance Control
NGI : Non-gaussianity Index
NLI : Nonlinearity Index
NPI : Non-predictability Index
OP : Controller output
QE : Quadratic Error
PSD : Power Spectral Density
PV : Process Variable
SISO : Single-input Single-output
SOPTD : Second Order Plus Time Delay
SWAT : Soil and Water Assessment Tool

LIST OF TABLES

Page

LIST OF FIGURES

Page

PERFORMANCE MONITORING OF CLOSED CONTROL LOOPS

SUMMARY

In industrial plants, large amount of process variables must be kept within the specified limits in order to maintain high quality and reliability of production. Potential limit violations can lead to problems in many aspects such as operational safety, environmental effects, product quality and plant profitability. Therefore, the concept of effective process control in plants is of great importance in creating an efficient and profitable facility. A good process control is carried out by regular maintenance and monitoring of the control system since the establishment of the plant. Today, these tasks are examined in the framework of the control-loop performance monitoring (CLPM). The basic idea behind CLPM is to determine the performance deterioration by monitoring the performance of the controller in real time and to be able to identify the root-causes that lead to poor performance. CLPM is widely used for SISO control loops, it has been also extended to include MIMO control systems.

In this study, the performance of the control loops in different refinery units has been evaluated. The minimum variance controller, designated as benchmark and the proximity to expected performance of the current performance has been quantified using performance index. For accurate calculation of the performance index, optimum values of certain parameters have been determined. It has been shown that sampling interval is insufficient for some loops and the estimated value of dead time is different from the actual value. The classification has been made on the basis of calculated performance index and root causes affecting the performance have been estimated with different methods. Diagnosing the root-cause has been initiated by the spectral analysis expressed as a classical and visual approach and oscillation has been detected by looking the magnitude of the peaks at the power spectral analysis. The results obtained have been supported by the methods depending on the auto-covariance function and time-domain. Equipment faults, controller parameter values and external disturbances cause the oscillation. To understand where the oscillation originated from, nonlinearity and stiction analysis were performed respectively. The higher-order statictics were used in nonlinearity analysis and interactions between frequency pairs have been examined. Stiction analysis has been made to reveal potential equipment faults in the control loops containing non-linearity. According to the results, it was concluded that valve is problematic in the presence of stiction. In the case of appearance of oscillating behavior has been emphasized that poor performance is arised from parameter settings or external disturbances.

KAPALI KONTROL DÖNGÜLERİNDE PERFORMANS İZLENME

ÖZET

Endüstriyel tesislerde, üretimin yüksek kalite ve güvenilirlik içerisinde sürdürülebilmesi için büyük miktardaki proses değişkenlerinin belirlenen limitler dahilinde tutulması gerekmektedir. Olası limit ihlalleri; operasyon güvenliği, çevresel etkiler, ürün kalitesi ve tesis karlılığı gibi birçok konuda problemlere yol açabilmektedir. Bu nedenle, tesislerde etkin proses kontrol kavramı verimli ve karlı tesislerin yaratılmasında büyük önem taşımaktadır. İyi bir proses kontrol, ünitenin kurulmasından itibaren kontrol sistemlerinin düzenli bakımı ve takibi ile gerçekleştirilmektedir. Günümüzde bu görevler kontrolör döngüleri performans izleme (CLPM) çerçevesinde incelenmektedir. CLPM arkasındaki temel fikir, kontrolör performansını anlık olarak izleyerek performanstaki kötüleşmeleri tespit etmek ve kötü performansa neden olan kök-nedenleri teşhis edebilmektir. CLPM, SISO kontrol döngüleri için yaygın olarak kullanılmakta olup, MIMO kontrol sistemlerini de içerecek şekilde genişletilmiştir.

Bu çalışmada, rafinerinin farklı ünitelerindeki SISO kontrol döngülerinin performansları değerlendirilmiştir. Kıyas noktası olarak, minimum varyans kontrolör belirlenmiş ve mevcut performansın beklenen performansa olan yakınlığı, performans indeks kullanılarak nicelleştirilmiştir. Performans indeks değerleri göz önünde bulundurularak, kontrol döngüleri performansa göre sınıflandırılmıştır. Performans indeksi; temelde aynı çıkarıma dayanan, farklı matematiksel algoritmalardan oluşan FCOR algoritması ve küçük kareler yöntemleri ile hesaplanmıştır. FCOR algoritması, tahmin edilen beyaz gürültü ile proses çıktı değişkeni arasındaki ilişkiden türetilmektedir. Diğer bir yöntem ise, proses varyansının minimum olduğu müdahale edilemeyen gürültü terimlerinin toplamıyla belirlenmektedir. Performans indeksinin doğru hesaplanması için, belli başlı parametre değerlerinin optimum değerleri farklı yöntemler ile tahmin edilmiştir. Bazı kontrol döngüleri için örnekleme zamanının yetersiz olduğu ve tahmin edilen ölü zamanların gerçek değerden farklı olduğu gösterilmiştir. Ölü zaman tahmini için genişletilmiş tahmin aralığı ve çapraz ilişki yöntemleri kullanılmıştır. Genişletilmiş tahmin aralığı yönteminde, değişen ölü zaman değerlerine karşılık performans indeksinin çok fazla değişmediği nokta ölü zaman değeri olarak belirlenmektedir. Çapraz ilişki yönteminde farklı veri setleri için farklı ölü zaman değerleri tahmin edilmiştir. Genişletilmiş tahmin aralığı ise, gerçek ölü zamandan daha büyük değerler vermekte; ancak diğer yöntemlere göre daha tutarlı sonuçlar göstermektedir. Dolayısıyla performans indeks hesaplamalarında ölü zaman değerleri genişletilmiş tahmin aralığı ile belirlenmiştir.

Hesaplanan performans indekse dayanarak sınıflandırmalar yapılmış ve performansı etkileyen kök-nedenler tahmin edilmiştir. Kök-neden teşhisine klasik ve görsel bir yaklaşım olarak ifade edilen güç spektral analizi ile başlanmış ve güç spektral analizlerindeki piklerin büyüklüğüne bakılarak, osilasyon tespit edilmiştir. Piklerin yer aldığı frekanslar, osilasyonun periyodunu vermektedir. Osilasyonun diğer bir özelliği

olan düzenlilik, güç spektrumuyla doğru şekilde elde edilememektedir. Osilasyonun özellikleri, oto-kovaryans fonksiyonuna bağlı yöntemler ile belirlenmiş ve güç spektrumu sonuçları desteklenmiştir. Oto-kovaryans fonksiyonunu kullanılarak, azalım oranı ve düzenlilik faktörleri belirlenmiştir. Azalım oranı, farklı çevrimlerdeki osilasyonların sönümlenmesinden yola çıkmaktadır. Osilatif bir sinyalin düzenli aralıklarla salındığı varsayılmakta ve düzenlilik faktörü ile sıfırı kesen noktaların aralıkları karşılaştırılmaktadır. Oto-kovaryanstan yararlanan yöntemlerin yanısıra, zamansal verilerden yola çıkılarak da osilasyon tespitleri yapılmıştır. Bu yöntem, verilerdeki gürültüden etkilenmekte ve çoklu osilasyon durumlarında yetersiz kalmaktadır. Çoklu osilasyon durumlarında oto-kovaryans fonksiyonu daha doğru sonuçlar sunmaktadır. Bu durumda güç spektrum analizinde iki veya daha çok frekansta belirgin, güçlü frekanslar görülmüştür. Pikler, bant filtre ile filtrelenerek ayrıştırılmış ve ayrı ayrı osilatif davranışları incelenmiştir. İnceleme yöntemi, kök-nedenin tespitinde kolaylık sağlamaktadır.

Her bir farklı periyotta salınan osilasyon, farklı bir kök-nedene işaret etmektedir. Kök-nedenler; ekipman bozulmaları, kontrolör parametre değerleri, dış bozucu etkenlerden kaynaklanabilir. Osilasyonun nereden kaynaklandığı anlamak için, sırasıyla nonlineerlik ve aşınma analizleri gerçekleştirilmiştir. Nonlineerlik analizinde yüksek derecede istatistik kullanılmakta ve frekans çiftleri arasındaki etkileşim incelenmektedir. Etkileşim ikiz spektrumda görselleştirilmektedir. Etkileşimin büyüklüğü kritik değerler ile karşılaştırılarak, prosesin normalliği ve nonlineerliğine karar verilmektedir. Normal olmayan prosesler, lineer sinyal ürettiğinde muhtemel problemler, kontrolör parametreleri ve dışsal bozucu etkenlerdir. Normal olmayan prosesler, nonlineer sinyal ürettiğinde ekipman bozulmaları temel problemi oluşturmaktadır. Nonlineerlik tespiti için uygulanan bir diğer yöntemde, mevcut veriler ile aynı güç spektruma sahip test verilerini karşılaştırmaktadır. Test verilerine dayalı nonlineerlik tespitlerinin daha doğru tespitler sağladığı düşünülmektedir.

Nonlineerlik içeren kontrol döngülerinde olası ekipman arızalarını ortaya çıkarmak için aşınma analizleri yapılmıştır. Aşınma analizleri için çapraz ilişkiler ve polinom uydurma yöntemleri uygulanmıştır. Çapraz ilişkiler yöntemi, kontrolör ayarlamadan etkilenmekte ve agresif kontrolör parametreleri varlığında vanada aşınma olduğu görülebilir. Bu nedenle, aşınım analizleri için polinom uydurma yöntemi kullanılmıştır. Polinom uydurma yönteminde mevcut kontrolör çıktısı ya da kontrolör hatasına üçgen ya da sinüs dalgası uydurarak, hangi eğrinin veriyi daha iyi temsil ettiğine bakılmıştır. Yöntem, kolaylığı açısından tercih edilmekle birlikte aşınma indeksinin aldığı değere göre kesin karara varılamayabilir. Aşınmaya karar verilemediği durumda, aşınmayı sayısallaştıran ve vanada hangi problemin olduğunu gösteren yöntemlerin kullanılması gerekmektedir. Analizler sonucunda, aşınmanın varlığında vananın problemli olduğu sonucuna varılmıştır. Nonlineer proseslerde, aşınma yoksa sensör arızası ya da prosesin nonlineer olduğu belirlenmektedir.

Literatürde önerilen algoritmaya göre; osilatif davranışın görünmediği durumda, kötü performansın parametre ayarlamalarından ya da dışsal etkenlerden kaynaklandığı üzerinde durulmuştur. Bazı vanadaki aşınma problemleri osilatif davranış göstermemekte ve algoritmaya göre aşınma tespit edilemeden problemin kontrolörden kaynaklandığı sonucuna varılmaktadır. Doğru kök-neden tespiti için tüm analizler tekrar edilmeli ve Hammerstein modeller uygulanmalıdır.

Kontrolör performansının kötüleşmesine sebep olan kök-nedenler belirlendikten sonra performansın iyileştirilmesi için önlemler alınmalıdır. Önlemler; ekipman bakımı, kontrolör parametre ayarlama olabileceği gibi, yeni ekipman değişikliği olabilir.

1. INTRODUCTION

In this chapter, the motivation and the structure of the thesis will be given and topics which are included in each chapter will be mentioned.

1.1 Purpose of Thesis

There are several hundred control loops in industry, especially in refineries and the performance of the control loops directly affect the process. Adjustments on the control system are made during the start-up of process unit to make sure that controllers are in good health. However, control performance starts deteriorating over time due to various reasons such as plant modifications and changes in process conditions. Generally, this situation is recognized when there appeared to be an inability to process in desired quality and then the process is realized under variable conditions using more raw materials. Thus, it is concluded with negative economic effects. Economic effects are increased by the reduction of variances of current performance as seen in Figure 1.1. These benefits can only be achieved through continuous performance monitoring. The motivation of this thesis is that constituting the continuous monitoring of closed loops and by this way, minimizing the losses.

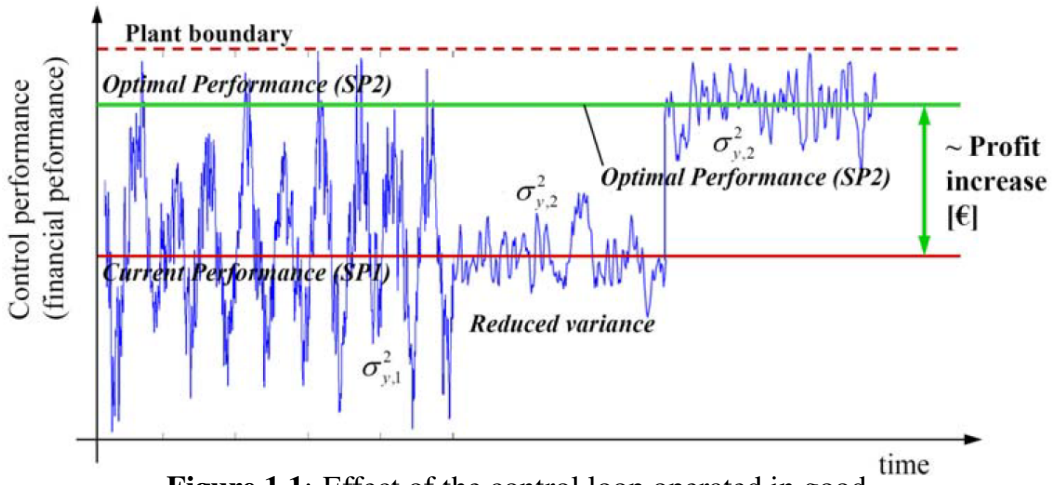

Figure 1.1: Effect of the control loop operated in good.

1.2 Thesis Outline

Thesis consists of a review of the possible advantages of CLPM applications and the detailed explanation of the basic steps for performance monitoring in the industry. In Chapter 1, it is focused on the state of the trend in manufacturing and introduced financial, environmental benefits of CLPM applications. Chapter 2 include analysis, research and applications devoted to this issue that has seen significant attention in recent years. Moreover, the main stages of CLPM systems are presented as performance management procedure.

Chapter 3 describes the assessment, diagnostic and improvement functions which are applied by combining different control performance metrics and assessments. Performance assessment approaches are grouped under two headings as deterministic and stochastic performance monitoring. Stochastic assessment only uses the routine operating data and minimal knowledge of the process. Also, this assessment employs the Harris index which is based on minimum variance control principles and has various algorithms for calculation. First, the calculation of Harris index for SISO feedback control loop is given and then it is extended to cascade and feed-forward/feed-back control. On the other hand, deterministic performance monitoring provides the data-driven indices about the robustness and process performance. Recommendations are provided for conducting both of the assessments simultaneously. After the evaluation phase, the algorithm widely used in the literature is introduced to describe how to proceed. According to algorithm, detection of oscillation and nonlinearity should be performed when the control loops are showing poor performance due to some causes. For oscillation diagnosis, the methods that can be applied in frequency or time domain has been described and the advantages and also drawbacks of each method is discussed. There may be multiple causes for system oscillation. To diagnose the root causes, techniques that are needed on the detection of nonlinearity, stiction are given in detail.

The concept of the performance monitoring has been implemented on SISO refinery control loops. The start of Chapter 5 is formed with the description of some of the control loops which have different controller types. Afterwards, the assessment of performance against the selected control performance and also the classification of the loops with respect to performance index are presented. The results of the diagnostic

techniques used to understand the underlying causes are provided in this chapter. This study is applied in the Tüpraş İzmit Refinery.

In Chapter 6, the obtained metrics, described in Chapter 5, in the view of performance assessment are summarized and actions are proposed to be taken.

2. CLOSED-LOOP PERFORMANCE MONITORING

Closed Loop Performance Monitoring (CLPM) concept has become of interest in recent years. In this chapter, the reasons for why CLPM is needed, what its benefits are and what steps are included for implementation will be discussed.

2.1 Values and Benefits of Process Control

The purpose of process control is to cope with disturbances and natural consequences of all process operations. The ability of a control system to maintain the stability of the process or to keep track of the desired path gives the way to reach some objectives such as safer operation and reduced environmental impact, more sustainable manufacturing, improved bottom line returns, efficiency gains, quality and agility gains [1]. The first goal in production is to maintain the process securely without damaging the environment. To achieve this, it is attempted to keep process conditions at steady state. The advantages alongside safer operation obtained by good control are the reduction of raw material consumption and the achievement of sustainable production. Nowadays, ensuring efficient use of raw materials has become an important factor in producing good quality products with flexible manufacturing.

At first glance, the control system seems only consisting of regulatory controllers classified as closed-loop feed-back and feed-forward control. However, advanced process control (APC) has been integrated to increase the output in the lower level of process control applications. In control theory, APC is a broad term of techniques implemented within control systems, but the most common advanced method is model predictive control (MPC) that utilizes a sequence of linear algebraic calculations to predict the result of controlled variable manipulations. Though MPC and regulatory control are distinct control functions embedded to different layers in control hierarchy, the function of a given layer is affected from the function placed in the next layer [2]. The generic representation of control hierarchy is given in Figure **??**.

Hierarchical control appears as a pyramid of control functions based on the process. It

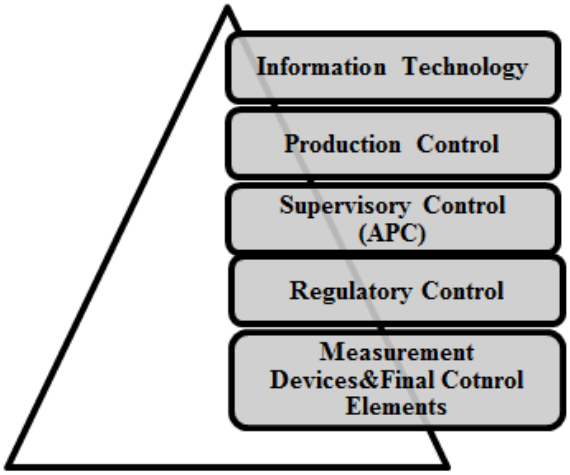

Figure 2.1: Hierarchy of control functions.

can be easily deduced from the arrangement of pyramid that APC needs well-structured regulatory control to improve performance. Many MPC applications are installed on the SISO regulatory controllers to track set-points given by MPC. Whilst the performance of regulatory controllers that are usually of the PID type is bad, APC cannot deliver benefits usually in financial terms [1]. Because if the PID controller does not work properly and the accurate measurements cannot be collected then it is not possible to specify the correct set-points by taking account wrongly measured dependent variables. The relation between MPC and PID control loops are shown in Figure 2.2. Thus, PID control loop should be considered as a priority for the performance monitoring.

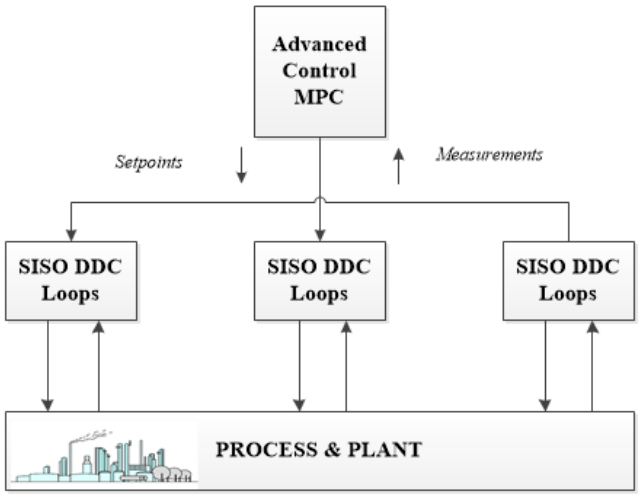

Figure 2.2: Implementation of advanced Control.

2.2 Need for Closed-Loop Performance Monitoring

Control problems are solved by using two-phase process that focus on the design and continuous implementation of control system without performance degradation. The first phase, related to the installation of the control system, respectively involves design, tuning and implementation of control strategies and controllers. If the first phase is applied as specified, well-designed and also well-performing control system could be attained. But changes in the quality of the product and operation strategies over time and modifications associated with equipment may require work on more distant conditions from the initial operation conditions. Thereupon, deterioration in performance is emerging even if equipment has been designed well. This situation necessitates the second-phase for the early detection of performance degradation by observing the control loops just because a noticeable deterioration in performance can be translated to a reduction in the profit. Moreover, the plants must operate at the highest performance to increase the market share of the company in a competitive environment and so overall implemented controllers should always show good performance. That is the reason why the demand of monitoring and modifying of control systems is increasing [3].

The emergence of the idea of monitoring the control system has led to many surveys about the status of PID control loops in the industry. These surveys reveal that 60% of all industrial controllers show poor performance [4–6]. Paulonis and Cox give a good example on the situation of the industry which contains more than 9000 PID controllers [7]. In this set, 20% of controllers have the adequate performance, 30% of controllers have poor performance because of process variability, 30% of them are oscillatory because of problems with instrumentation and 15% of them have incorrect controller design. Several reasons like inadequate controller tuning, equipment malfunction and inappropriate control structure might lead to poor performance as it appears [8]. Therefore, not only the performance of the controllers, all equipments in the control loops and control strategies must be analyzed. Components of a control loop are shown in Figure 2.3.

After making sure that the equipment is functioning correctly in the control loop, methods for the improvement of performance should be carried out.

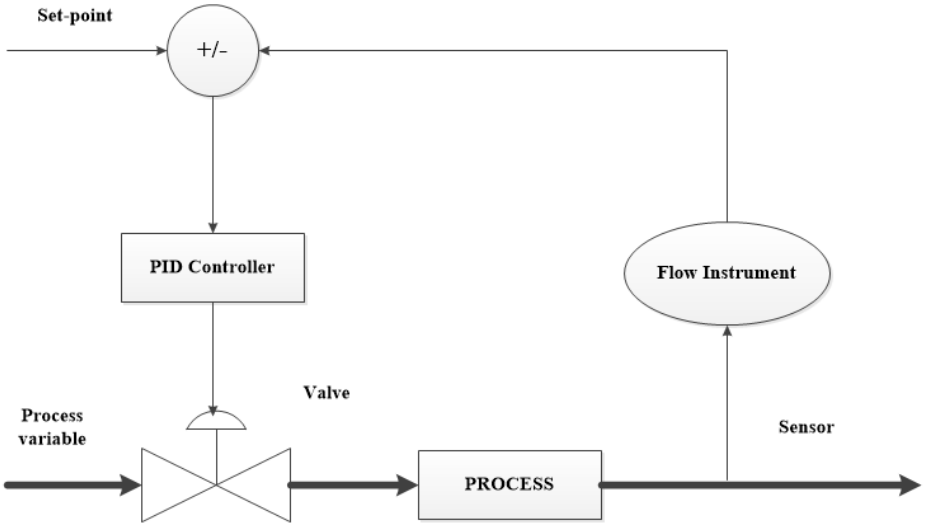

Figure 2.3: Closed control loop with its components.

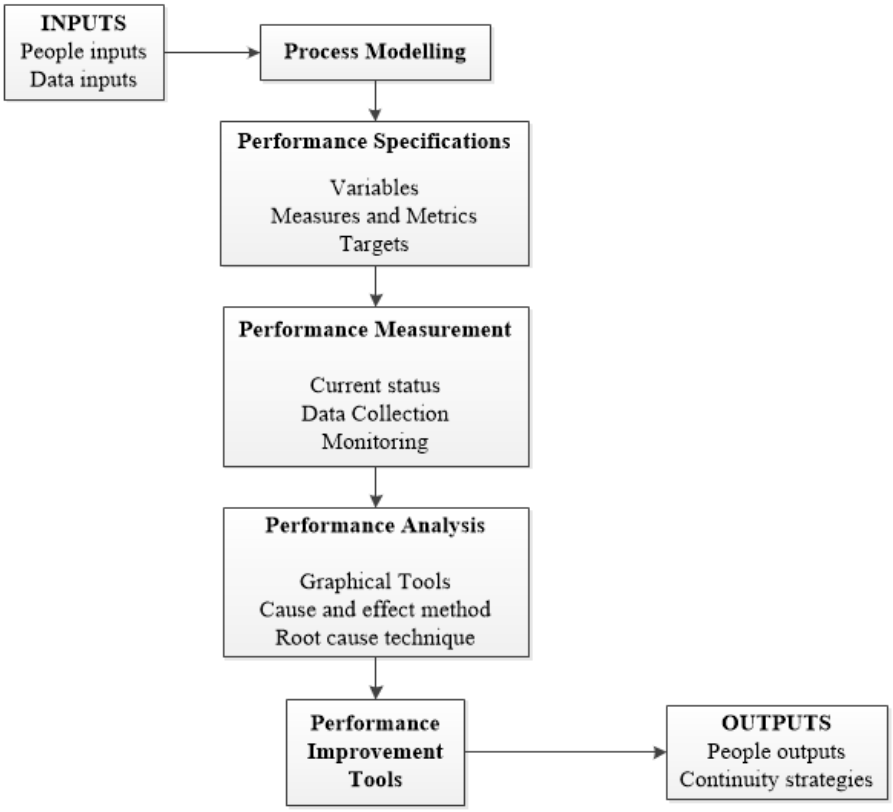

Figure 2.4: Steps in performance assessment.

2.3 Key Steps for Implementation of Performance Management

A good financial performance is directly associated with enhanced production performance and then performance is a remarkable measure to be observed by several key steps. Monitoring key steps are various and complex in themselves, consequently, they should be combined to build performance management procedure illustrated in Figure 2.4.

Evaluation of multiple process performances is possible with the identification of some inputs which are gathered by organization personnel. Indeed, all data are not required and so necessary information should be extracted with certain techniques. The next step is modelling of the process using measured data which are set-point, controller output and process output for a control system. After that, the step to be considered is deciding the process variable that is intended to capture the desired control performance in system and then suitable performance measure, metrics. The performance measures obtained are subsequently utilized for the monitoring of the performance and if the performance is getting worse, problem that causes this deterioration is analyzed by some tools or techniques. Performance improvements should be applied as a solution to this problem. Finally, the outcomes obtained from the performance monitoring are applied with the help of people-based mechanisms. Also mechanisms are used for continuing performance monitoring and announcing the outcomes [9].

2.4 Sources of Implementation Problems

Performance analysis only needs routine operating data without excitation input signal that provides a great advantage in the application of CLPM. Although considered to be easier in terms of data, the analysis of performance is recognized as a complex task due to repetition for thousand different control loops. Even though analysis section is usually automated and results are presented by online reports, interpretation of diagnostic task is left to engineers.

3. PERFORMANCE MANAGEMENT OF THE CONTROL LOOPS

The performance of a control system is related to its ability to hold the controlled variables at their desired set-points for maintaining the production in an efficient way. Control loop performance can be analyzed by evaluating suitable statistical data which reflect the performance of the existing system. This analysis is referred to as performance assessment or performance monitoring in the literature [3]. The performance assessment of control loops is the main stage in the CLPM procedure. In this stage, poorly or not adequately performing control loops are observed by monitoring methods and selected for the following diagnostic steps. Monitoring methods can be classified as stochastic and deterministic methods. Stochastic performance monitoring assesses the variance of process output associated with unmeasured stochastic measures, whereas deterministic performance monitoring relates to the traditional performance such as set-point, settling time, etc. Best performance of control loop cannot be achieved in both methods at the same time due to different strategies [10].

3.1 Performance Assessment of the Control Loops

3.1.1 Deterministic Performance Indices

Deterministic performance monitoring analyzes how the system responses to the set-point changes and load disturbances via some performance indices. The step response characteristic of a system with set-point changes may be represented by the following time domain measures [3, 11]. Related scalar values are shown in Figure 3.1.

- Rise time (T_r): The time interval between the first moments at which step response reaches to 10% and 90% of final value.

- Settling time(T_{set}) : It refers to the elapsed time between time when step set-point change occurs and time when system reaches $\pm$ 5% of the steady-state value.

- Decay ratio: It is the ratio between adjacent positive errors from the new stead-state value and formulated as (c/a) where a and c are the heights of the first and second peaks, respectively.

- Overshoot: It is the ratio of the first maximum deviation from steady-state value and steady-state of output and formulated as (a/b).

- Steady-state error: It implies the process output deviation from set-point.

Time domain measures are the main indicators of the process behavior under closed-loop control. A sluggish control is observed as a result of the large rise time value. Also large decay ratio and increased overshoot imply a process with aggressive controller.

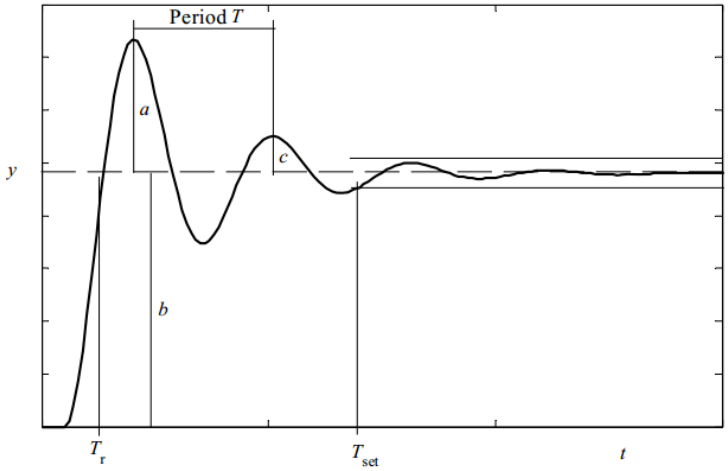

Figure 3.1: The step response of feedback control to set-point change.

In contrast to the set-point response criterion, integral absolute error (IAE) criterion describes the whole step response curve instead of paying attention to single point of curve. The related IAE criteria are listed as follows [3, 12]:

- Integral of the squared error (ISE): This criterion penalizes large controller errors and results in aggressive controller settings.

$$\int_0^\infty e^2(t)dt \tag{3.1}$$

- Integral of the absolute value of the error (IAE): This criterion is calculated by the sum of the areas between the response curve and steady-state value. When the

magnitude of deviation is changing linearly with the performance, it can be chosen as specification for assessment. It neither produces aggressive controller settings as ISE criterion nor conservative controller parameters as ITAE criterion.

$$\int_0^\infty |e(t)|dt \tag{3.2}$$

- Integral of the time-weighted absolute error (ITAE): The criterion penalizes errors that endure for a long time and also provides conservative controller parameters.

$$\int_0^\infty t|e(t)|dt \tag{3.3}$$

- Integral of the multiplied absolute error (ITNAE): The ITNAE illustrates the same features as IAE criterion.

$$\int_0^\infty t^n|e(t)|dt \tag{3.4}$$

- Quadratic error (QE): To design optimum controller, QE criterion can be used as specification.

$$\int_0^\infty [e^2(t) + \rho u^2(t)]dt \tag{3.5}$$

where e(t) is the difference between set-point value and controlled variable.

Deterministic assessment of PI or PID controller performance should be established upon the control strategies to be achieved. Controller settings may be appropriate for rejection of load disturbances, but not demonstrate satisfactory performance against set-point changes. Hence, the assessment should be done considering different control objectives separately via different techniques [13].

Shinskey proposed the delay time as a significant tool to determine the best achievable performance [14]. On the other hand, Swanda and Seborg have proposed a new methodology on the basis of set-point response to evaluate performance of PI and

PID controllers [15, 16]. The methodology is recommended to compare the available performance with the achievable performance of a PI controller tuned with the IMC rule based on a FOPTD process model. This technique utilizes dimensionless indices such as normalized settling time and normalized IAE given by:

$$T_s = \frac{t_s}{L} \tag{3.6}$$

$$IAE_d = \frac{IAE}{|A|L} \tag{3.7}$$

where t(s) is settling time, L is process time delay, IAE is measured integral absolute error and A is the size of step change. The values of apparent time delay, integral absolute error and setting time can be obtained by carrying out a set-point response experiment with closed-loop system. There are some methods for time-delay estimation which constitutes an important point in control performance assessment. Looking at how to model a step response curve, time delay estimation techniques are studied under two headings as approximating the step response by FOPTD and SOPTD models [17, 18]. As a result of determined dimensionless indices, the performance of PI/PID controller can be classified with respect to benchmarks attained by the IMC design.

Horch and Stattin have further discussed Swanda and Seborg's method to assess the control performance by a practical way. The new method has been proposed to cope with the inadequate experimental data sets leading to determination problems in settling time or overshoot. The first computational step is dead time estimation which is applied as in the original set-point response analysis. Contrary to previous method, settling times and overshoots of the closed-loop step responses are found by use of Kautz models. After identification of all these parameters, normalized indices are calculated as described above [19].

Another control objective is that control loops should be properly tuned to retain good control loop performance. Supposing that controllers are conservatively tuned, then sluggish response will be observed in terms of rejecting input load disturbances. To detect the sluggish control loops, Hagglund described a new method on the basis of measurement referred to as idle index [20]. Idle index assesses the recovery time to

distinguish between well-tuned and sluggish control loops subjected load disturbances. Index is formed with the times described by positive and negative correlations between the control signal (δ_u) and the process output increments (δ_y). When the load disturbance is applied, the control signal and process output response are initially in opposite directions which means that the multiplication of the increments is negative. After that, the process output goes back to the set-point and thus the multiplication of the increments is positive. The formulation of idle index I_i is then given as:

$$I_i = \frac{t_{pos} - t_{neg}}{t_{pos} + t_{neg}} \tag{3.8}$$

where t_{pos} and t_{neg} are updated according to sign of the correlation at each sampling instant.

$$t_{pos} = \begin{cases} t_{pos} + T_s & \text{if } \Delta u * \Delta y > 0 \\ t_{pos} & \text{if } \Delta u * \Delta y \leq 0 \end{cases} \tag{3.9}$$

$$t_{neg} = \begin{cases} t_{neg} + T_s & \text{if } \Delta u * \Delta y < 0 \\ t_{neg} & \text{if } \Delta u * \Delta y \geq 0 \end{cases} \tag{3.10}$$

The value of idle index can change between -1 and 1. When I_i takes positive value close to 1, control will exhibit sluggish responses to load disturbances. The I_i index of approximately zero values means that the controller tuning is acceptable. The index value close to 1 indicates that control is finely tuned, but oscillatory control can also cause the index to get a close value to 1. It should be noted that if the measurement data are corrupted by noise, the value of idle index does not fully reflect the behavior of process control loop. Khuel and Horch proposed some techniques for data pre-treatment to handle noisy data and enable to compute the correct value of idle index. Data pre-treatment techniques comprise of steady-state detection, filtering and signal quantization [21].

Beside sluggish responses, the oscillatory behavior of controller should be considered for the adjustment of controller settings. It is well-known that aggressive controller causes the oscillatory behavior in the closed-loop system. To recognize it, the new index so-called as area index (AI) is proposed to define how the control signal reject abrupt load disturbance. When the abrupt load disturbance is employed on the process,

the control signal approaches the new steady-state value after transient response, denoted as $\bar{u}$. The first time instant and the subsequent time instants when the control signal gets steady-state value are denoted by t_0 and $t_1,\ldots,t_N$ respectively. The area between two consecutive time instants is limited by the function created with the control signal values at each time and steady-state value.

$$A_i = \int_{t_i}^{t_{i+1}} |u(t) - \bar{u}| dt \tag{3.11}$$

Then, the devised area index is formulated as the ratio of maximum area determined and sum of all areas.

$$AI = \begin{cases} 1 & \text{if } n < 3 \\ \dfrac{\max\{A_1,\ldots,A_{n-2}\}}{\sum_{i=1}^{n-1} A_i} & \text{elsewhere} \end{cases} \tag{3.12}$$

The index is bounded in the interval of [0, 1]. The closer the AI value to zero, the more oscillatory behavior will be occurred. Likewise, the closer the AI value to one, the more sluggish behavior will be deduced [13]. On the other hand, the simultaneous evaluation of the area index and the idle index provides guidance on how the PI controller settings can be set for improvement of load disturbance rejection performance. A detailed description of performance assessment rules is presented by Visioli [22].

Through this thesis, controller performance will be assessed based on both monitoring methods except when determining the control loops which are considered in the subsequent diagnostic steps.

3.1.2 Stochastic Performance Indices

In the past applications, standard deviation of process output from the set-point has commonly been applied and used as an appropriate statistic to monitor. According to the perspective on this topic, this statistic has limited and misguiding information and also depends on the magnitude of load upsets. The statistic changes with process conditions rather than reflecting the controller performance. High standard deviation can be expected in spite of the desired controller performance for periods of large upsets, whereas low standard deviations with poorly design controllers can be seen for

periods of undisturbed process [23].

The most widespread used performance criterion is the variance of CV error, even though the statistic measure demonstrates sensitivity to load upsets. This criterion represents level of product quality, energy and raw material consumptions. The decrease in standard deviation generally means reduced energy consumption and increased product quality. However, the control system doesn't have the ability to adjust the effect of some random disturbances which are naturally occurred in process. This restricts the control loop to the achievable and certain lower bound of variance. The only way to decrease the variance below this limit is replacing the plant equipment [24].

In order to evaluate the performance of controller objectively, performance indices, which define the comparison of the current performance of the loop with the optimum one, are required. The concept of optimal controller serves as a benchmark which represents a significant contribution to the performance assessment. With the aim to quantify the current performance against benchmark, controller performance index (CPI) is defined as a relative measure. CPI should be scaled within [0, 1] and generally described by the following representation:

$$\eta = \frac{J_{des}}{J_{act}} \tag{3.13}$$

where J_{des} is any optimal value for performance criterion and J_{act} is the actual value of the performance criterion. CPI has grade equal to 1 for better control and 0 for worse control. The formulation is well accepted in control performance monitoring framework, but various definitions of CPI mentioned before are also available.

The selection of benchmark for the quantification has long been recognized as the early stage in assessment procedure. Different benchmarks such as perfect control, best-possible linear control, minimum variance e.g. exist and these are classified in terms of process output variance which denote the tightness of control. Among benchmark types, minimum variance is the most suitable control for the evaluation of closed-loop and linear systems. That is the reason why minimum variance benchmark will be discussed through thesis.

3.1.2.1 Harris Index

The minimum variance control (MVC) strategy, first introduced by Astrom [25] and Box-Jenkins [26], is the best optimal benchmark for the feedback control. The idea behind the MVC is to minimize the noise effect of the disturbance on the controlled variable. This refers to the performance that can be achieved with an ideal controller. The representation of generic single input-single output (SISO) feedback controller and the formulation of the MVC are given in Figure 3.2.

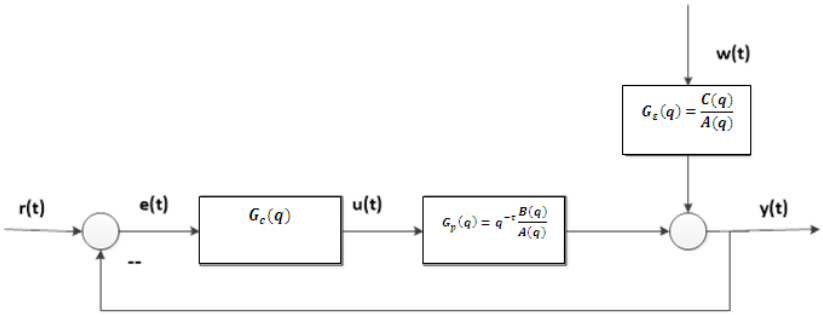

Figure 3.2: The generic single input-single output (SISO) feedback controller.

where G_C,G_p and G_ε are the transfer functions respectively represent the controller, process and disturbance dynamics, r(t) is the set-point for process output, e(t) is the control error, u(t) is the controller output, w(t) unmeasured noise and y(t) is the process output. The derivation of MVC is based on the following structured process model which is the result of linear and time-invariant assumptions.

$$y(t) = \frac{B(q^{-1})}{A(q^{-1})}q^{-d}u(t) + \frac{C(q^{-1})}{A(q^{-1})}w(t) \tag{3.14}$$

where w(t) is the Gaussian white noise, time delay d is known and A(q^{-1}), B(q^{-1}), C(q^{-1}) are nth order polynomials depending on shift operator(q^{-1}). The underlying purpose under MVC strategy is to minimize the variance of the process output at time (t+d) by manipulating the u(t) together with all given information at time t [13]. The formulation for minimization is defined as:

$$J(t) = E\{(r - y(t+d))^2 | Y(t)\} \tag{3.15}$$

where Y(t) is a conditional operator and E is the conditional expectation operator. This formula is rewritten by combining with process model and assuming that future values

of controller output is zero, disturbance values consist of causal and non-causal parts.

$$y(t+d) = \frac{B(q^{-1})}{A(q^{-1})}u(t) + [E(q^{-1} + z^{-d}\frac{F(q^{-1})}{A(q^{-1})}]w(t+d) \quad \textbf{(3.16)}$$

where the expression inside parenthesis satisfies the Diophantine equation. The polynomials E(q^{-1}), F(q^{-1}) and Diophantine equation can be written as respectively:

$$E(q^{-1}) = 1 + e_1 q^{-1} + ... + e_d q^{-d} \quad \textbf{(3.17)}$$

$$F(q^{-1}) = f_0 + f_1 q^{-1} + ... + f_{n-1} q^{-(n-1)} \quad \textbf{(3.18)}$$

$$A(q^{-1})E(q^{-1}) + q^{-d}F(q^{-1}) = C(q^{-1}) \quad \textbf{(3.19)}$$

The last equation for the optimal output prediction includes the present and past output values, present and past controller output values and future disturbance values. As a consequence, the minimization function can be regulated as:

$$J(t) = E\{[\frac{E(q^{-1})B(q^{-1})}{C(q^{-1})}u(t) + \frac{F(q^{-1})}{C(q^{-1})}y(t)]^2\} + E\{[E(q^{-1})(t+d)]^2\} \quad \textbf{(3.20)}$$

Future noise terms are independent from process outputs which are collected until time t, so the minimum can be achieved when the first part of the above equation equals to zero [13]. The model of MVC and the process output under MVC are shown below.

$$u(t) = \frac{F(q^{-1})}{B(q^{-1})E(q^{-1})}y(t) \quad \textbf{(3.21)}$$

$$y(t) = E(q^{-1})w(t) \quad \textbf{(3.22)}$$

where $E(q^{-1})$ is the noise-to-output transfer function.

The implementation of actual MVC law requires to know the process and disturbance models. However, the conception of MVC can be applied by the minimum variance estimate techniques which give CPM tools opportunity to assess the performance.

Harris [27] suggested the calculation of the minimum variance from closed-loop operational data and the comparison of single-loop controller performance against MVC in this way. The first step of the proposed procedure is describing the system by an autoregressive moving average (ARMA) model comprising the known process time delay. After constructing the model, impulse response of this model should be determined as follows [27].

$$y(t) = (\sum_{i=0}^{\infty} e_i q^{-i})\varepsilon(k) = (e_0 + e_1 q^{-1} + e_2 q^{-2} + ... + e_{d-1} q^{-(d-1)})\varepsilon(k) + (e_d q^{-d} + ...)\varepsilon(k) \tag{3.23}$$

where e_i is the impulse coefficient of the model. The impulse coefficients are found by solving linear Diophantine equations. MVC is not able to interfere the process output until time d, denoted by first parenthesis. Hence the minimum variance is designated as lower achievable limit and estimated by the first d impulse terms. To compute actual variance, the rest of the terms is incorporated to the MV formulation. The series expansion of actual and minimum variance are formulated as shown [27].

$$\sigma_{mv}^2 = \sum_{i=0}^{d-1} e_i^2 \sigma_\varepsilon^2, \ \sigma_y^2 = \sum_{i=0}^{\infty} e_i^2 \sigma_\varepsilon^2 \tag{3.24}$$

The comparison of the current performance with respect to MV benchmark is identified by Harris Index. Harris index is the ratio of the minimum variance to the actual variance and bounded between 0 and 1. The value of Harris index close to zero indicates poor performance controller. Likewise, the Harris index equal to one shows the best performance controller.

$$\eta_b = \frac{\sum_{i=0}^{d-1} e_i^2}{\sum_{i=0}^{\infty} e_i^2} \in [0,1] \tag{3.25}$$

It should be noted that the minimum variance control cannot be achieved in practice, so the index where values close to one is considered as acceptable in terms of good performance criteria.

Based on the idea of minimum variance, Desborough and Harris [28] introduced the normalized performance index that bounded like original index. Moreover, they proposed another estimation algorithm with the aim of computing index. This

algorithm utilizes the linear regression solution methods instead of solving a Diophantine equations. By this way, Harris index is easily obtained from the closed-loop operational data by simple matrix solution. Though the mentioned algorithm provide a simple way for estimation, it is inconvenience for online applications. To update the index sequentially in time, it is preferable to use recursive least square approach. The detailed description of how these algorithms are carried out given in Appendix. They also show the relation of index with the squared correlation coefficient which provides the dependence of index on sample length, time delay etc.

Another commonly used algorithm for estimation of MV is filtering and correlation (FCOR) method which was proposed by Huang and Shah [29]. The algorithm consists of forming the moving average (MA) model between the process output and the estimated white noise ($\hat{w}$). This white noise sequence can be obtained by use of whitening filter that receive the process output as an input to produce white signal output. In literature, some methods have been recommended to fit the filter model and estimate the white noise [30–32]. The widespread approach originated from Chatfield [33] is that white noise sequence can be assumed as difference between the actual closed-loop data and predicted process output. After modeling the relation between w(t) and y(t), model equation is multiplied by the white noise excitations respectively to attain minimum variance formulation. Minimum variance formulation include cross-correlation terms (r_{yw}) and defined as below.

$$\sigma_{mv}^2 = [r_{yw}^2(0) + r_{yw}^2(1) + r_{yw}^2(2) + ... + r_{yw}^2(d-1)]/\sigma_w^2 \qquad \textbf{(3.26)}$$

The performance index is regulated considering the above formulation given as:

$$\eta(d) = \frac{\sigma_{mv}^2}{\sigma_y^2} = \rho_{yw}^2(0) + \rho_{yw}^2(1) + \rho_{yw}^2(2) + ... + \rho_{yw}^2(d-1) \qquad \textbf{(3.27)}$$

where ρ_{yw} is the cross-correlation coefficient for lags from 0 to d-1. The general schematic representation of FCOR algorithm is shown in Figure 3.3.

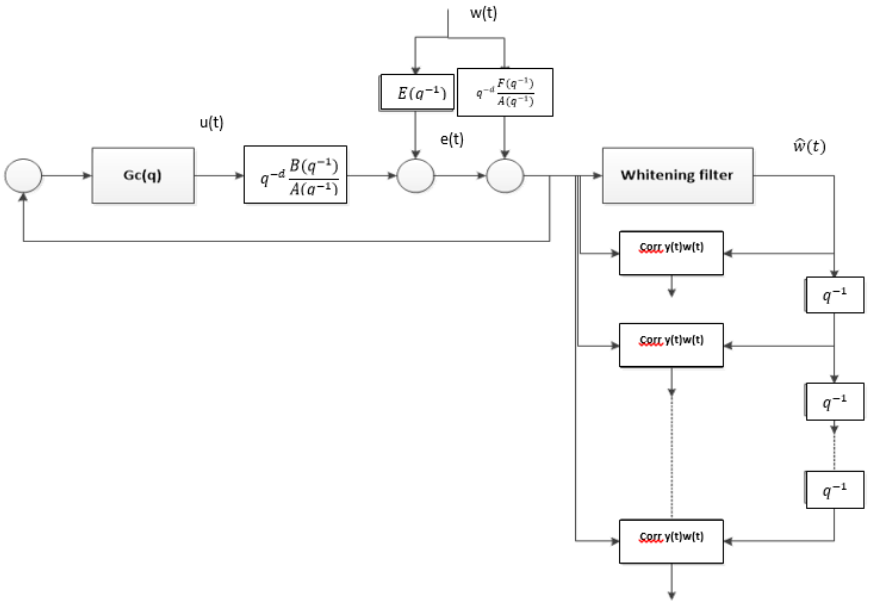

Figure 3.3: Schematic representation showing the filtering and correlation (FCOR) algorithm.

MV approach has been extended from the feedback control (FBC) to feed-forward (FFC)/feedback control loops. The objective with this extension is to evaluate the FBC/FFC loops and reveal which loops affect the process output variance. However, the MV calculation of FFC/FBC loops necessitates some changes in model and components of output variance. The model of relation between process outputs and unmeasured disturbances has some differences in terms of model type and time delays. The mentioned type formed as AR(I)MA time-series model consists of measured disturbance beside the unmeasured disturbance. After identifying model type, closed-loop models are created by use of model order and time delays due to FF and FB loops. These models provide a basis for variance analysis which include the effect of the disturbances on the overall variance. The overall variance is:

$$\sigma_y^2 = \sigma_{MV,w}^2 + \sigma_{FB,w}^2 + \sum_{j=1}^{n_w} (\sigma_{MV,\varepsilon_j}^2 + \sigma_{FF,\varepsilon_j}^2 + \sigma_{FB/FF,\varepsilon_j}^2) \qquad \textbf{(3.28)}$$

where $\sigma_{MV,w}^2$ is the MV of FBC resulting from unmeasured disturbance w, $\sigma_{FB,w}^2$ is caused by the non-optimality of the FBC,$\sum_{j=1}^{n_w} \sigma_{MV,\varepsilon_j}^2$ is the MV of FFC resulting from n_w measured disturbances, $\sum_{j=1}^{n_w} \sigma_{FF,\varepsilon_j}^2$ and $\sum_{j=1}^{n_w} \sigma_{FB/FF,\varepsilon_j}^2$ are caused by the non-optimality of the FFC and FBC/FFC respectively. The analysis of overall variance is a proper way to indicate the quantity of the improvement in performance. Desborough and Harris have given detailed description for the calculation of variance

components [34].

Although above-mentioned methods were developed based on the different procedures, the common aspect of them is that MVC should be designed in the presence of dead time. Thus, the key point of assessment analysis is the dead time estimation arising from true process dead time or the determination methods. The preference for determination methods versus actual time delay results from the fact that determination methods can be applied easily with approximate estimates. Indeed, the precise determination of the time delay can only be obtained by actual process delay with the use of time consuming open-loop test. Therefore, Desborough and Harris, and Thornhill et al. proposed another index to be called as extended horizon performance index (EHPI) to avoid estimating the time delay [28, 34, 35]. EHPI is defined as:

$$\eta_b = \frac{\sum_{i=0}^{b} e_i^2}{\sum_{i=0}^{\infty} e_i^2} \tag{3.29}$$

where b is the prediction horizon and greater than time delay. Otherwise, when b is equal to time delay, η_b is implied as Harris index. Thornhill used this index to choose the time delay without requiring any prior knowledge. Index values are primarily determined against different prediction horizons and then the best appropriate prediction horizon, where the index value does not vary so much, is selected [35].

The minimum variance benchmark constitutes an important part of the performance assessment and gives the theoretical minimum value based on the routine operating data. However, the minimum variance is widely used approach because of its simplicity, the variance under MVC can only be achieved in a theoretical manner. Furthermore, the interpretation of Harris index might be misleading and could not take into account the deterministic criterion. To compensate this limitation of MVC, Bezergianni and Georgakis devised the new index to be called relative variance index (RVI) to compare the actual controller performance with the open-loop control and the minimum variance control. The RVI index is formulated as following:

$$RVI = \frac{\sigma_{OL}^2 - \sigma_y^2}{\sigma_{OL}^2 - \sigma_{MVC}^2} \tag{3.30}$$

where σ^2_{OL} is variance under open-loop case, σ^2_y is the variance obtained by current control action and σ^2_{MVC} is the minimum variance of process output. When the controller performs like an open-loop control system, value of the RVI index is zero; conversely when the performance of controller is good enough as the MVC, the RVI index is equal to one [36]. The actual variance and minimum variance of process output are only required to be known when dealing with the Harris index. By considering this new index, the calculation of open-loop output variance must also be introduced, apart from the actual and minimum variance terms. For this purpose, the methodology is primarily trying to capture the dynamics of the system with system identification which provides an estimate of approximate models for controller, process and disturbance.

The above-mentioned MV approach needs modification with different control schemes except the single loop FBC. Cascade control (CC) scheme is widely used to reject load disturbances and eliminate the nonlinear behaviors originating from the final control element [12, 37]. To achieve these control strategies, CC has been designed with primary and secondary control loops. Primary control loop can be assessed like single FBC loop with constant set-point, but these techniques could not evaluate the effect of secondary unmeasured disturbance. For this purpose, the extension of the MV assessment to cascade control (CC) has been handled by Ko and Edgar [38]. The model of primary process output can be established based on the unmeasured disturbances (ε_1,ε_2) and process outputs of secondary loops. After some arrangements, the expression for process output of primary control loop can be reduced into the MA process relating the primary process outputs to both disturbances. As a result, the MV of primary output can be determined by two methods which are the correlation analysis between the process outputs and the estimated sequences or the Diophantine identity regarding the estimated parameter matrix polynomial.

The extension of MV to MIMO system requires a sequence of complicated calculations, although, the concepts related to the MVC of SISO system are relatively straightforward. The starting point for MVC approach of MIMO system is the simplification of assessment by partitioning into p MISO systems. However, this strategy does not reflect the improvement potential of all loops, only gives an idea of the improvement potential for each loop [3]. New techniques for accurate assessment of multivariable systems have emerged in the literature [29, 39–41]. Some approaches

such as FCOR algorithm and the spectral-factorisation-based approach use the routine operating data of MIMO systems. It is worth noted that a key point in these approaches is to construct the multivariate generalization of the time delay referred to as the interactor matrix. The interactor matrix can be estimated from the plant process transfer function or the plant data proposed by Rogozinski et al. and Huang, Shah, respectively [29, 42]. These approaches provide an introduction to estimation algorithms, but they require the knowledge of the process transfer matrix as well as the Markov matrices of the system transfer function matrix. Whenever the process matrix is not possible to be completely known, the difficulties have been encountered in the estimation of the interaction matrix. Thus, Ko and Edgar devised the new method to overcome the obstacle without need for knowledge of the process transfer matrix, but the Markov matrices are still necessary [41]. By this method, calculation of the lower achievable value for each output variance is proposed to weaken the need for interactor matrix instead of the estimation of performance index. This alternative way is based on the combination the interactor matrix with the estimation of performance index without the calculation of interactor matrix in an explicit manner. The other studies in this direction have been proposed by Ettaleb and McNabb and Qin [3, 43]. Although various improvements in this field have been recorded, theoretical developments and industrial applications of MIMO assessment are considerably limited.

3.2 Diagnosis of the Control Loops

The next step of the performance assessment is the diagnosis of the source that cause the performance degradation. To this end, a series of analyzes are performed and an algorithm is implemented as shown in Figure 3.4.

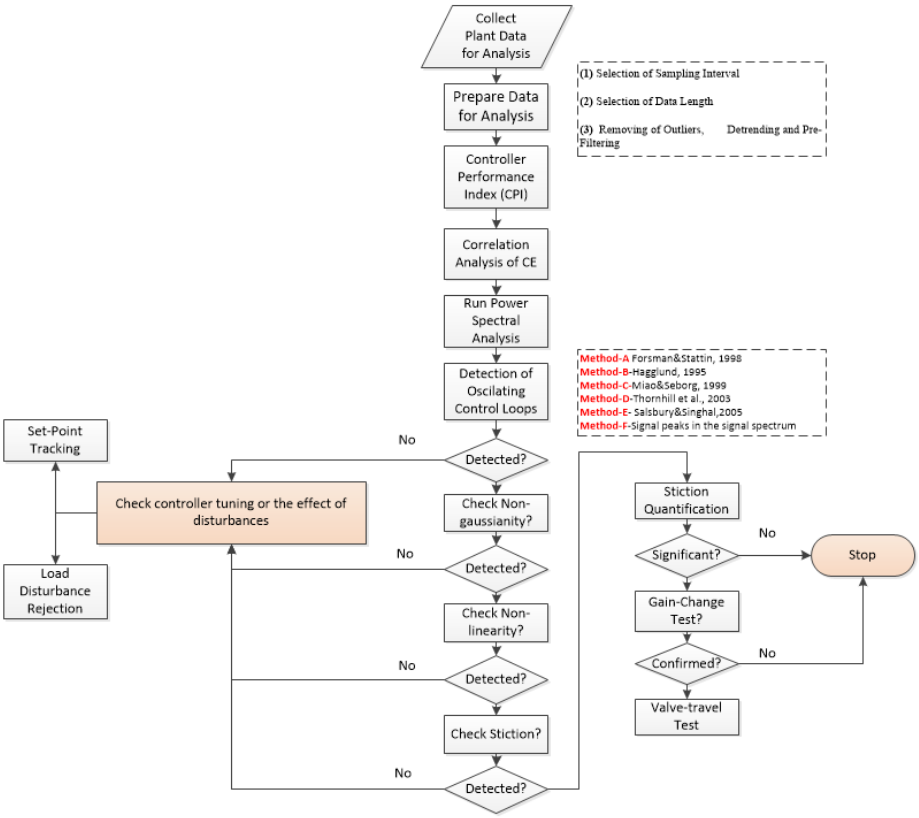

Figure 3.4: Algorithm for performance monitoring to assess and diagnose root-causes.

3.2.1 Oscillation Detection

Oscillation in the controlled and manipulated variables is stemmed from various root-causes such as nonlinearities in the hardware, external disturbances, aggressive tuning and loop interactions. The most common problems in the control loop are static friction, dead zone, backlash, saturation and quantization which are considered as nonlinearities in the hardware. External disturbances may be originated from the loop interactions, fluctuations in the quality of raw-material e.g. The realization of external and internal oscillations is a key point to diagnose the oscillations. The other root-cause is the aggressive tuning that occurs when the parameters of control loop are set to be unstable. Controller gain higher than ultimate gain or excessive integral action may lead to oscillation in the controlled variables. Finally, loop interactions as a result of poor design of control structures may be the origin of plant-wide oscillations. If an oscillation appears in a control loop, it will progress and affect another loop because of the poor design of control system. A general representation of problematic components of control loop is shown in Figure 3.5.

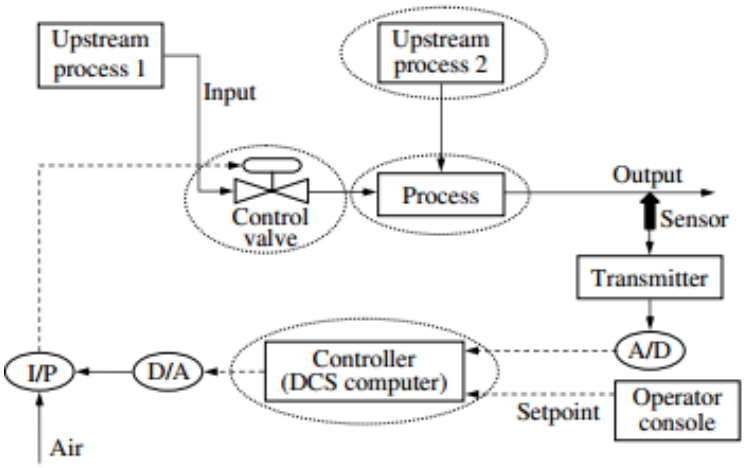

Figure 3.5: Schematic representation of possible faulty components.

Since no significant mathematical formula representing the oscillation, the oscillation comes up as a relative concept with various definitions. Horch defined the oscillation as visible periodic changes which are not affected by noise. Shoukat et al. also introduced similar definition that oscillation signal is a periodic signal with well-defined amplitude and frequency [44]. In addition to these definitions, there are several ways to interpret the periodicity of oscillations such as auto-covariance function (ACF), power spectral density (PSD) and quantification of the strength of oscillations by period, regularity and power. ACF gives a measure of the correlation of data series with itself at two different times, but when these data are stationary, it is sufficient to know the difference between sampling times, referred to as lag. ACF is defined as:

$$r_{xx}(k) = \frac{\sum_{t=1}^{N-k}(x(t)-\bar{x})(x(t+k)-\bar{x})}{\sum_{t=1}^{N}(x(t)-\bar{x})^2} \tag{3.31}$$

where k is the lag number, x(t) is the data measured at time t and x is the mean of N sample data [45, 46] . The value of ACF is bounded between -1 and 1. Power spectrum is another tool to help identifying the periodicity by decomposing the signal into available frequencies in the process. For a stationary random process, the power spectrum is the Fourier transform of the ACF, written in Eq.3.32.

$$P(f) = \sum_{k=-\infty}^{\infty} r_{xx} e^{-2\pi j f k} \tag{3.32}$$

The power spectrum is a positive real-functioned value, since the autocorrelation of time series data consists of imaginary values [45, 46]. Sharp peak in the power

spectrum reveals the periodic signal at a frequency where peak is located.

Assessment of the features of oscillations is an important point that must be understood to reveal whether the degree of fault is significant and maintenance is required. One of the features is the period which is twice the time-instant between two successive zero-crossings and at the same time, it corresponds to the reciprocal of the oscillation frequency. This period may take values around the mean due to the changes in the interval between zero-crossings arising from the stochastic components and noise term. The regularity is the function of mean and standard deviation of the oscillation period that is used as an indication of the non-randomness behavior. Finally, power is a feature that compares the amplitude of oscillation in the selected frequency according to total power. By use of these features, some techniques for detection which are classified as in Figure 3.6 are developed.

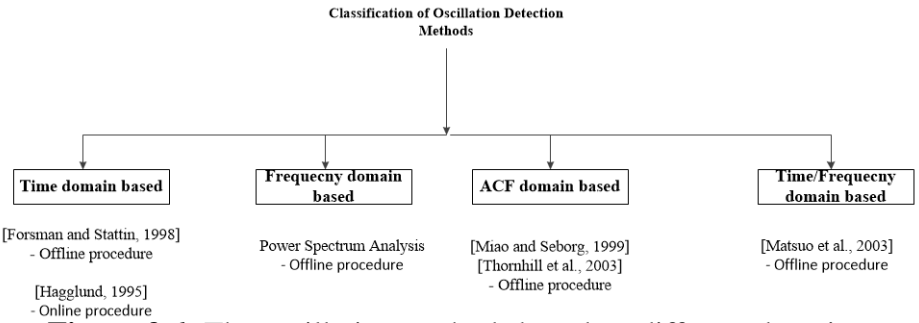

Figure 3.6: The oscillation methods based on different domains.

Hagglund proposed the first online procedure to detect oscillation using integral absolute error (IAE) between two successive zero-crossings of the control error [47] . IAE is a widely used performance metric deciding whether load-disturbance acts on the process input. With load-disturbance acting, the interval bracketing two zero-crossings is wide and the value of IAE becomes large. For quantization of this error, limit value, IAE_{lim}, is defined by the use of ultimate frequency which means that all frequencies up to ultimate frequency are included. Ultimate frequency can be obtained from the relay feedback test suggested as an alternative to generate sustained oscillation. In cases where the ultimate frequency is unknown, integral time of the reasonably tuned controller corresponds to the ultimate period. Although this method easily detects oscillation by observing the number of load disturbances during the supervision time, there may be some problems with the assumptions. This method is associated with loops oscillating at the ultimate frequency, but this situation is not always valid.

Besides, the ultimate frequency may not be known and also the integral time may not show the accurate results. Despite these disadvantages, it is a preferred method for online oscillation detection.

Forsmann and Stattin inspected both zero-crossings and IAE for detecting oscillations in time domain [48] . It is assumed that when control error is approximately periodic, time instants between a sequence of zero-crossings and IAE values corresponding these time instants should not change with time. Firstly, all zero-crossings and all IAE values are computed, then separated into negative part, denoted as A_i,δ_i and positive part, denoted as B_i,ε_i. All related parameters for this method are illustrated in Figure 3.7. IAE and zero-crossings of both parts are used in pairs.

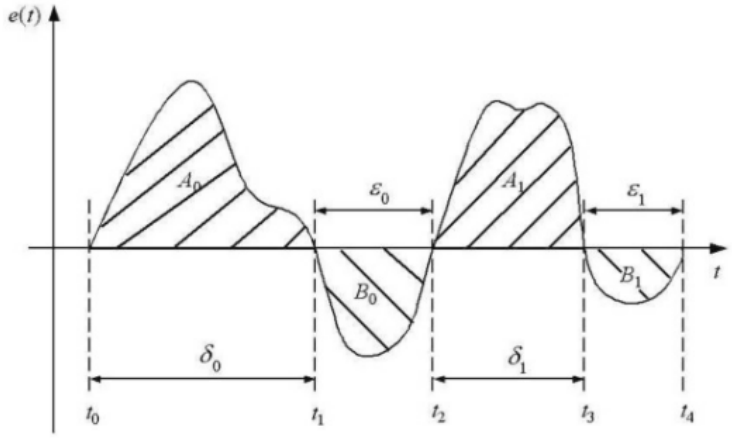

Figure 3.7: Parameters related to the oscillation index calculation.

Secondly, the number of pairwise parameters that satisfy certain conditions in both parts are counted. Oscillation index (h) is the ratio of total number of pairwise parameters to total number of zero-crossings. The general formulas are written as following:

$$h = \frac{h_A + h_B}{N} \tag{3.33}$$

where h_A is the number of parameters in positive parts, h_B is the number of parameters in negative parts and N is total number of zero-crossings. The conditions for determining h_A and h_B are given in Eq3.34 and 3.35.

$$h_A = \#\{i < \frac{N}{2}; \alpha < \frac{A_{i+1}}{A_i} < \frac{1}{\alpha}\Lambda\gamma < \frac{\gamma_{i+1}}{\gamma_i} < \frac{1}{\gamma}\} \tag{3.34}$$

$$h_B = \#\{i < \frac{N}{2}; \alpha < \frac{B_{i+1}}{B_i} < \frac{1}{\alpha}\Lambda\varepsilon < \frac{\varepsilon_{i+1}}{\varepsilon_i} < \frac{1}{\varepsilon}\} \tag{3.35}$$

This method is sensitive to signal noise, thus pre-filtering is essential before index calculation. Simple low pass filter and a moving average filter are usually recommended filter types, and these are also preferred for reduction of high-frequency noise and smoothing data respectively [45] .

Miao and Seborg developed a patented approach based on the auto-covariance function (ACF). This method produces some advantages over oscillation detection methods defined in the time domain. Firstly, the ACF reduces the influence of noise as a kind of filter, since ACF of white noise is theoretically zero for lags greater than zero. Secondly, auto-covariance function of an oscillating signal shows behavior in the same manner as the oscillatory signal. Based on this idea, damping of oscillatory signal is expected to be seen in a similar way in the ACF. Thus, the damping factor in time domain is corresponding to the damping ratio of the ACF, known as decay ratio (R_{acf}). To determine the decay ratio, the ACF of controller error or process output is primarily computed using only normal operating data without a need to process model or special excitation input. Two different lines are formed by combining the first two minimum points of ACF and by combining the first maximum point with zero-lag auto-covariance coefficient. The decay ratio is then defined as the ratio between distance from the first maximum to line connecting minimum points and distance from the first minimum to remaining line. If the decay ratio exceeds a specified threshold, the possibility of an oscillation is inferred. ACF and the actual signal must contain a certain number of cycles. To achieve this, the methods of indicating what should be the data collection period are used [49] .

Thornhill et al. inspected the regularity of zero-crossings of ACF. If the intervals between zero-crossings are regular, the signal has oscillating behavior. To decide whether a signal is regular or not, the comparison with the mean value of period and standard deviation of time period are used and this comparison can be termed as regularity factor.

$$r = \frac{1}{3}x\frac{\bar{T}_p}{\sigma_{T_p}} \tag{3.36}$$

where σ_{T_P} is the standard deviation of the period that twice the standard deviation of intervals and $\bar{T_p}$ is the mean of the period formulated as

$$\bar{T_p} = 2\frac{\sum_{i=1}^{n} \triangle T_i}{n} \tag{3.37}$$

where n is total number of zero-crossings. Thornhill et al. suggested to use the first 11 zero-crossings for calculating period which means that taking 10 intervals except the interval zero-lag to the first zero-crossing. As a result of calculations, when the regularity factor takes a value greater than one, a signal indicates a regular oscillation with a well-defined period [50] .

Detection of oscillation can be also carried out by observing the apparent peaks in power spectrum. This approach is a conventional method performed in the frequency domain and identify the control loops affected by control-valve nonlinearity, poor controller tuning or external disturbances. A signal oscillating at a certain frequency produces a dominant peak in the power spectrum in the same frequency. To distinguish the dominant peak, the magnitude of these peaks outside the low frequency range are proportioned to the total power located in this frequency range. Although it is an easier method for visual inspection of oscillation detection, it is difficult to automatically apply and sometimes provides inaccurate information for the period and regularity of oscillations. Thornhill et al. define the regularity of a signal as the ratio between the frequency of peak and its bandwidth [50] . There is an obstacle to clearly determine the bandwidth of peak in case of noisy signal. Also, if trend of signal is intermittent and changes with time, oscillation detection becomes more difficult, so an appropriate method for peak detection should be specified.

The next step in the detection of oscillation is the combination of time and frequency domain analysis. Contrary to intermittent oscillations, persistent oscillations are clearly seen as sharp peaks in power spectrum. To examine the intermittent oscillations in power spectrum, collected data should be divided into subsets according to trend changes over time. Apart from this technique, Matsuo et al. provide an alternative method, referred as Wavelet analysis, to deal with multiple frequencies as well as intermittent oscillations [45, 51] .

3.2.2 Nonlinearity Detection

Root-cause diagnosis of oscillations due to some sources prevents the loss of the money by identifying the oscillations before spreading through the plant and affecting the operation so much. The success of this stage lies in properly addressing what the oscillation sources are because it can be more than one source that creates the same root-cause for the oscillating behavior such as nonlinearity. Controller performance within the CPM framework is mostly evaluated by assuming that nature of the process is linear and therefore degradation of performance will be sensed whenever the nonlinearity is appeared in the closed-control loop. Nonlinearity may be generated by such an external source as disturbances or such an internal source as valve stiction, and so on. For each of the oscillation sources, appropriate corrective action should be implemented after non-linearity test methods make distinction between types of nonlinearities in time series.

To measure the nonlinearity of the process, basically, methods are categorized into two main concepts, namely model-based and time-series based. Several authors addressed model-based concept for quantification of nonlinearity and proposed two main approaches which are based on best-linear approximation and curvature [52,53] . Since model-based approaches benefit from the relationship between input and output or the system model, time series-based nonlinearity measures are preferably used. Haber et al. gave a review of all classical non-linearity detection methods based on time-series that used for decision of whether a process is linear or not . These methods are treating the open-loop nonlinearity system with excitation input signals that are not present in the actual system, so quantification of nonlinearity is a challenging task.

Another method has been proposed for the nonlinearity detection in time series by use of the higher order statistics analysis of closed loop data. First and second order moments are utilized for the analysis of signals from linear processes assuming that the data are sampled from a normal distribution. However, when the nonlinear signal is analyzed, higher order statistics tools such as cumulants, bispectrum and bicoherence are needed to quantify nonlinearity of process. Bispectrum is the frequency domain counterpart of the third-order moments and defined as

$$B(f_1,f_2)\underline{\underline{\triangle}}\, DDFT[c_3(\tau_1,\tau_2)]\underline{\underline{\triangle}}E[X(f_1)X(f_2)X^*(f_1+f_2)] \tag{3.38}$$

where X(f_1) is the Fourier transform of time-series data $x(t)$ and $E[]$ is the expectation operator. Part of bispectrum plot with the sufficient information is called as non-redundant principal domain which consists of the inner and outer triangular regions [44] . Each point wherein principal domains represents the bispectral content of the interaction between two frequencies. Scalling is used to bring all bispectrum values into the range [0, 1] and as a result, normalized values referred to as bicoherence are obtained.

$$bic^2(f_1,f_2)=\frac{|B(f_1,f_2)|^2}{E\{|X(f_1)X(f_2)|^2\}E\{|X(f_1+f_2)|^2\}} \tag{3.39}$$

where bic is denoted for bicoherence function. Higher-order statistic-based methods present a practical way to detect nonlinearities in time series and help to decide whether linear system is affected by Gaussian white noise or the output of the nonlinearity system. Some authors made an attempt to this area by testing bispectrum and then modified to simplify the calculations [54, 55] . These methods are mainly concerned with squared bicoherence which is a clear indication of nonlinear system. System is analysed based upon whether the squared bicoherence is zero or constant. The squared bicoherence is zero meaning that the signal is Gaussian and the system is also linear [56] . On the other side, the squared bicoherence is constant which means that the signal is non-Gaussian, but the system is linear. The equation for Gaussianity is formed as below:

$$\overline{bic^2{}_{crit}}=\frac{1}{4KL}[c\alpha^z+\sqrt{4L-1}] \tag{3.40}$$

$$NGI=\overline{bic^2}-\overline{bic^2{}_{crit}} \tag{3.41}$$

where K is number of data segments, L is the number of bifrequencies including in the principal domain and is the one-sided critical value obtained from the standard normal distribution corresponding to confidence level α. A non-Gaussian signal must be examined later for nonlinearity. Nonlinearity is formulated due to the fact that nonlinearity disrupt the flatness of the graph.

$$NLI = |\overline{bic^2}_{max} - (\overline{bic^2} + 2{\sigma_{bic}}^2)| \tag{3.42}$$

where and are the average of the estimated squared bicoherence respectively. If NLI is equal to zero, the system is linear and if NLI is greater than zero, the system is nonlinear.

Theiler et al. formulated another approach that detect the nonlinearity behavior by observing the phase coupling in time series. As a result, time series capture the regular pattern and there exist predictable nonlinearities. This situation gives an alternative way to identify nonlinearities statistically that comparing the test data with synthetic data sets known as surrogate data having the same power spectrum as test data. Although different methods are available for generating surrogate data, the most commonly employed method is the randomizing the phase while maintaining the same spectral feature [57, 58] . To produce surrogate data, the FFT of the test data is primarily calculated and then randomize the phase at each frequency over [0, 2π] range. After that, inverse discrete Fourier transform is calculated and finally achieve the key property for each of the data set.

$$z = FFT(test\ time\ series) \tag{3.43}$$

$$z = FFT(\text{test time series}) \tag{3.44}$$

$$z_{surr} = \begin{cases} z[i] & i = 1 \\ z[i]e^{j\Phi_{i-1}} & i = 2,\ldots,N/2 \\ z[i] & i = \dfrac{N}{2}+1 \\ z[i]e^{-j\Phi_{N-i+1}} & i = 2\left(\dfrac{N}{2}+2\right),\ldots,N \end{cases} \tag{3.45}$$

$$\text{surrogate data} = IFFT(z_{surr}) \tag{3.46}$$

$$surrogate\ data = IFFT(z_{surr}) \tag{3.47}$$

If difference between the key property of test data and mean of property for surrogate data is greater more than standard deviations, it is clear indication of nonlinearity formulated as [59] :

$$NPI = \frac{\overline{\Gamma_{surr}} - \Gamma_{test}}{3\sigma_{surr}} \tag{3.48}$$

Values of NPI >1 are taken to indicate a nonlinearity. Indeed, periodicity of time series, peaks and discontinuities in data set should be taken into account to avoid misleading results.

3.2.3 Stiction Detection

Nonlinearities of the valve such as stiction, hysteresis, dead-band or dead zone limit the control loop performance and cause oscillations in the control loop. Among them, one of the most common problems is valve stiction and many techniques have been proposed that attach great importance to it. Some of these techniques are cross-correlation method, the area-peak method, the relay method, the curve-fitting technique, the bicoherence and ellipse fitting method, using only OP and PV signals [60–65] . Another part of detection techniques requires extra information about the valve characteristics and is not recommended as an automated detection method for industrial applications [66, 67] . The present study is aimed to evaluate stiction in control loops by using the routine operating data that are always available.

Horch's easy method to diagnose oscillations is based on the cross-correlation between controller output (u) and process output(y) [60] . This technique distinguishes oscillating loops that are caused by external disturbances and static friction. However, there are several assumptions in the method about types of process and controller and also the amplitude of oscillation. For the application of method, process should not have an integral action and controller should be PI type. Additionally, control loop with a large amplitude oscillation can be detected. The basic idea underlying the method is that odd cross-correlation function values indicate the case of stiction-induced oscillations, but if the cross-correlation values are even then oscillations is not induced in the control loop due to stiction. Although Horch's method has been applied in many industrial applications, it sometimes gives incorrect results.

He et al. formulated a theory for the detection of valve stiction from piece-wise fitting of the process variable or controller output [64] . In this method, firstly, sinusoidal or triangular segments so as to minimize objective function are fitted on each half cycle of PV or OP. Sinusoidal and triangular segments in Figure 3.8(a) and (b) display how

to define a piece-wise fitting objective function.

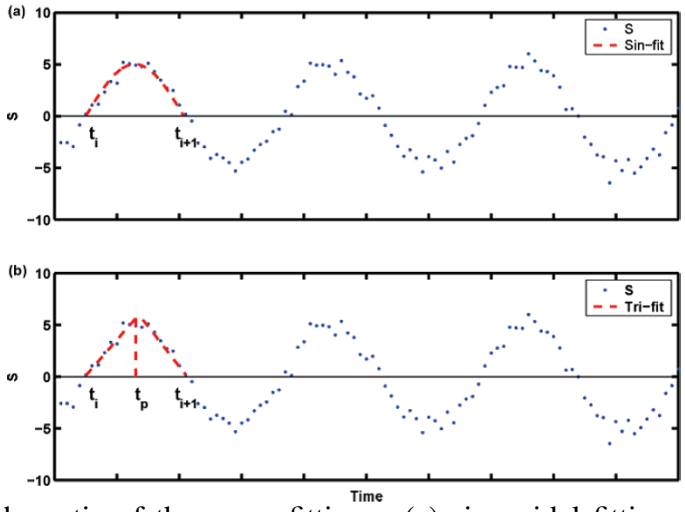

Figure 3.8: Schematic of the curve fittings: (a) sinusoidal fitting and (b) triangular fitting.

Objective function of sinusoidal segments constitutes a single fitting using a LS method for each half-period of oscillation, but for triangular fitting, each half period of oscillation is investigated under two time periods, such as first time period endured until time t_p and second time period endured after time t_p. Then the error between the actual data and segments is analyzed to decide which model represents better. If the real data is represented by the sinusoidal wave, there is no stiction; otherwise stiction is concluded.

Choudhury et al. presented a bicoherence-based technique for distinguishing the stiction from other valve problems and quantifying the stiction [65] . First, nonlinearities stemmed from process or valve are detected in a control loop by use of higher-order statistical based indices. Next, if the nonlinearities occur, pretreatment of data by Wiener filter is primarily realized and an ellipse is fitted to the filtered PV and OP signals, denoted as PV_f and OP_f. If the relation between PV_f and OP_f is tracking the elliptic pattern, stiction can be quantified.

3.2.4 Basic Statistics

Horch and Heiber introduced a considerable number of measures to realize the performance analysis on large data sets [68] . These measures are computed using only operating data without requiring any additional knowledge about process. The simple indices are shown in Table 3.1.

Table 3.1: Simple performance indices that have been evaluated for all data sets. The units [%] refer to the operating ranges of OP and PV.

Index	**Description**
CE mean[%]	Mean of control error
CE std.[%]	Standard dev. of control error
OP std.[%]	Standard dev. of controller output
CE skewness	Skewness of control error
CE kurtosis	Kurtosis of control error
Std. ratio	Ratio of std. of control error and controller output
Maximum bicoherence	Maximum bicoherence
Correlation coefficient	Correlation coefficient between control error and controller output

4. RESULTS AND DISCUSSIONS

4.1 Industrial Data

Industrial data Loops 1-5 are data sets collected from different units of the İzmit Refinery, located in Kocaeli. Two trends from different flow control loops, one from a temperature control loop, one from a level control loop and one from a pressure control loop were used. Time trends are shown in Figure 4.1, 4.2, 4.3, 4.4 and 4.5. Data have been obtained to cover three shifts at an operation day when the control system experienced problems. Control engineers have identified sampling interval as 15 s for some loops and 30 s for some others.

Loop 1 is controlling the flow of light crack naphtha (LCN) withdrawn from the splitter column and is not operating in cascade with any control loop.

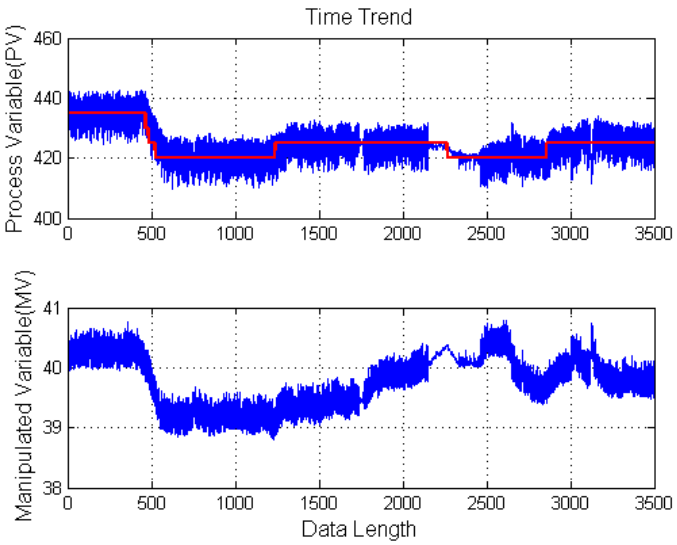

Figure 4.1: Data from Loop 1.

Loop 2 is controlling the reflux flow of naphtha-splitter column in crude-oil unit and is not operating in cascade with any control loop.

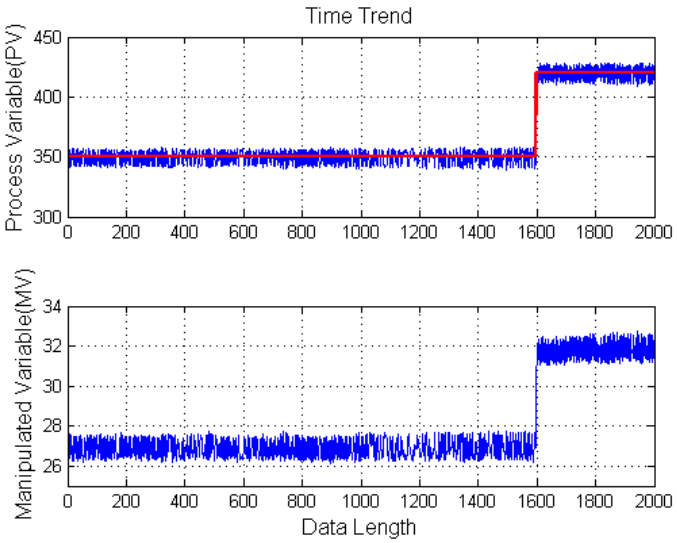

Figure 4.2: Data from Loop 2.

Loop 3 is placed after the furnace and controls the temperature of the flow that is supplied to the fractionator column. It operates as cascade with the fuel system of furnace.

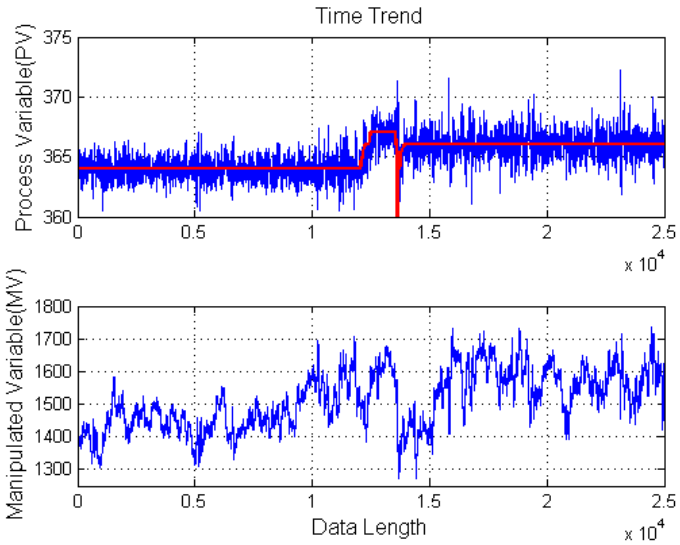

Figure 4.3: Data from Loop 3.

Loop 4 is controlling the level of top drum in splitter column and working cascade with the flow controller, interfering the distilate.

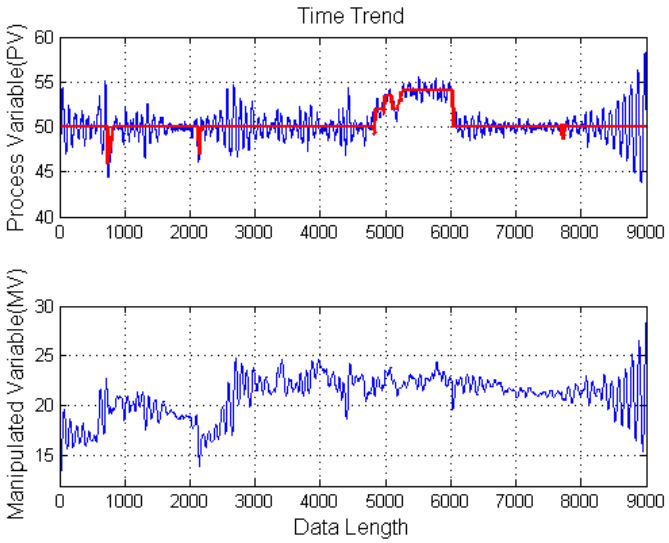

Figure 4.4: Data from Loop 4.

Loop 5 is interfering the fuel gas to control the pressure at the top drum of ethanizer column.

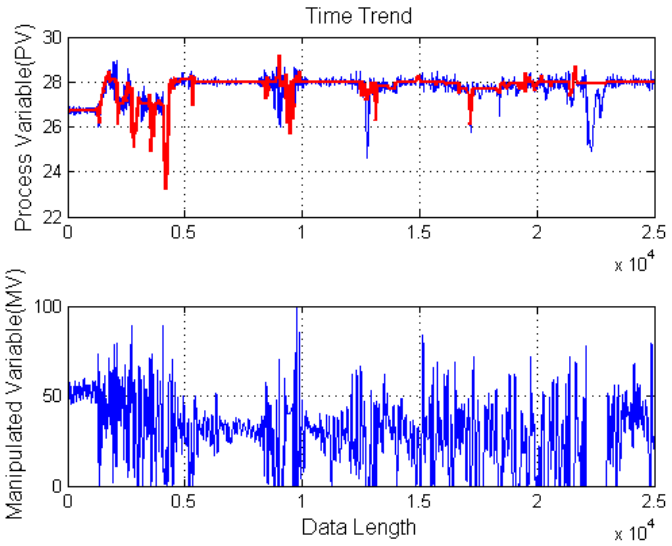

Figure 4.5: Data from Loop 5.

4.2 Loop 1-Flow Control Loop

Controller performance monitoring techniques require some parameters such as the number of terms in the model (m), the sampling interval, data ensemble length (n) and the prediction horizon (b) to create auto-regressive (AR) model. Sampling time and number of terms in the model are not independent from each other and so, when deciding on the sampling interval, the number of terms is taken as 30. After the terms are constant, the required sampling interval is determined using the estimated closed

loop impulse response plot which demonstrates the response of the system until it becomes steady. When selecting the sampling interval, it should be noticed to capture the impulse response in 30 samples.

Figure 4.6(a) and 4.6(b) shows the estimated impulse response of Loop 1 at 15 s and 30 s. 30 s samples capture the estimated impulse response, but the estimated impulse response from 15 s is captured within 20-25 samples. Therefore, 30 s is recommended for sampling interval.

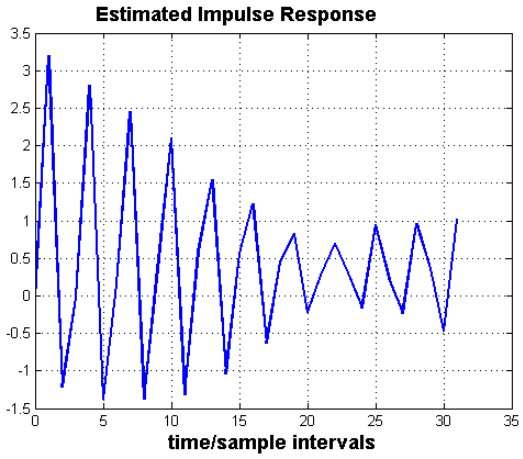

(a)

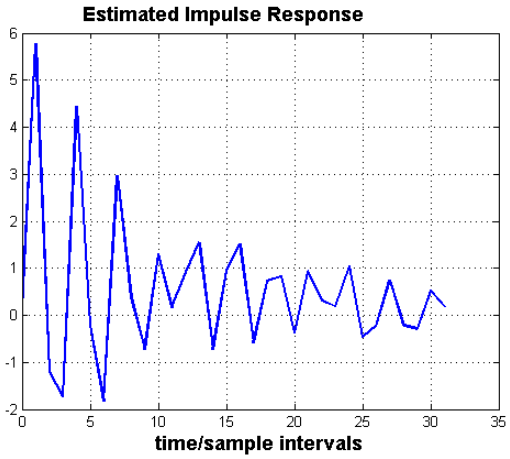

(b)

Figure 4.6: Estimated impulse response plots (a) for Loop 1 with 15 s sampling interval, (b) for Loop 1 with 30 s sampling interval

Another parameter to be considered in the performance index calculation is time delay. When the actual value of the dead time is unknown, the dead time can be estimated from the data obtained under closed-loop by use of some methods. One of them is the cross-correlation method. This method is based on analysing the cross-correlation between manipulated variable and controlled variable. Lag, where the maximum cross-

correlation occurs, gives the time delay. Figure 4.7 shows the cross-correlation plot for Loop 1.

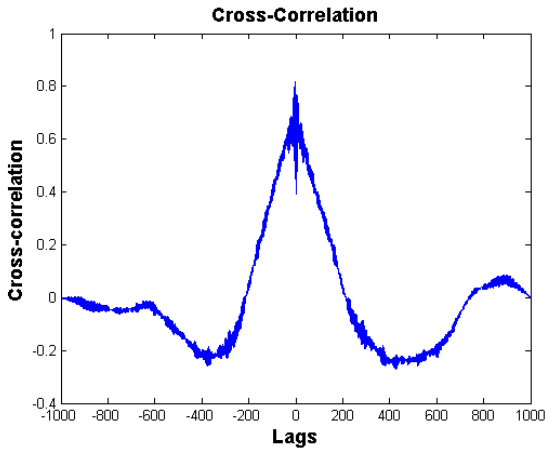

Figure 4.7: Cross-correlation plot for Loop 1.

According to cross-correlation, 1 sampling interval is recommended for time delay. This value is compatible with the real value observed by engineers and so, it is used in the assessment calculations.

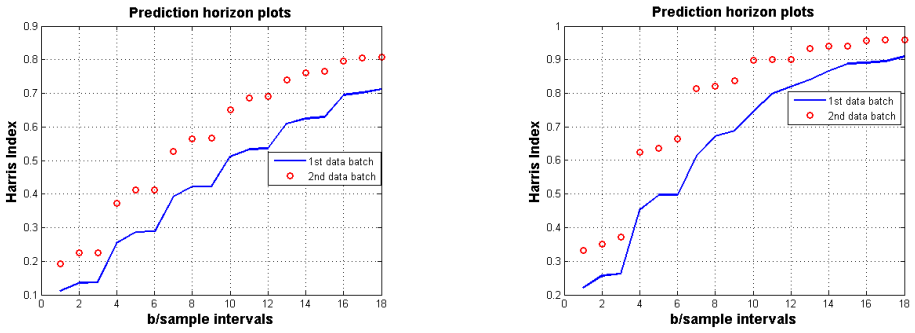

(a) (b)

Figure 4.8: Extended prediction horizon plots (a) for 15s samples, (b) for 30s samples.

However, sometimes the time delay estimates may be different from each other and prediction horizon should be set to the dead time. Choice of prediction horizon depends on the changes in performance index with prediction horizon. Once the model order is fixed, change of the performance index is investigated by increasing the value of prediction horizon. The first point with no significant change in index provides the prediction horizon. Figure 4.8(a) and 4.8(b) present the change in performance index and interpretation of this chart is a challenging task for the case.

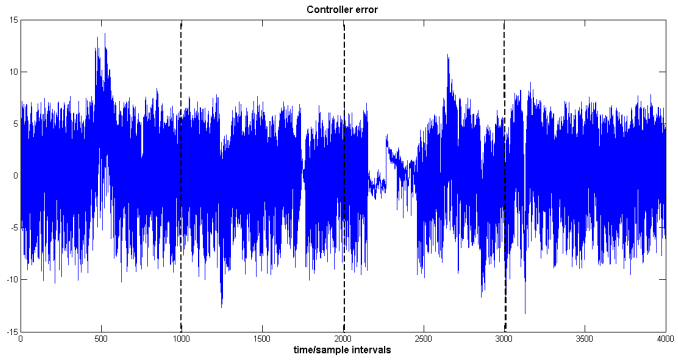

Figure 4.9: Time trend of the controller error from Loop 1.

The data ensemble length also influences the statistical confidence of performance index that likely to remain within the limits and increases by incremental data length. Time trend of controller error in Loop 1 is shown in Figure 4.9.

Values and changes in performance index are examined with data ensembles of 400, 500 and 1000, results shown in Figure 4.10(a), 4.10(b) and 4.10(c). A change in operation mode appears between samples 1000 and 1200. In the case of working with 400 samples, the performance index of last data ensemble is 0.0311 with a standard deviation of 0.2044 that is much higher than the confidence limit. On the other hand, the standard deviations with 500 samples and 1000 samples, as shown by the error bars are slightly smaller. When working with data size of 1000 samples, it has decreased deviation of changes in the performance index. 1000 samples is recommended to achieve the stability of the loop response and statistical confidence, but 500 samples give a reasonable result.

After all parameters required for index calculation are specified, the performance index is found by two algorithms, and results are given in Table 4.1. Poor control performance is detected with respect to performance index.

Table 4.1: Performance indices for Loop 1-Flow control loop

Parameters	
Data Batch	1000 samples
Model Order	30
Time Delay(s)	30
Sampling Interval(s)	30
Performance Indices	
FCOR	0.2574
Harris index	0.2592

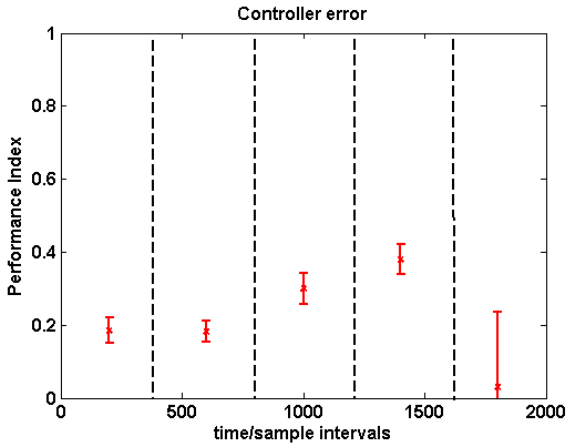

(a)

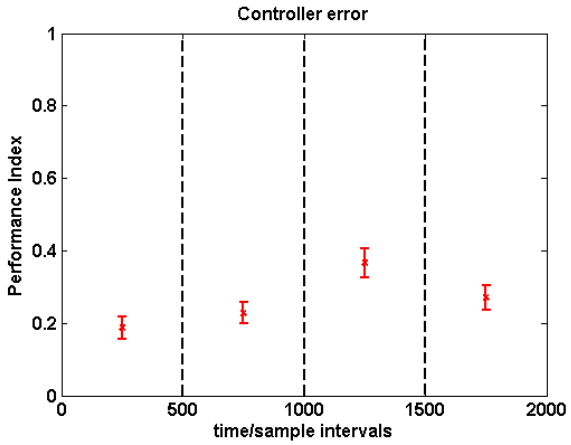

(b)

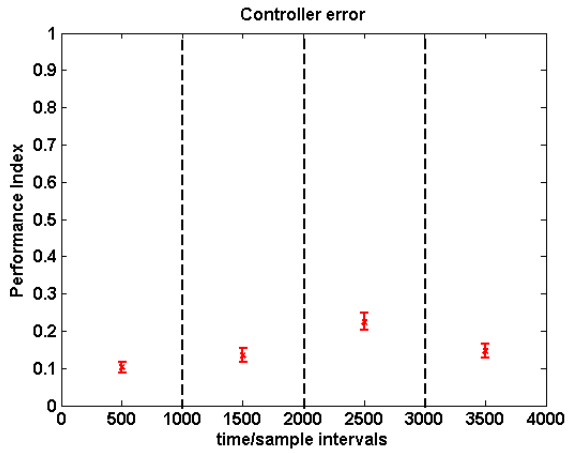

(c)

Figure 4.10: Performance index values for longer data ensembles. (a) Data ensembles of 400 samples (b) Data ensembles of 500 samples (c) Data ensembles of 1000 samples

For diagnosis of the root-cause for poor performance, the oscillation detection is firstly carried out by spectral density analysis. Power spectrum of this loop in Figure 4.11, reveals that there are two peaks, including the dominant one. Peaks in size greater than 0.1 are the indicative of oscillation at different periods. But sometimes peak,

whose power is smaller than 0.1, is a possible indicator of the oscillation and it may not be noticed visually due to lowest and highest frequencies. The magnitude of the dominant peak in Fig.4.11, is close to 0.1, so certainly there is an oscillation. By contrast, small peak having power that equals to 0.014 (just above zero) should not be ignored immediately and so low and high frequency components must be pre-filtered from the power spectrum. Filter boundary is determined considering the sampling frequency and total recorded samples. Moreover, filter type is chosen as finite-impulse-response (FIR), which is designed by use of Parks-McClellan iterative algorithm. The filtered power spectrum is illustrated in Fig.4.12 and it is also agree with Figure 4.12.

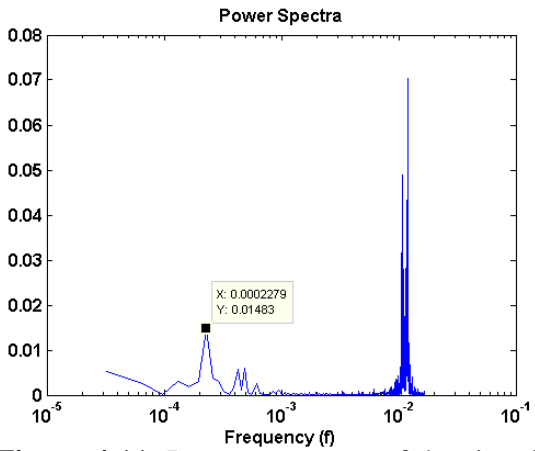

Figure 4.11: Power spectrum of the signal.

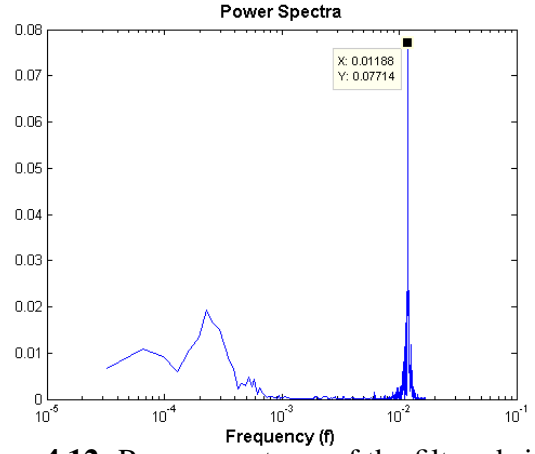

Figure 4.12: Power spectrum of the filtered signal.

The oscillation can be detected by visual inspection of spectra, but the characteristics of oscillation such as period and regularity can not be determined clearly. Also, difficulties have been encountered in the use of power spectrum in an automatic manner, even though providing good benefits visually. Once the oscillation is observed by power spectrum, the detection of oscillation should also be supported

by the methods based on ACF function or time-domain. The representation of ACF of pre-filtered power spectrum is given in Figure 4.13(a) and zero-crossings are distributed on a regular basis as illustrated by red points in Figure 4.13(b). The values of oscillation measures are provided as in Table 4.2. Decay ratio and oscillation index are above the threshold and regularity is close to the threshold for decision. All of the measures indicate that control loop shows an oscillating behaviour and period is compatible with frequency where the dominant peak is situated at 0.01188 Hz(84.175 s).

Table 4.2: Oscillation indices for Loop 1-Flow control loop

Decay Ratio(R_{ACF})	**Regularity(r)**	T_{period}**(s)**	**Oscillation index(h)**
0.9605 (threshold:0.5)	0.9875(threshold:1)	84.4246	0.7487(threshold:0.4)

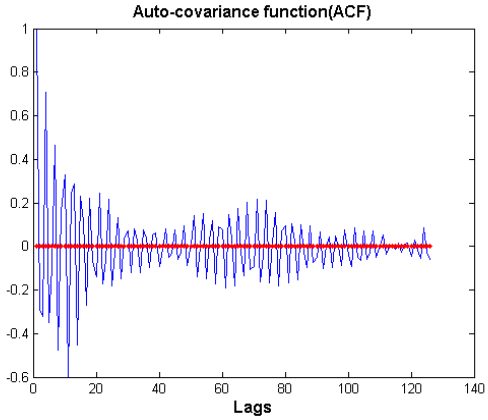

(a)

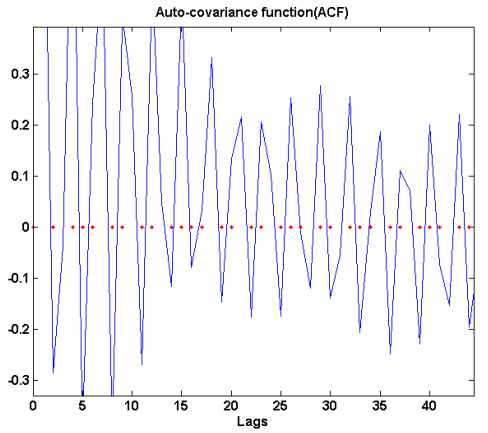

(b)

Figure 4.13: Auto-Covariance Function. (a) ACF (b) Regularity of the ACF

After the determination of the oscillation, the effect of nonlinearity on oscillation

is investigated. Nonlinearity analysis is performed with bicoherence function, in Figure 4.14, and surrogate data, in Figure 4.15.

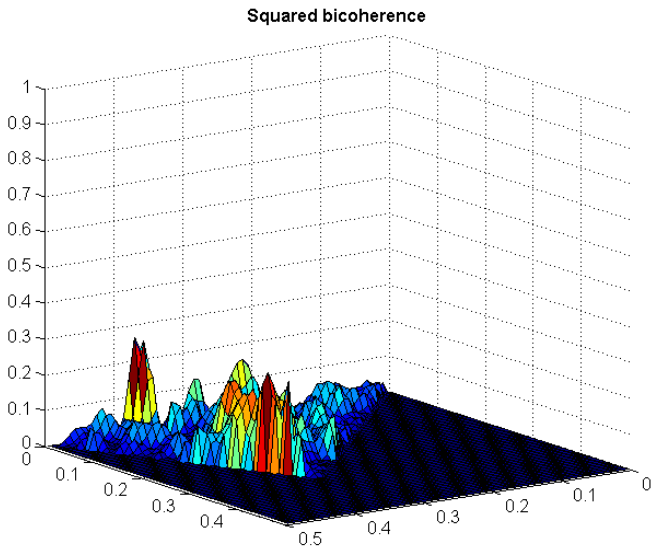

Figure 4.14: Bicoherence function in the principal domain.

Bicoherence function shows the interaction between frequency and the high interaction at which pair frequency is represented in red. Strong interactions in two bifrequencies proceeding from two different faults are available in bispectrum. The nonlinearity indices, given in Table 4.3 are utilized from the squared bicoherence value and surrogate data. When NGI is greater than zero, signal is non-Gaussian at a confidence level of 0.05. Also, when NLI is greater than zero, the signal generating process is non-linear. NPI is calculated based on distribution of surrogate data and if NPI is >1, the process is specified as nonlinear.

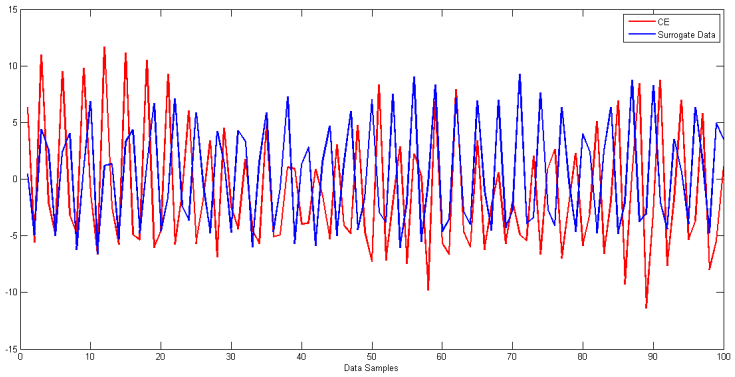

Figure 4.15: Time trend of the surrogate data.

All of the nonlinearity indices are concluded that the flow control loop is detected as nonlinear. Nonlinearity may be arised from problems in valve, controller parameter

Table 4.3: Nonlinearity indices for Loop 1-Flow control loop

Data Batch	NGI	NLI	TNLI	NPI
3000 samples	0.0516	0.1035	20.2348	1.8989

settings or external disturbances. One of the main valve problem is the stiction and it usually gives rise to the nonlinearity. To diagnose the stiction of valve, the stiction index is computed by curve-fitting method. The obtained sinusoidal and triangular fittings are presented in Figure 4.16(a), 4.16(b) and Table 4.4.

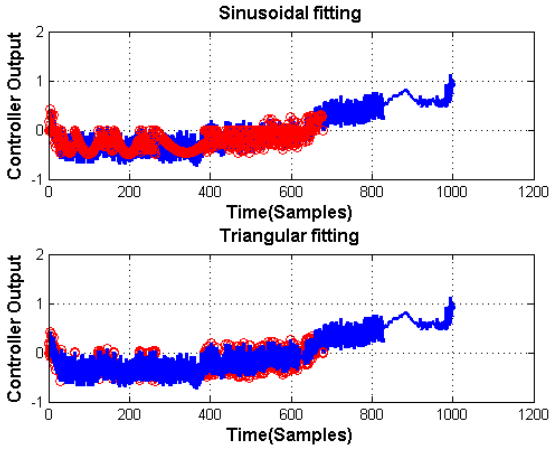

(a)

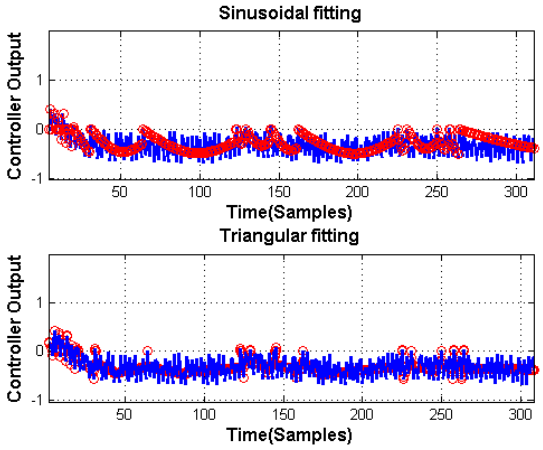

(b)

Figure 4.16: Curve fitting method. (a) All raw data (b) Some of the data after filtering

The value of stiction index 0.5437 is between 0.4 and 0.6 which means that the presence of stiction is undetermined.

Analysis of this data detected oscillation and also nonlinearity. Tuning of the controller parameters is the most likely source of the oscillation in this case. However, the

Table 4.4: Mean square error of curve fitting- Loop 1

Data Batch	MSE_{sin}	MSE_{tri}	Stiction Index
1st data batch	0.0122	0.0102	0.5437(threshold:0.6)

oscillation may be caused by multiple sources such as controller parameter settings and valve stiction or another valve problems.

4.3 Loop 2- Flow Control Loop

The plot which attempted to choose the sampling interval of Loop 1 will be repeated for all other loops. Figure 4.17(a) and 4.17(b) show the estimated impulse response of Loop 2 at 30 s and 60 s. The estimated impulse responses from 30 s and 60 s are captured within 20-25 samples and 5-7 samples, respectively. It should be used the sampling time that is shorter than 30s.

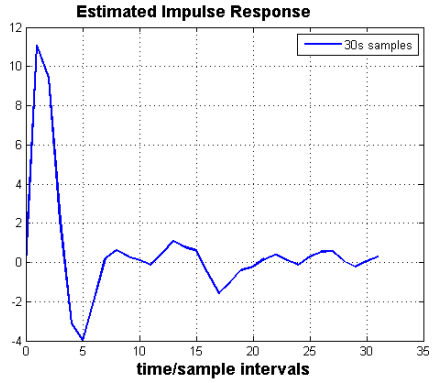

(a)

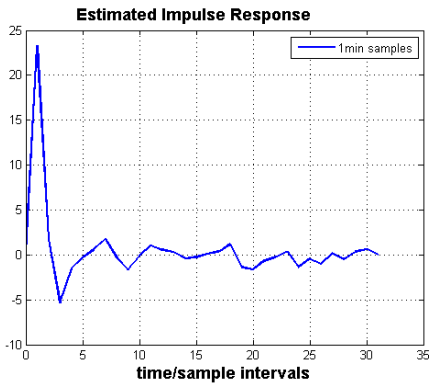

(b)

Figure 4.17: Estimated impulse response plots. (a) for Loop 2 with 30s samples (b) for Loop 2 with 60 sec samples

Another parameter needs to be determined is time delay. Cross-correlation method provides consistent value as 1 sample lag, shown in Figure 4.18(a). Besides, extended prediction horizon plots in Figure 4.18(b), give the 5 sample intervals for each data

batch that is greater value than actual time delay. Flow control loop where the process variable responses quickly due to a change in manipulated variable should have 1 sample lag. The first two studied cases have the same dead time, and so 1 sample lag is accepted as the generic value for dead time estimate of all flow control loops in refinery.

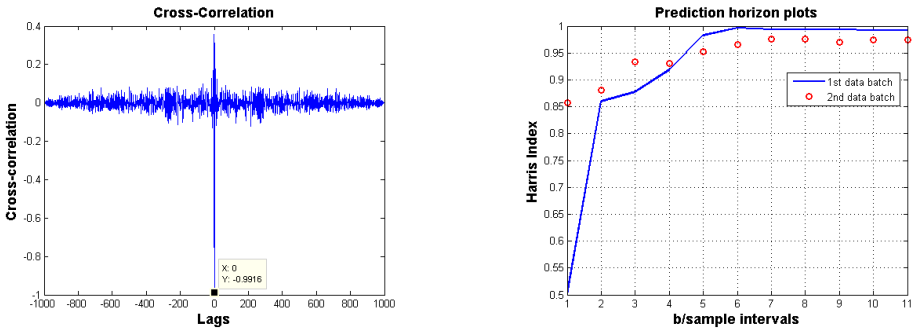

(a) (b)

Figure 4.18: Methods for time delay estimates (a) Cross-correlation plot for Loop 2. (b) Extended prediction horizon plots for 30s samples.

Another parameter to be taken into consideration is the data ensemble length. Time trend of controller error in Loop 2 is shown in Figure 4.19. A brief part of disturbance is occurred between samples 1550 and 1600 due to set-point change. The optimum value of this parameter for Loop 2 is specified with the examination of changes in performance index for data ensembles of 500, 700 and 1000, as given in Figure 4.20(a), 4.20(b) and 4.20(c). The set-point change at sample 1598 leads to quite large performance index for three data ensemble length. The performance indices of 500 samples and 1000 samples including the abrupt change are calculated as 0.8316 with 0.040 standard deviation and 0.7810 with 0.0210 standard deviation, respectively. It is concluded that shorter data batches are more sensitive to the disturbances even though reasonable results are obtained. When working with data size of 1000 samples, it has decreased deviation of changes in the performance index and abrupt changes such as set-point change and external disturbance can be noticeable. However, 500 and 700 samples can also be used.

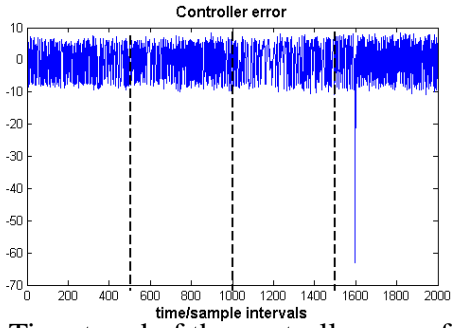

Figure 4.19: Time trend of the controller error from Loop 2.

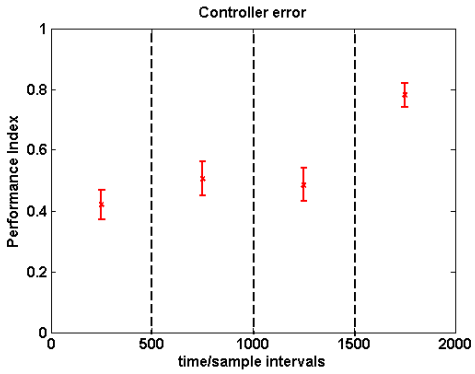

(a)

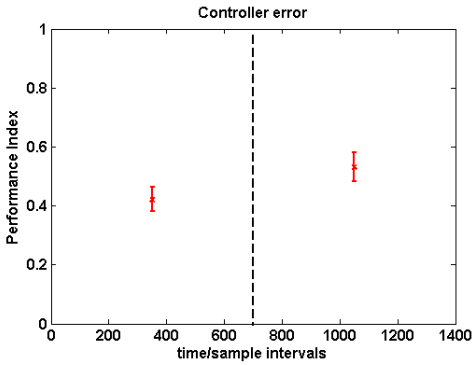

(b)

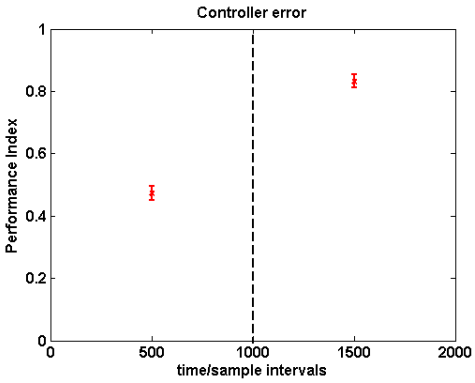

(c)

Figure 4.20: Performance index values for longer data (a) Data ensembles of 500 samples (b) Data ensembles of 700 samples (c) Data ensembles of 1000 samples.

After all parameters required for index calculation are specified, the performance index

is found by two algorithm, results given in Table 4.5. Poor control performance is detected based on the performance index.

Table 4.5: Performance indices for Loop 2-Flow control loop

Parameters	
Data Batch	1000 samples
Model Order	30
Time Delay(s)	30
Sampling Interval(s)	30
Performance Indices	
FCOR	0.4722
Harris index	0.5009

When judged that controller shows poor performance, analysis is continued with oscillation detection by performing the spectral density analysis. Besides the power spectrum of signal, in Figure 4.21, power spectrum of filtered signal is analyzed as in Figure 4.22. It is concluded that there is no oscillation in Loop 2.

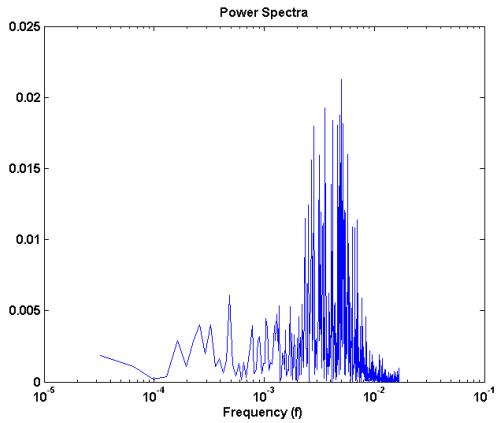

Figure 4.21: Power spectrum of the signal.

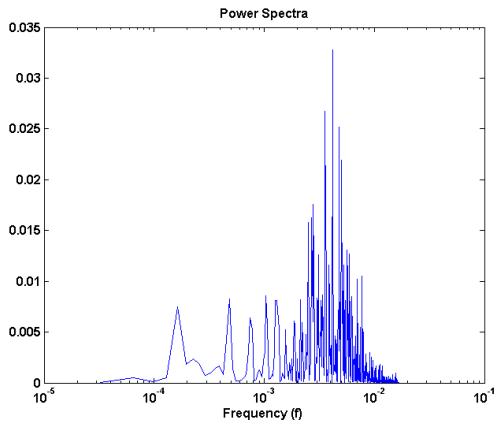

Figure 4.22: Power spectrum of the filtered signal.

The result obtained by power spectrum is confirmed by decay ratio and regularity factor which are given in Table 4.6. Conversely, the oscillation detection has failed, when the oscillation index depending on the method of Forsmann and Stattin method is observed. In the case, oscillation index is larger than threshold due to the fact that the control error signal is corrupted by noise. In order to eliminate the effect of noise, it should be utilized from the smoothing filter in time-domain. Savitzky-Golay filter is designated as smoothing filter to protect the location of peaks in data trend. After filtering, the oscillation index is obtained as 0.2921. According to oscillation measures, the process has not oscillating behaviour.

Table 4.6: Oscillation indices for Loop 2-Flow control loop

Decay Ratio(R_{ACF})	**Regularity(r)**	**Oscillation index(h)**
0.5045(threshold:0.5)	0.3886(threshold:1)	0.4265(threshold:0.4)

In the case of process without oscillation, it is usually examined for controller tuning problems or external disturbances instead of nonlinearity analysis. Sometimes valve problems may not lead to oscillation and nonlinearity. Therefore, whether the valve has stiction problem, nonlinearity and stiction analyzes are carried to find out. Nonlinearity analysis is performed with bicoherence function, in Figure 4.23, and surrogate data, in Figure 4.24.

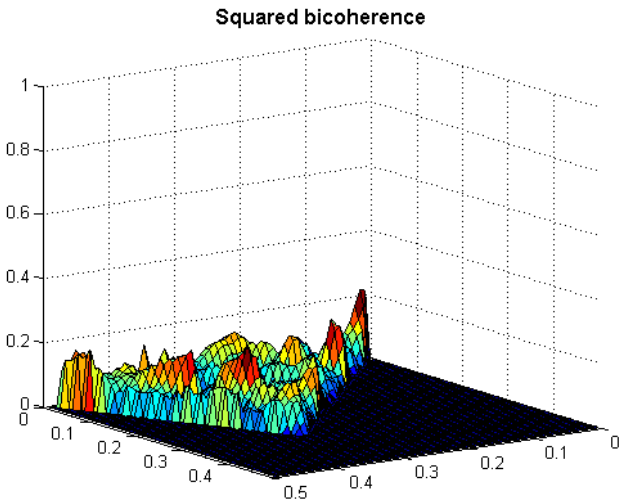

Figure 4.23: Bicoherence function in the principal domain for Loop 2.

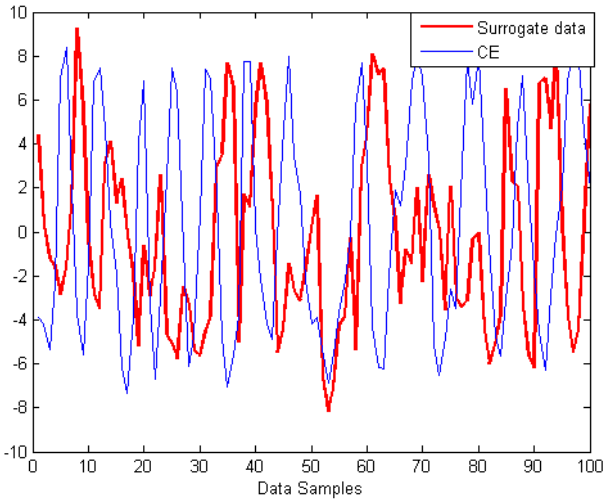

Figure 4.24: Time trend of the surrogate data for Loop 2.

The nonlinearity indices based on the bicoherence function and surrogate data are presented in Table 4.7. Considering the NGI, NLI and TNLI indices, it can be assumed that the process is nonlinear. Otherwise, surrogate data analysis can not be performed because it requires the characteristics of the oscillation. Whereas, based on the earlier studies, the surrogate analysis points out the real analysis and NPI is a better measure. Thus, it can not reach a definite conclusion about the nonlinearity.

Table 4.7: Nonlinearity indices for Loop 2-Flow control loop

Data Batch	**NGI**	**NLI**	**TNLI**
1000 samples	0.0741>(threshold:0)	0.0768>(threshold:0)	76.2911

Generally, when the signal is assumed oscillating, it is considered to be stiction in the valve. In this case, stiction is detected by curve-fitting method without oscillating behaviour. Fitted sinusoidal and triangular functions are demonstrated in Figure 4.25(a) and Figure 4.25(b).

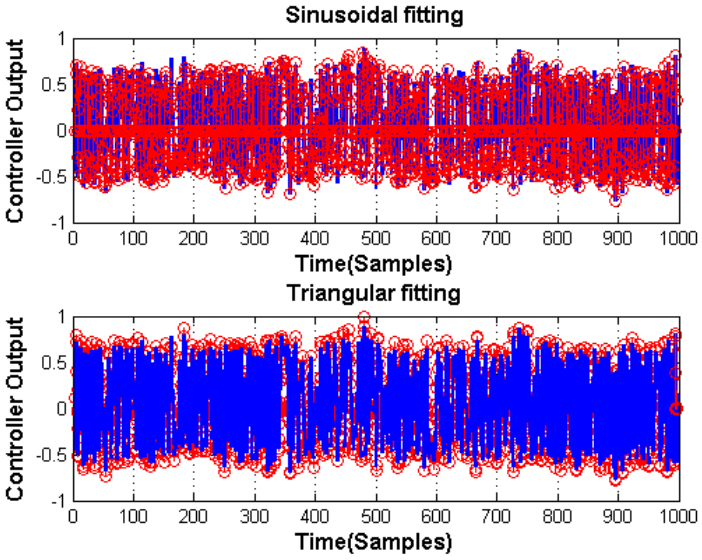

(a)

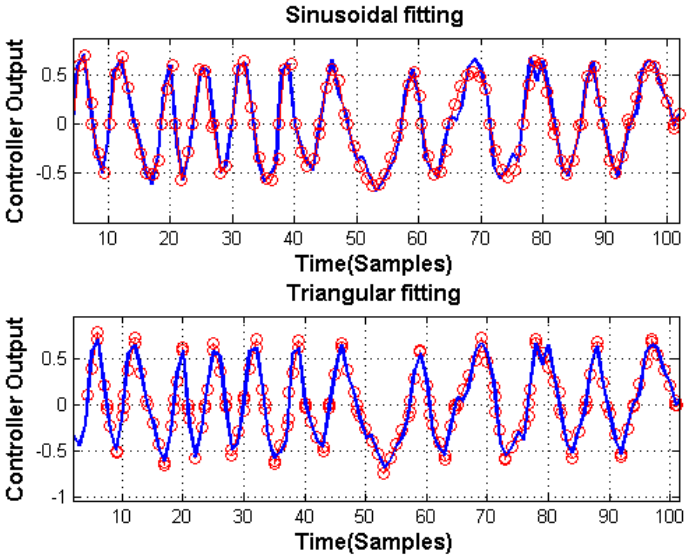

(b)

Figure 4.25: Curve fitting method for Loop 2. (a)All raw data (b) Some of the data

The computed mean square error of curves and stiction index are as given in Table 4.8. The value of stiction index 0.6525 is greater than the threshold value 0.6.

Table 4.8: Mean square error of curve fitting- Loop 2

Data Batch	MSE_{sin}	MSE_{tri}	**Stiction Index**
1st data batch	0.0152	0.0081	0.6525(threshold:0.6)

According to the literature, if the oscillation is not detected, the most likely problems in control loop are controller parameter settings and external disturbances. As a result, poor performance is due to the controller parameters of this controller. Although the stiction in valve needs to be examined since it is concluded that there might be stiction

in the valve. Therefore, analysis based on the Hammerstein model should be carried out to arrive at the right decision about root-cause.

4.4 Loop 3- Temperature Control Loop

The sampling interval is primarily chosen for performance assessment. Figure 4.26(a), 4.26(b) and 4.26(c) show the estimated impulse response of Loop 3 at 1 min, 2 min and 4 min. For 1 min sampling, the estimated impulse response cannot reach the steady-state within 30 samples. Meanwhile, the estimated impulse response from 2 min is captured within 20-25 samples and so, the sampling interval should be between 1 min and 2 min sampling.

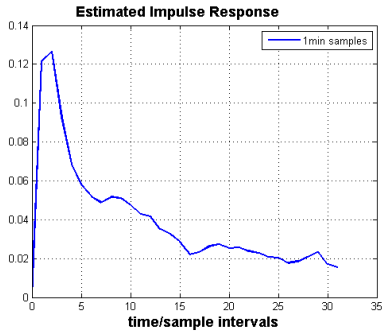

(a)

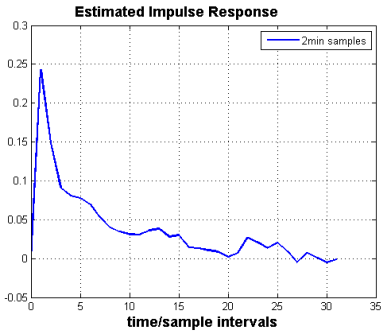

(b)

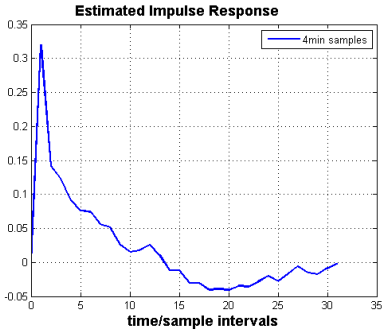

(c)

Figure 4.26: Estimated impulse response plots. (a) for Loop 3 with 1 min samples (b) for Loop 3 with 2 min samples (c) for Loop 3 with 4 min samples

Another parameter needs to be determined is time delay. Time delay values estimated by cross-correlation method in Figure 4.27(a) and 4.27(b), varies by data batches. That is the reason why the time delay value for temperature control loop is determined by extended horizon prediction plots as presented in Figure 4.28(a) and 4.28(b). The graphics are formed by 60s data samples and 120s samples. It can be seen that the estimated dead time is inversely proportional to the sampling interval. 8 sampling

intervals and 14 sampling intervals are recommended as time delays for 120s samples and 60s samples, respectively.

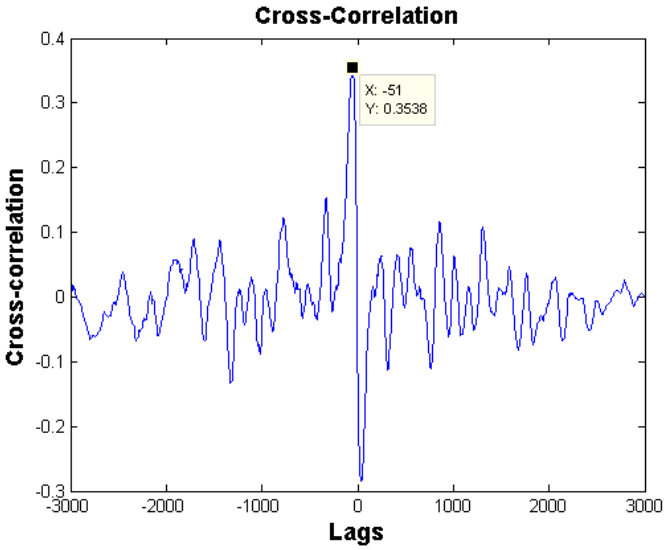

(a)

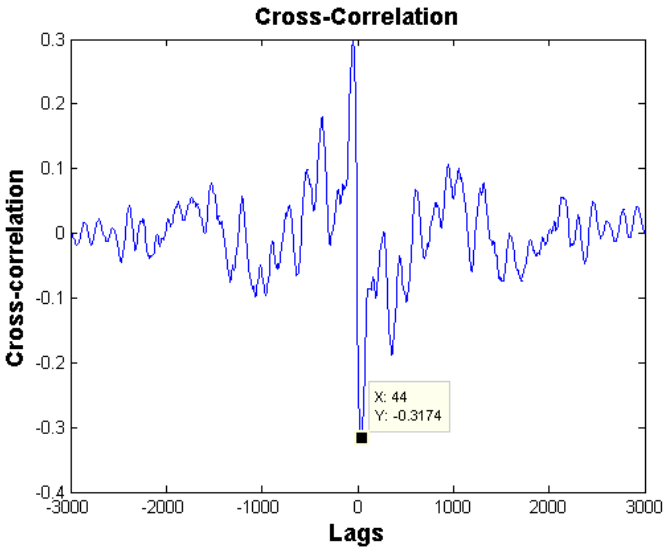

(b)

Figure 4.27: Cross-correlation plots (a) for 60s samples (b)for 120s samples

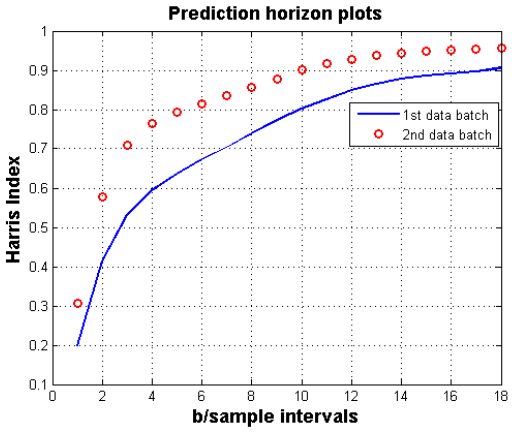

(a)

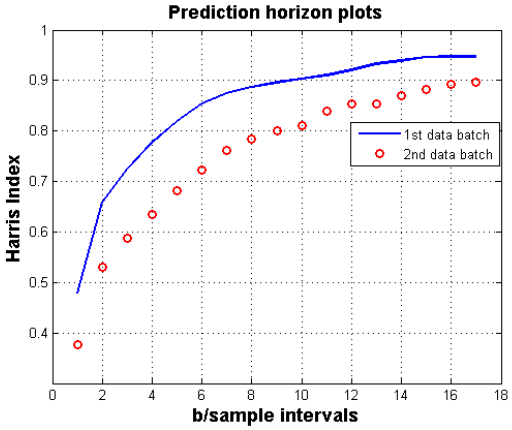

(b)

Figure 4.28: Extended prediction horizon plots for Loop 3 (a) for 60s samples (b) for 120s samples

It is aimed by the specification of data ensemble length to examine the statistical confidence of performance index which is generally increased with large data ensembles. Time trend of controller error in Loop 3 is shown in Figure 4.29.

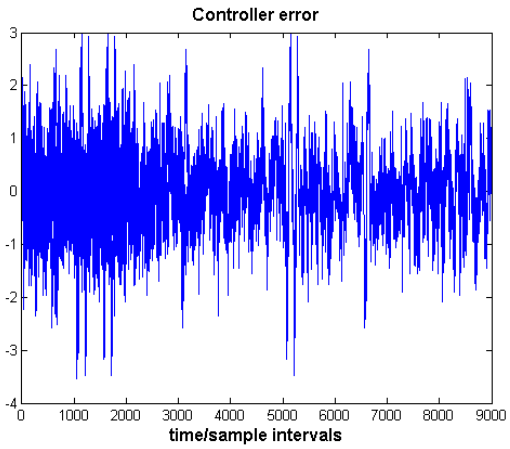

Figure 4.29: Time trend of the controller error from Loop 3.

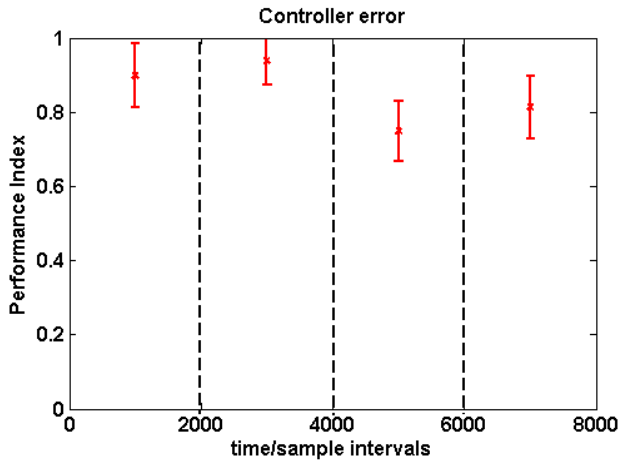

(a)

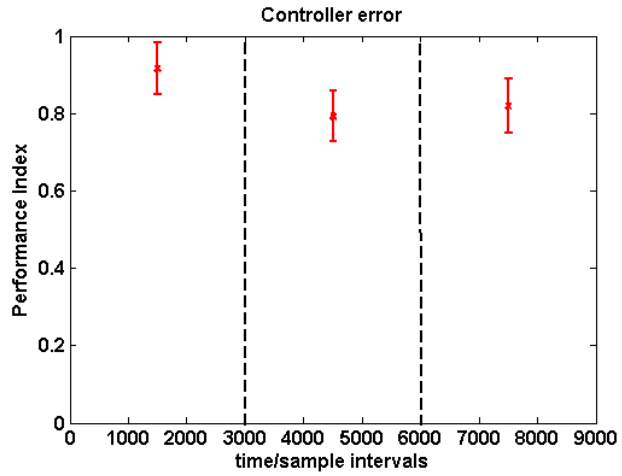

(b)

Figure 4.30: Performance index values for longer data (a) Data ensembles of 2000 samples (b)Data ensembles of 3000 samples.

Based on the collected data from Loop 3, data ensemble length is determined so as to enable both disclosure characteristic of loop and remaining within confidence limits. Thus, standard deviations and performance indices for different shorter data ensembles are studied and results are given in Figure 4.30(a) and 4.30(b). In the upper figure, the data ensembles are formed by 2000 points and in the second figure, the data ensembles are 3000 points each. The error bars for 2000 samples are larger and the error bar could exceed the maximum value of performance index which is not possible in real situation. Conversely, standard deviations for 3000 samples, which are represented by error bars are somewhat smaller. The stability of the loop response and also statistical confidence can be achieved with 3000 samples.

Once the optimum parameter values are specified, performance indices can be obtained by the use of two algorithms as in Table 4.9. It is concluded that the control loop

performance is not so bad, but it can be improved slightly.

Table 4.9: Performance indices for Loop 3-Temperature control loop

Parameters	
Data Batch	3000 samples
Model Order	30
Time Delay(s)	120 x 8 lag
Sampling Interval(s)	120
Performance Indices	
FCOR	0.7966
Harris index	0.7935

After that, detection of oscillation is carried out firstly by power spectrum in Figure 4.31(a). The bandpass filtering is applied to remove the noise effect on the data by equripple FIR filter and then power spectrum of the prefiltered signal is performed as illustrated in Figure 4.31(b). There is no peaks with the amplitude higher than 0.1. Based on ACF and time-domain, oscillation measures are calculated as in Table 4.10.

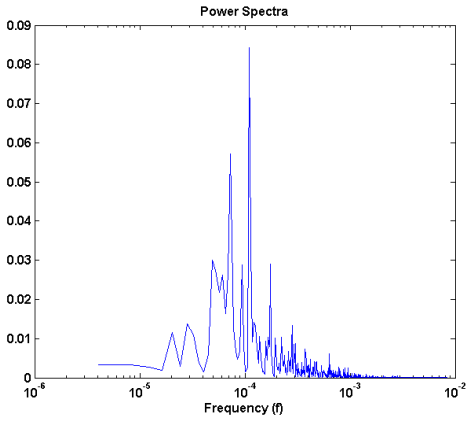

(a)

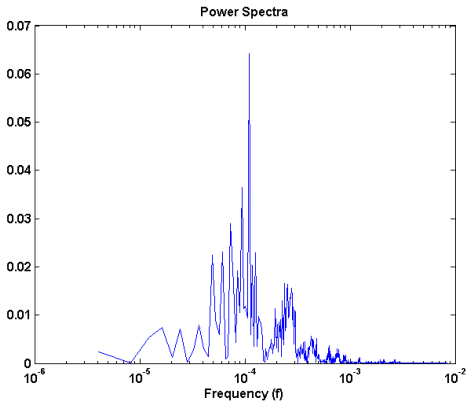

(b)

Figure 4.31: Power spectrum of. (a)the signal (b)the filtered signal.

Table 4.10: Oscillation indices for Loop 3-Temperature control loop

Data Batch	Decay Ratio(R_{ACF})	Regularity(r)	Oscillation index(h)
1000 samples	0.0380(threshold:0.5)	0.5744(threshold:1)	0.1199(threshold:0.4)

Oscillation is not detected and so the possible root-causes are tuning problems or external disturbances. Nevertheless, nonlinearity and stiction analyses are performed. Nonlinearity indices based on the bicoherence function as in Figure 4.32, are calculated and the results are shown in Table 4.11. Whereas measures have values around zero, the nonlinearity is not dominant in the control loop.

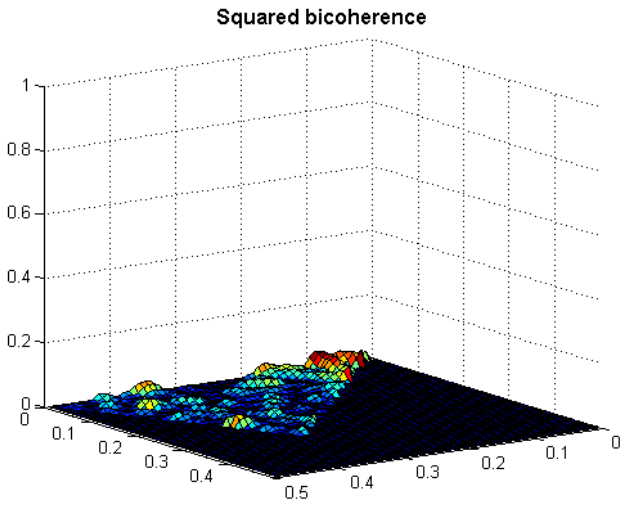

Figure 4.32: Bicoherence function in the principal domain.

Table 4.11: Nonlinearity indices for Loop 3-Temperature control loop

Data Batch	NGI	NLI	TNLI
3000 samples	0.0323>(threshold:0)	0.0287>(threshold:0)	0.0287

Afterwards, the stiction analysis is carried out by curve fitting method, represented in Figure 4.33(a), 4.33(b) and the stiction index for different data batches are shown in Table 4.12. All of the measures are above 0.6, so that the stiction is detected. However, the curve is not fitted very well so that the calculated value of the sitction index is indefensible. Thus, more detailed analysis should be performed for stiction detection.

Table 4.12: Mean square error of curve fitting-Loop 3

Data Batch	MSE_{sin}	MSE_{tri}	Stiction Index
1st data batch[1500 samples]	529.12	63.22	0.8933
2nd data batch[3000 samples]	950.50	108.77	0.8973
1st data batch[1500 filtered samples]	1294.60	139.31	0.9028
2nd data batch[3000 filtered samples]	2006.10	222.09	0.9003

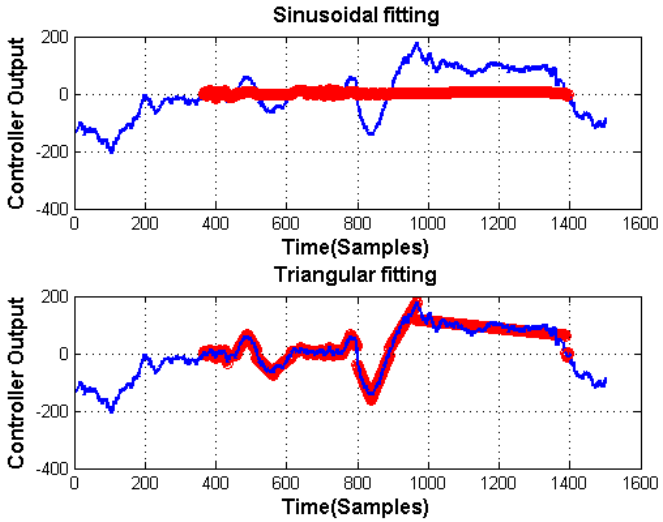

(a)

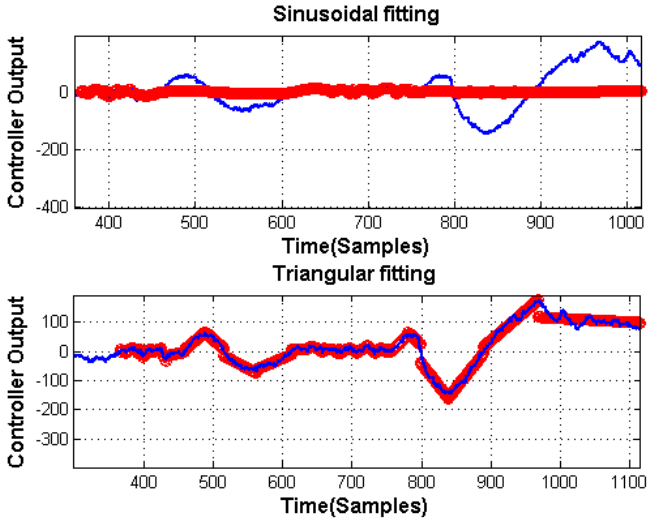

(b)

Figure 4.33: Curve fitting method for Loop 3. (a) All raw data (b)Some of the data.

The root-cause of the bad performance may be the external disturbances and therewith tuning parameters may be another cause.

4.5 Loop 4- Level Control Loop

To construct the AR model for performance monitoring, first, the sampling interval should be specified. Figure 4.34(a), 4.34(b), 4.34(c) and 4.34(d) show the estimated impulse response of Loop 1 at 1, 2, 3 and 11 min and only the estimated impulse response from 11 min is captured within 30 samples. These values may seem too long, but changes in the level are noticeable after a long time in the system.

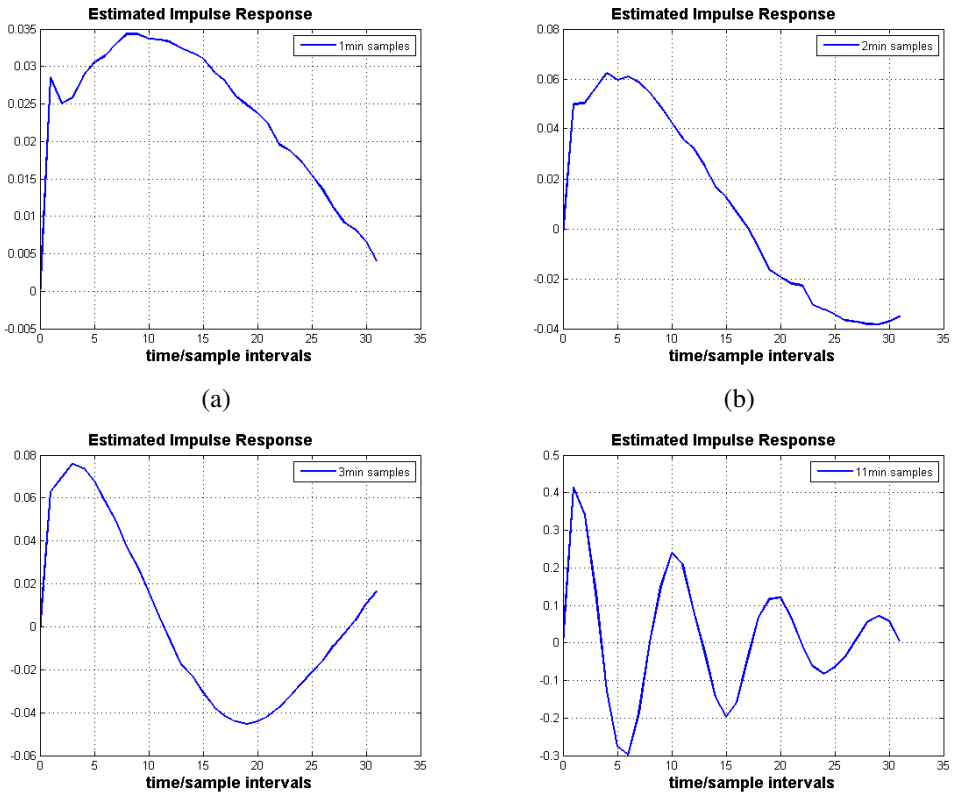

Figure 4.34: Estimated impulse response plots. (a) for Loop 4 with 1 min samples (b) for Loop 4 with 2 min samples (c) for Loop 4 with 3 min samples (d) for Loop 4 with 11 min samples

Time delay values estimated by cross-correlation method in Figure 4.35(a) and 4.35(b) vary by data batches. Time delay value for temperature control loop is determined by extended horizon prediction plots for each data batches as presented in Figure 4.36(a), 4.36(b) and 4.36(c). Even if different data ensembles which contain disturbances and set-point changes are used, changes in prediction horizon are similar. 8 and 14 sampling intervals are respectively recommended as time delays for 180s samples and 120s samples, respectively. Since dead time values are proportional to the time sampling, the dead time estimate of 60s samples must be greater than 14 sampling intervals.

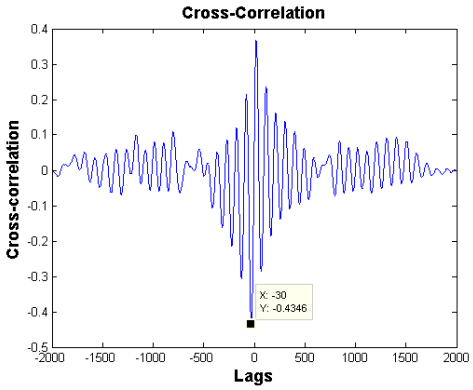

(a)

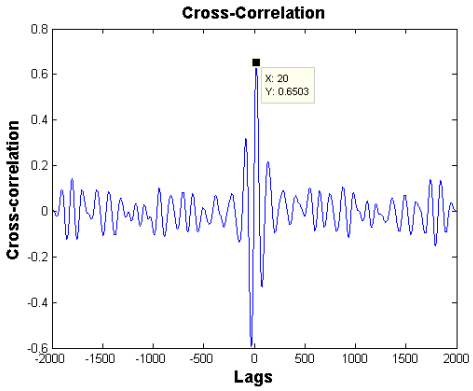

(b)

Figure 4.35: Cross-correlation plots (a) for 1min samples (b) for 2min samples

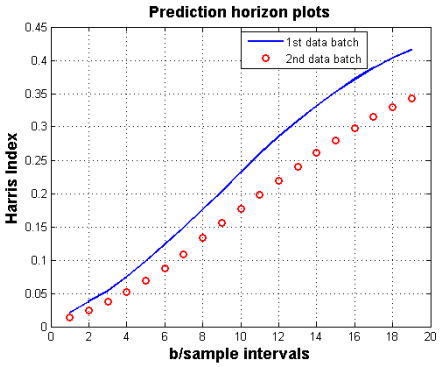

(a)

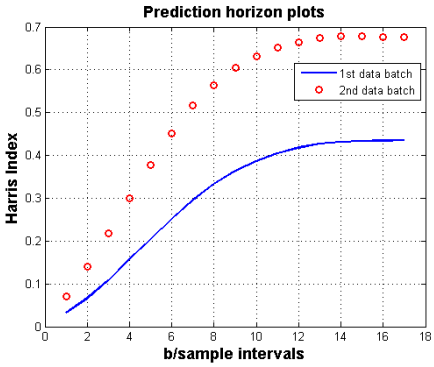

(b)

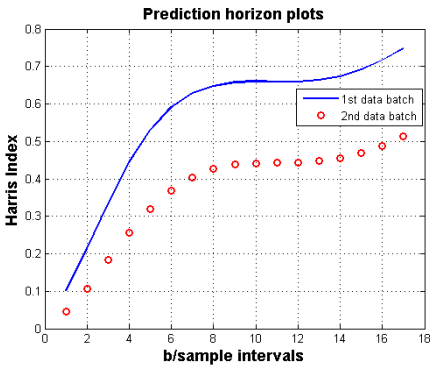

(c)

Figure 4.36: Extended prediction horizon plots of Loop 4 (a) for 60s samples (b) for 120s samples (c) for 180s samples

It is aimed by the specification of data ensemble length to examine the statistical confidence of performance index. Time trend of controller error in Loop 4 is shown in Figure 4.37. In the first and last data ensembles of 3000 samples, a disturbance appears in the trend.

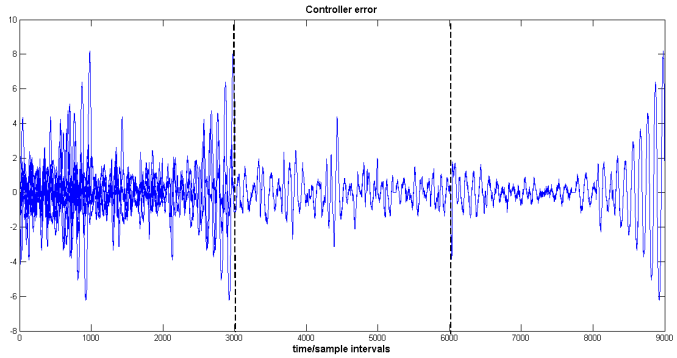

Figure 4.37: Time trend of the controller error from Loop 4.

Standard deviation of performance index for 1000, 2000 and 3000 samples are studied and results are given in Figure 4.38(a), 4.38(b) and 4.38(c). The upper figure is generated by 1000 points and the error bars for 1000 samples are quite large. Also performance index takes value greater than 1 which is not expected in real situation. The standard deviations of data ensemble of 2000 samples are more sensitive to disturbances in the trend. Conversely, it is possible to cancel out the stability of the loop response and statistical confidence with 3000 samples.

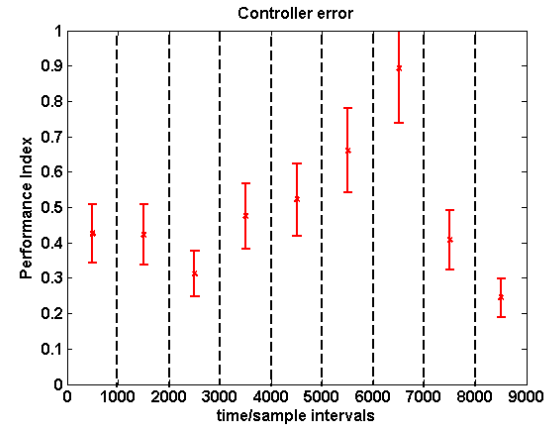

(a)

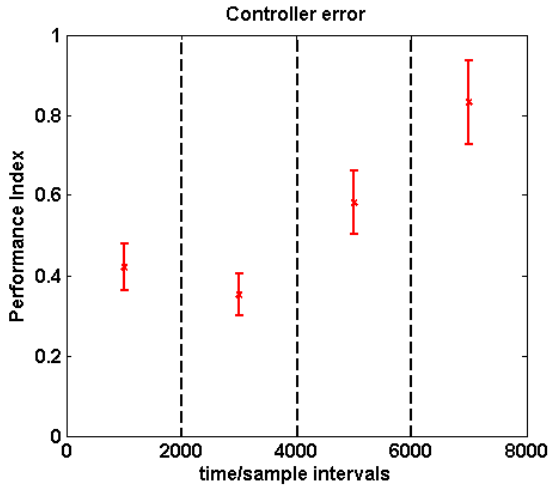

(b)

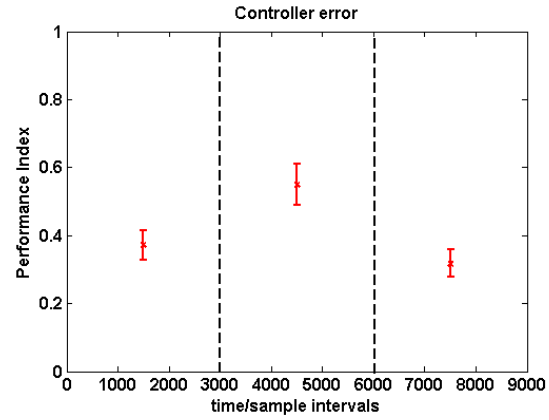

(c)

Figure 4.38: Performance index values for longer data (a) Data ensembles of 1000 samples (b) Data ensembles of 2000 samples (c) Data ensembles of 3000 samples

After all parameters required for index calculation are specified, the obtained performance index values are given in Table 4.13. Poor control performance is detected with respect to performance index.

Table 4.13: Performance indices for Loop 4-Level control loop

Parameters	
Data Batch	2000 samples
Model Order	30
Time Delay(s)	60 x 19 lag
Sampling Interval	>3min
Performance Indices	
FCOR	0.1421
Harris index	0.1203

The oscillation detection is firstly carried out by power spectrum of this loop in Figure 4.39. It reveals that there is a strong oscillating frequency. Owing to the fact that low frequency oscillations may be suppressed by frequency components, the data is filtered by band-pass FIR filter in the frequecny range of [0.0013,0.9934]Hz. Boundaries of the equiripple filter are determined taking into account the sampling frequency and the length of collected data set. The pre-filtered power spectrum is illustrated in Figure 4.40.

Table 4.14: Oscillation indices for Loop 4-Level control loop

Decay Ratio(R_{ACF})	**Regularity(r)**	**Period(min)**	**Oscillation index(h)**
0.7973>(threshold:0.5)	7.9360>(threshold:1)	93	0.1452<(threshold:0.4)

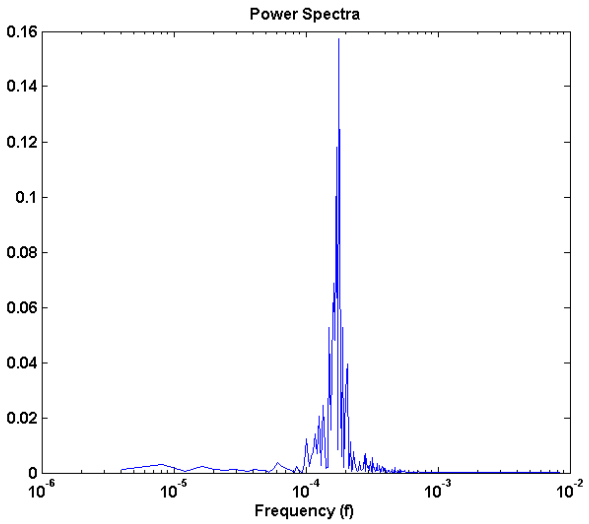

Figure 4.39: Power spectrum of the signal.

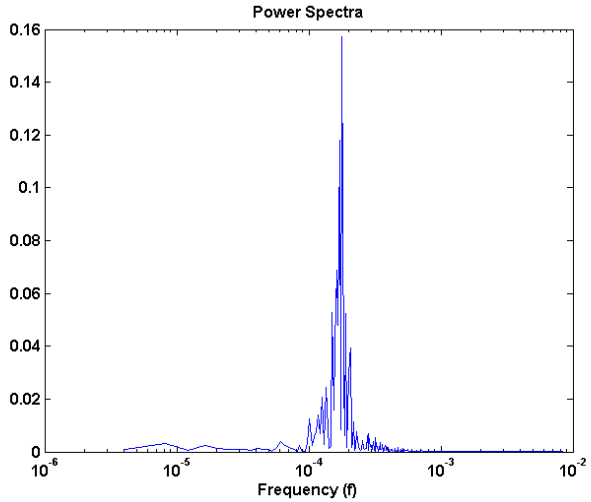

Figure 4.40: Power spectrum of the filtered signal.

Then oscillation index values are computed by ACF using pre-filtered data. Oscillation period is compatible with frequency where the dominant peak is situated at 0.000179 Hz. The measures except oscillation index agree with power spectrum. Oscillation index can be influenced by the noise and the smoothing filter whose type specified as Savitzky-Golay is applied so as to remove the effect of the noise. Afterwards, the oscillation index has a value of 0.3085, close to the threshold.

Once the oscillation is detected which nonlinearity and stiction analyses are repeated. Nonlinearity indices based on the bicoherence function as in Figure 4.41, are calculated and the results are shown in Table 4.15. NGI, NLI and TNLI indices are above the zero value and the process has a strong nonlinearity which designated by NPI much greater than 1.

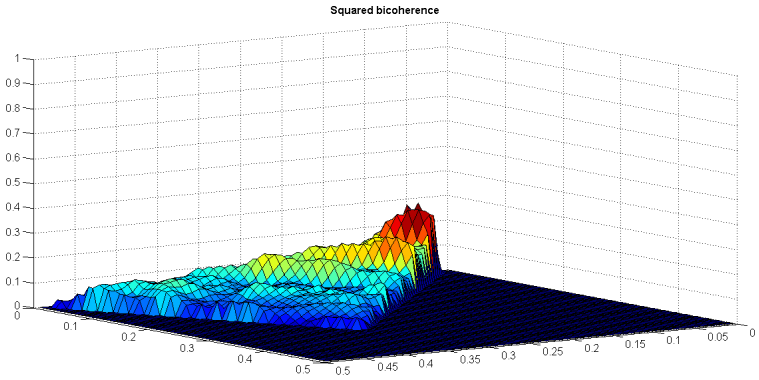

Figure 4.41: Bicoherence function in the principal domain.

When judged that controller shows oscillating behavior, stiction in valve should be detected by performing the curve fitting method, in Figure 4.42(a) and 4.42(b).

Table 4.15: Nonlinearity indices for Loop 4-Level control loop

Data Batch	NGI	NLI	TNLI	NPI
3000 samples	0.0863	0.1160	103.0324	5.20

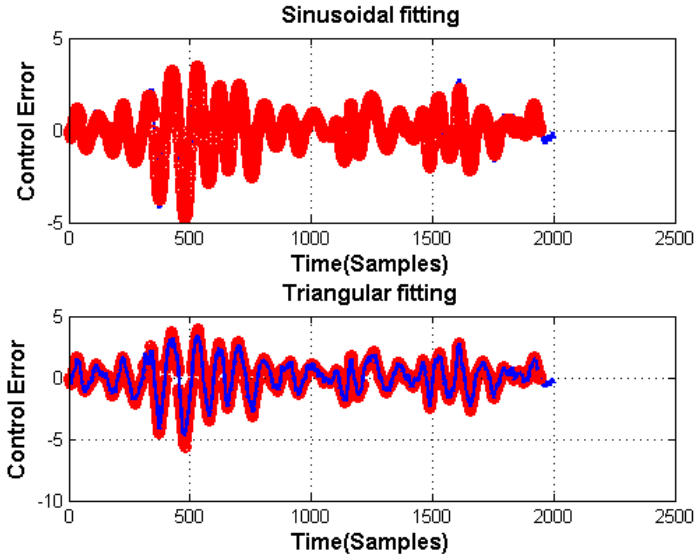

(a)

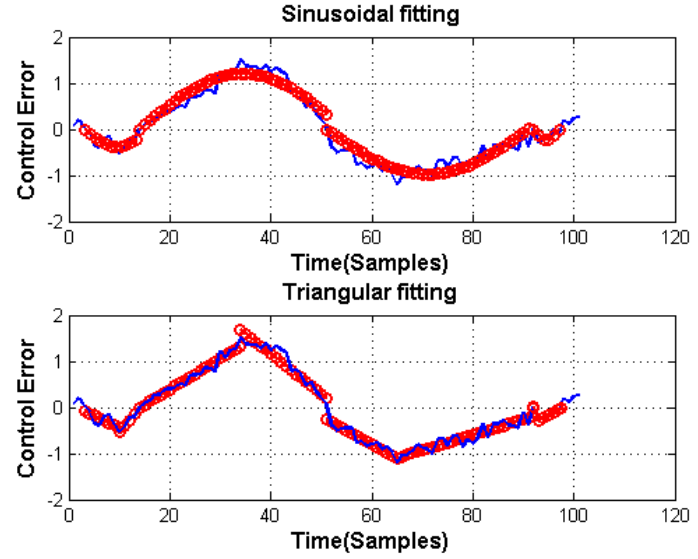

(b)

Figure 4.42: Curve fitting method for Loop 4 (a) All raw data (b)Some of the data

All the stiction index results calculated on the basis of different data batches are demonstrated in Table 4.16. Stiction index sometimes is affected by noise, thus the effect of the pre-filtering on the stiction analysis is investigated. The stiction index is found below the threshold value of 0.4 for each data batch.

Table 4.16: Mean square error of curve fitting-Loop 4

Data Batch	MSE_{sin}	MSE_{tri}	Stiction Index
1st data batch[2000 samples]	0.0213	0.0346	0.3814
1st data batch[2000 filtered samples]	0.0282	0.0431	0.3953
2nd data batch[1000 filtered samples]	0.0373	0.0684	0.3529

The control loop has no valve stiction in the presence of nonlinearity. Thus, the main root-cause is nonlinear characteristic of the process. Possible causes related with sensor or other valve problems can also be examined.

4.6 Loop 5-Pressure Control Loop

The analysis applied for other control loops is repeated in the pressure control loop. Figure 4.43(a), 4.43(b) and 4.43(c) show the estimated impulse response of Loop 5 at 30 s, 1 min and 2 min. The estimated impulse responses from 30 s and 1 min are not captured within 30 samples and 2 min is recommended for sampling interval.

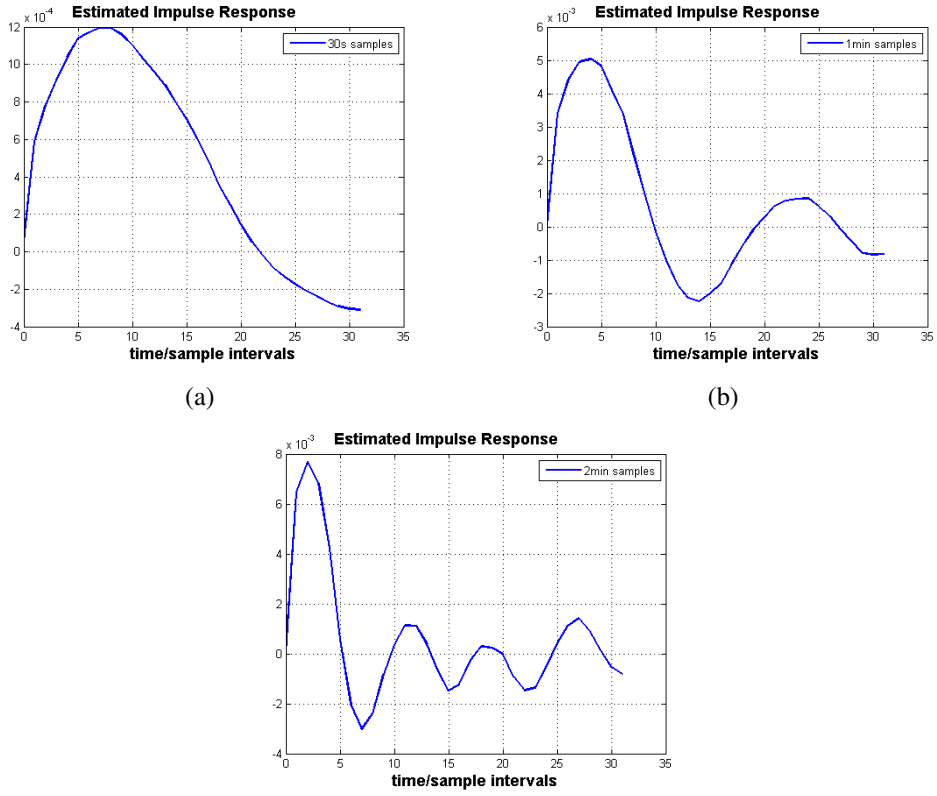

(a) (b)

(c)

Figure 4.43: Estimated impulse response plots (a) for Loop 5 with 30s samples (b) for Loop 5 with 1min samples (c) for Loop 5 with 2min samples

Time delay estimation problem is also valid for pressure control loop. Estimated time

delay values are not consistent by cross-correlation method given in Figure 4.44(a) and 4.44(b). The fair value can be obtained by the extended prediction horizon plots as given in Figure 4.45(a) and 4.45(b). The estimated values by these plots for 30s samples and 60s samples are 12 sampling interval and 6 sampling interval, respectively.

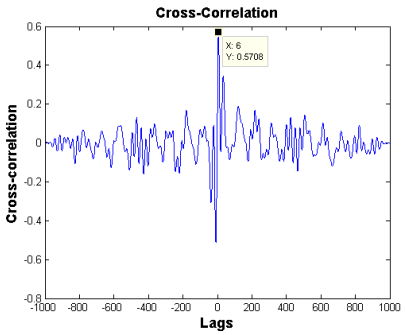

(a)

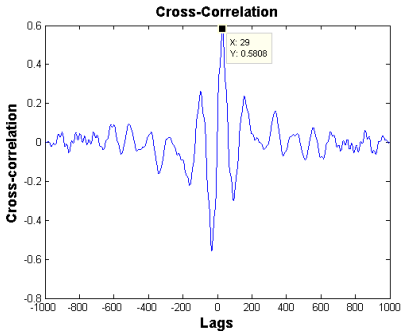

(b)

Figure 4.44: Cross-correlation plots (a) for 30s samples (b) for 60s samples

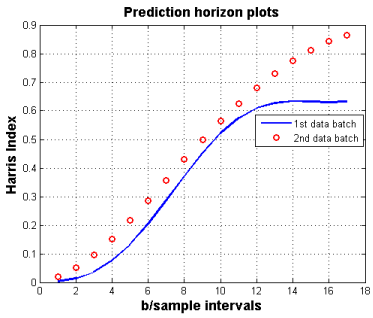

(a)

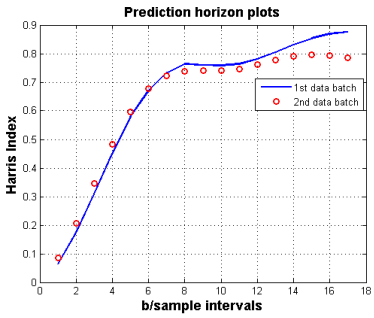

(b)

Figure 4.45: Extended prediction horizon plots of Loop 5, (a) for 30s samples (b) for 60s samples

The effect of the data ensemble length on the confidence limit of performance index is studied with different data ensemble lengths as 2000, 3000 and 3500 samples. The time trend of controller error for Loop 5 and the effect of data size worked on are presented in Figure 4.46 and Figure 4.30(a), 4.30(b), 4.47(c).

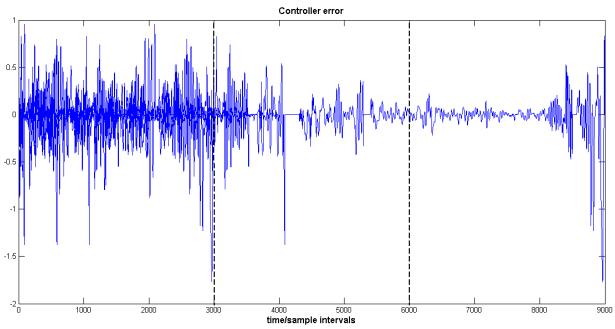

Figure 4.46: Time trend of the controller error from Loop 5.

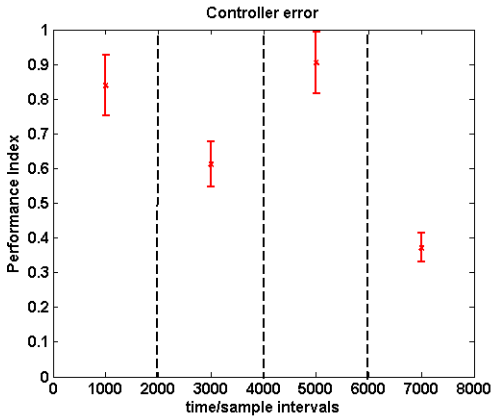

(a)

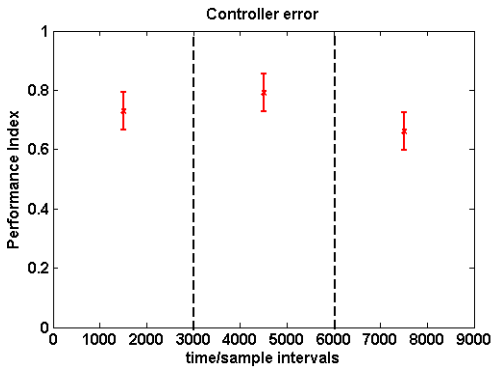

(b)

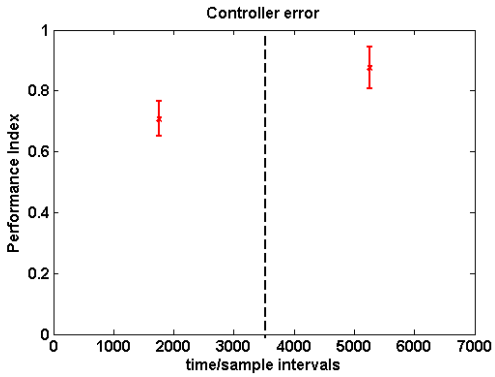

(c)

Figure 4.47: Performance index values for longer data. (a) Data ensembles of 2000 samples (b) Data ensembles of 3000 samples (c) Data ensembles of 3500 samples

When working with 3500 samples, the standard deviation is within the confidence limit of 0.05, although the change in trend cannot be captured. For instance, the performance index is 0.7074 and standard deviation is 0.0570 for the first data ensemble of 3500 samples. As for each data set index take varied values, the use of data ensembles of 2000 samples is not recommended. Therefore, the use of 3000 samples is more appropriate.

After all parameters specified, the controller performance index can be computed as in Table 4.17. It is concluded that the control loop performance is not so bad, but it can be improved slightly.

Table 4.17: Performance indices for Loop 5-Pressure control loop

Parameters	
Data Batch	3000 samples
Model Order	30
Time Delay(s)	30 x 12 lag
Sampling Interval	3min
Performance Indices	
FCOR	0.6948
Harris index	0.7011

The oscillation detection is firstly carried out by power spectra analysis of this loop in Figure 4.48(a). It reveals that two strong oscillating frequencies present which are at 0.0003255 Hz and 0.001335 Hz. Each peak value refers to a separate oscillating source, so each sharp peak should be analyzed separately. Before detailed detection, the data is pre-filtered, in Figure 4.48(b), so as to eliminate the effect of low and high frequency components. The result illustrated in Figure 4.48(b) is not confirmed by regularity and oscillation index, given in Table 4.18. The regularity of oscillations is destroyed in the presence of the multiple oscillations and this makes it difficult to analyse. To handle this problem, band-pass filter is applied by including the peaks that should be analyzed. After performing filtering in frequency domain by equripple filters, the illustrations in Figure 4.49(a) and 4.49(b) show the amplitude of the sharp peak and the frequency at where the signal is oscillating. According to the power spectral analysis, Table 4.19 and Table 4.20 list all of the measures that are computed for each dominant frequency.

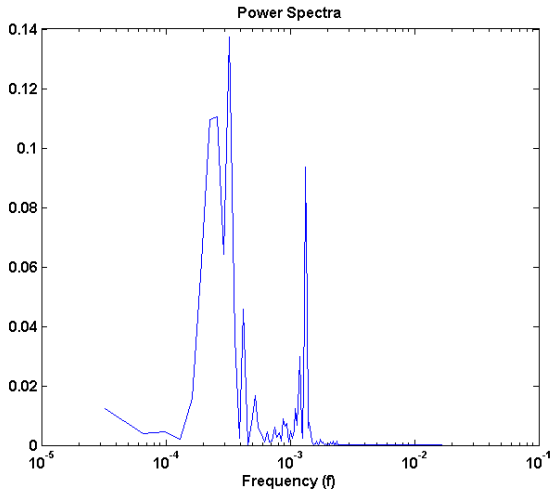

(a)

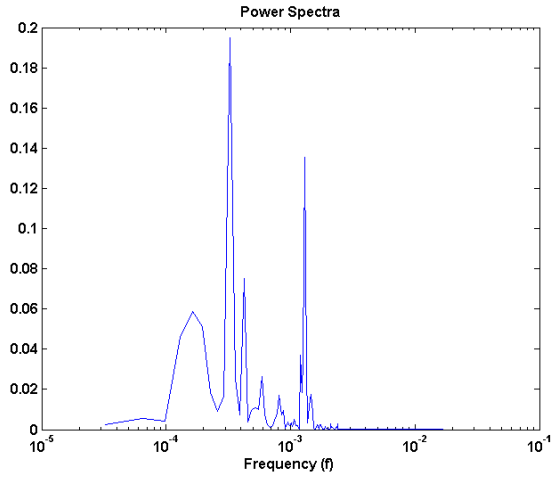

(b)

Figure 4.48: Power spectrum of , (a) raw data (b) filtered data

Table 4.18: Oscillation indices for Loop 5-Pressure control loop

Decay Ratio(R_{ACF})	**Regularity(r)**	**Period(s)**	**Oscillation index(h)**
0.8720	0.9131	758	0.2000

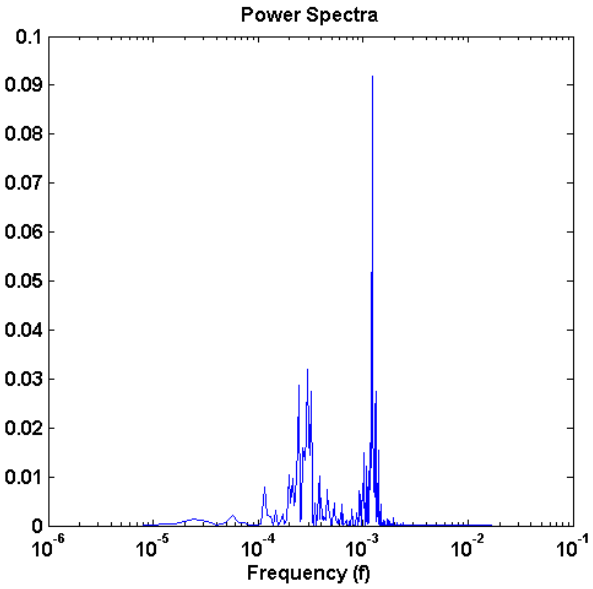

(a)

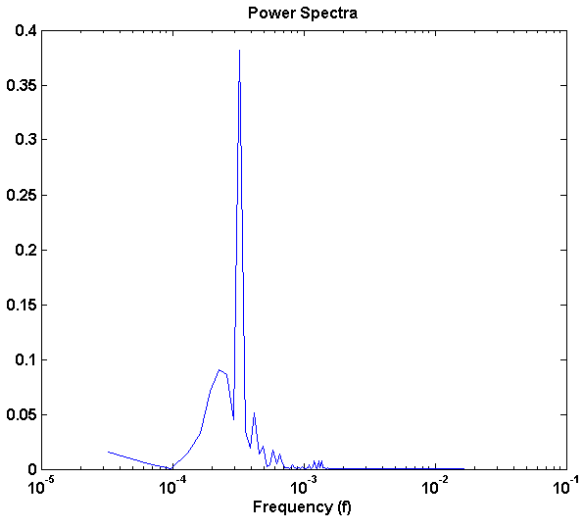

(b)

Figure 4.49: Power spectrum of , (a) raw data (b) filtered data

Table 4.19: Oscillation indices for the first peak- Pressure control loop

Decay Ratio(R_{ACF})	**Regularity(r)**	**Period(s)**	**Oscillation index(h)**
0.5291	4.1978	3117	0.2000

The data should be prefiltered in time-domain prior to index calculation by the smoothing filter and by this way, noise should be attenuated. However, the oscillation index has the value of 0.2 after filtering and this means that the method of Forsmann and Stattin cannot detect multiple oscillations properly.

Table 4.20: Oscillation indices for the second peak-Pressure control loop

Decay Ratio(R_{ACF})	Regularity(r)	Period(s)	Oscillation index(h)
0.8485	6.0045	747	0.2000

Nonlinearity and stiction analyses are repeated to find the root cause of multiple oscillations. Nonlinearity indices based on the bicoherence function given in Figure 4.50 are calculated and the results are shown in Table 4.21. Based on the indices, the process is considered to be non-Gaussian and includes nonlinear signal generating process.

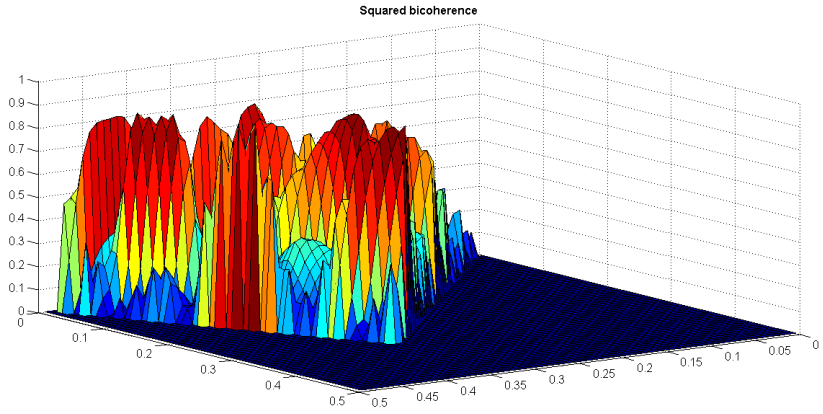

Figure 4.50: Bicoherence function in the principal domain.

Table 4.21: Nonlinearity indices for Loop 5-Pressure control loop

NGI	NLI	TNLI	NPI
0.2918>(threshold:0)	0.1690>(threshold:0)	343.7175	6.20>(threshold:1)

Afterwards, the stiction analysis is carried out by curve fitting method, represented in Figure 4.51(a) and 4.51(b). and the stiction index for various data batches are shown in Table 4.22. The effect of the noise in stiction analysis is investigated by some batches and some of them is prefiltered prior to computing the stiction index. The technique for stiction quantification must be used to arrive at the right decision. Because the stiction index above 0.4 does not have any meaning.

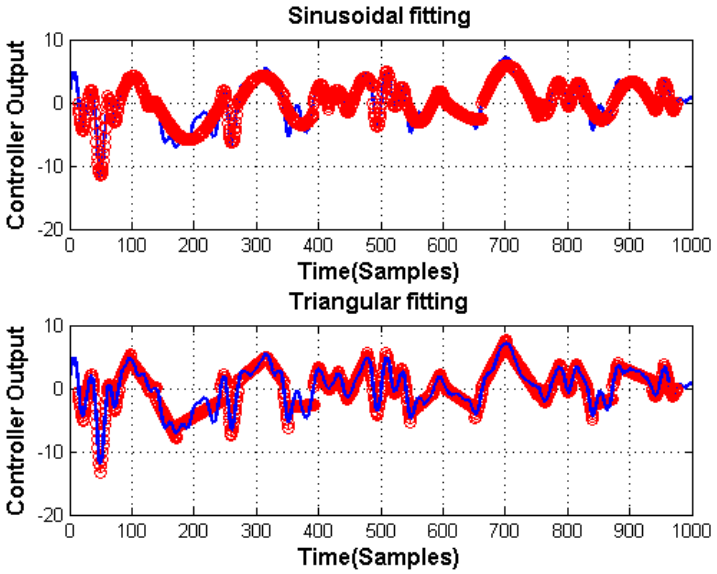

(a)

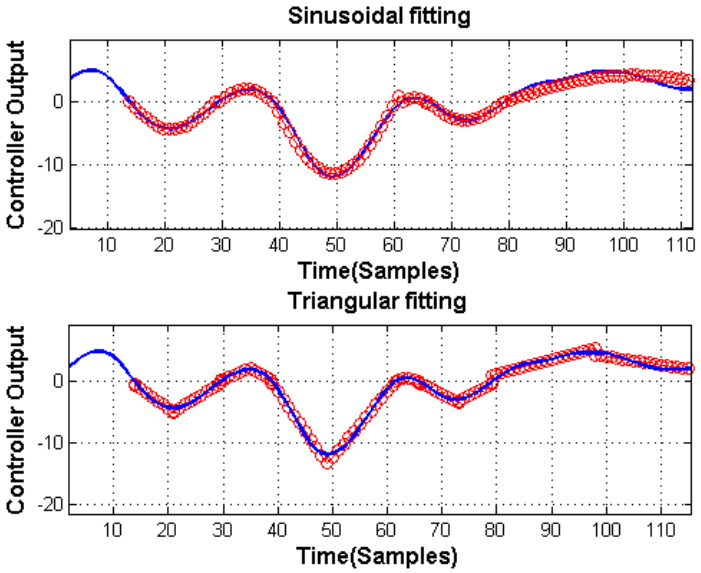

(b)

Figure 4.51: Curve fitting method for Loop 5. (a) All raw data (b) Some of the data

Table 4.22: Mean square error of curve fitting-Loop 5

Data Batch	MSE_{sin}	MSE_{tri}	**Stiction Index**
1st data batch[1000 samples]	0.5350	0.8305	0.3918
2nd data batch[2000 samples]	76.8374	9.7529	0.8874
1st data batch[1000 filtered samples]	0.5917	0.9528	0.3831

According to the analysis, the stiction is not clearly detected, a more detailed analysis should be performed for stiction detection. The possible root causes are external

disturbances and valve saturation. Besides, the oscillation can be proceeded from the process where no interference with valve until the pressure is increased to a certain value.

5. CONCLUSIONS AND RECOMMENDATIONS

The issues require further research and contributions provided by the study are discussed in this chapter.

5.1 Practical Application of the Study

Researchers working on the control proposed numerous techniques for evaluation of performance. The most widely accepted technique among them is based on comparing the performance of a minimum variance controller with the current control performance, and the performance index, called as Harris index, is defined to quantify the difference. Although various modifications of the Harris index are available in the literature, first proposed definition is used in this scope of the work. Besides Harris index, conclusive metrics are utilized for the process performance and robustness. When bad control performance is judged, the underlying root causes of poor performance are diagnosed with a large number of techniques such as oscillation, nonlinearity and stiction detection. Nonlinearity detection techniques are based on the higher-order statictics and also some techniques such as curve fitting, cross-correlation, quantification of stiction are applied to differentiate the valve stiction.

In this study, SISO refinery control loops are evaluated separately and classified in accordance with the control loop performance. First of all, the values of the parameters included in Harris index are decided. It is shown that sampling interval is insufficient for some cycles and time delay estimate has not reflect the actual value and then, the data ensemble length is determined considering the standard deviation of performance indices not exceeding the confidence limit. Performance indices of control loops are computed with the available parameters. Based on the result of performance evaluation, respectively oscillation, nonlinearity and stiction diagnostics are carried out. When the loops show both the oscillating and nonlinear behavior, stiction analysis is performed to decide whether the valve is problematic. If stiction index is low, the valve is not possible source of oscillation and the nonlinearity can be induced by

tuning, external disturbances or sensor fault. Meanwhile, the amplitude of oscillation is too small to be noticed and so performance is affected by tuning, external disturbances or both of them.

5.2 Recommendations for Further Actions

5.2.1 Time Delay Estimation

Dead time is one of the parameters to be taken into account in computing MVC based performance index. In the literature several methodologies have been proposed to estimate, although each individual technique gives different result and uselessly long delays. If the estimated value is longer than the process dead time, benchmark will no longer be the minimum variance comparison and the difference between minimum variance cannot be quantified. It should be noted that time delay is not typically estimated and process engineer informs about time delay values that should be included in performance index. Hence, the computation of time delay should be automated and close to the actual values.

5.2.2 Detail Analysis of Oscillation

The number of independent oscillations, oscillations with the same period and oscillations which have different periods can be determined by the detection techniques of oscillation. All of them may occur due to multiple faults and so some of the problems are encountered in diagnosis of root-cause. Therefore, further studies in this area should be carried out for the accurate diagnosis of faults.

REFERENCES

[1] **Brisk, M.** (2004). Process control: potential benefits and wasted opportunities, *5th Asian Control Conference*, pp.10–16.

[2] **Smith, C.** (2009). *Practical Process Control: Tuning and Troubleshooting*, Wiley.

[3] **Jelali, M.** (2012). *Control performance management in industrial automation*, Springer.

[4] **Bialkowski, W.**, (1993). Pulp & Paper Canada Magazine, volume 94, chapter Dreams vs. reality: a view from both sides of the gap, Pulp & Paper Canada, pp.19–27.

[5] **Ender, D.**, (1993). Control Engineering, volume 40, chapterProcess control performance: not as good as you think, Control Engineering Magazine, pp.180–190.

[6] **Desborough, L.** (2002). Increasing customer value of industrial control performance monitoring - Honeywell's experience, *AIChE Symposium*, volume 98 of *Series No:326*, pp.153–186.

[7] **Paulonis, M.A. , Cox, J.W.** (2003). A practical approach for large-scale controller performance assessment, diagnosis, and improvement, *Journal of Process Control*, ***13***, 155–168.

[8] **Jelali, M.** (2006). An overview of control performance assessment technology and industrial applications, *Control Engineering Practice*, ***14***, 441–466.

[9] **Ordys, A.W., Uduehi, D., Johnson, M.A.** (2006). *Process control performance assessment: From theory to implementation*, Springer-Verlag.

[10] **Qin, S.** (1998). Control performance monitoring- a review and assessment, *Computers and chemical engineering*, ***23***, 173–186.

[11] **Connor, N.O., O'Dwyer, A.** (2004). Control loop performance assessment: A classification of methods, *Proceedings of the Irish Signals and Systems Conference*, pp.530–535.

[12] **Seborg, D.E., Mellichamp, D.A.** (2004). *Process Dynamics and Control*, John Wiley & Sons.

[13] **Visioli, A.** (2006). *Practical PID Control*, Springer-Verlag, London.

[14] **Shinskey, F.** (1994). *Feedback Controllers for the Process Industries*, McGraw-Hill Professional.

[15] **Swanda, A. P., Seborg, D. E., International Federation of Automatic Control** (1997). Evaluating the Performance of PID-Type Feedback Control Loops using Normalized Settling Time, *Advanced Control of Chemical Processes -IFAC Symposium-*, Pergamon , Oxford, pp.301–306.

[16] **Swanda, A., Seborg, D.E.** (1999). Controller performance assessment based on set-point response data, *American Control Conference, 1999, San Diego, CA*, volume 6, IEEE, pp.3863–3867.

[17] **Yuwana, M., Seborg, D.E.** (1982). A new method for on-line controller tuning, *AIChE Journal*, ***28***(3), 434–440.

[18] **Rangaiah, G.P., Krishnaswamy, P.R.** (1994). Estimating second-order plus dead time model parameters, *Industrial & Engineering Chemistry Research*, ***33***(7), 1867–1871.

[19] **Horch, A., Stattin, A.** (2002). A complete practical implementation of a method for step response performance assessment, Proceedings of the IEE Seminar Control Loop Performance Assessment, London, UK, *IET Conference Proceedings*, 4–4(1), `http://digital-library.theiet.org/content/conferences/10.1049/ic_20020221`.

[20] **Hägglund, T.** (1999). Automatic detection of sluggish control loops, *Control Engineering Practice*, ***7***(12), 1505–1511.

[21] **Kuehl, P., Horch, A.** (2005). Detection of sluggish control loops-experiences and improvements, *Control Engineering Practice*, ***13***(8), 1019–1025.

[22] **Visioli, A.** (2006). Method for Proportional-integral controller tuning assessment, *Industrial and engineering chemistry research*, ***45***(8), 2741–2747.

[23] **Kozub, D.** (2002). Controller performance monitoring and diagnosis: Industrial perspective, *Proceedings of the 15th IFAC World Congress, 2002*, volume 15, Barcelona, Spain, pp.1619–1619.

[24] **Shunta, J.** (2004). *Achieving World Class Manufacturing Through Process Control*, Prentice Hall.

[25] **Astrom, K.** (1979). *Introduction to Stochastic Control*, Academic Press.

[26] **Box, G.E.P, Jenkins, G.M., Reinsel, G.C.** (1970). *Time series analysis: Forecasting and control*, Wiley.

[27] **Harris, T.** (1989). Assessment of Control Loop Performance, *The Canadian Journal of Chemical Engineering*, ***67***, 856–861.

[28] **Desborough, L., Harris, T.** (1992). Performance assessment measures for univariate feedback control, *The Canadian Journal of Chemical Engineering*, ***70***(6), 1186–1197.

[29] **Huang, B., Shah, S.L.** (1999). *Performance Assessment of Control Loops: Theory and Applications*, Advances in Industrial Control, Springer London, `http://books.google.com.tr/books?id=DCngCzLG904C`.

[30] **Box, G.E.P., MacGregor, J.F.** (1974). The analysis of closed-loop dynamic-stochastic systems, *Technometrics*, ***16***(3), 391–398.

[31] **Söderstörm, T., Stoica, P.** (1989). *System Identification*, Prentice Hall.

[32] **Goodwin, G.C., Sin, K.S.** (1984). *Adaptive filtering prediction and control*, Prentice - Hall information and system sciences series, Prentice-Hall, `http://books.google.com.tr/books?id=6tUpAQAAMAAJ`.

[33] **Chatfield, C.** (1989). *The analysis of time series: an introduction*, Chapman and Hall, London.

[34] **Desborough, L., Harris, T.** (1993). Performance assessment measures for univariate feedforward/feedback control, *The Canadian Journal of Chemical Engineering*, ***71***(4), 605–616.

[35] **Thornhill, N.F., Oettinger, M. and Fedenczuk, P.** (1999). Refinery wide control loop performance assessment, *Journal of Process and Control*, ***9***(2), 109–124.

[36] **Bezergianni, S., Georgakis, C.** (2000). Controller performance assessment based on minimum and open-loop output variance, *Control engineering practice*, ***8***, 791–797.

[37] **Shinskey, F.** (1996). *Process Control Systems: Application, Design, and Tuning*, Chemical engineering books, McGraw - Hill, `http://books.google.com.tr/books?id=EqdTAAAAMAAJ`.

[38] **Ko, B.S., Edgar, T.F.** (2000). Performance assessment of cascade control loops, *AIChE Journal*, ***46***(2), 281–291.

[39] **Huang, B., Shah, S.L., Kwok, E.K.** (1997). Good, bad or optimal? Performance assessment of multivariable processes, *Automatica*, ***33***(6), 1175–1183.

[40] **Harris T., Boudreau, F., MacGregor, J.F.** (1996). Good, bad or optimal? Performance assessment of multivariable processes, *Automatica*, ***32***(11), 1505–1518.

[41] **Ko, B.S, Edgar, T.F.** (2001). Performance assessment of multivariable feedback control systems, *Automatica*, ***37***(5), 899–905.

[42] **Rogozinski, M., Paplinski, A., Gibbard, M.** (1987). An algorithm for calculation of nilpotent interactor matrix for linear multivariable systems, *IEEE Transactions, Automatic Control*, ***33***(3), 234–237.

[43] **McNabb, C.A., Qin, S.J.** (2003). Projection based MIMO control performance monitoring: I- covariance monitoring in state space, *Journal of Process Control*, ***13***, 739–757.

[44] **Choudhury, A.A.S., Shah, S.L., Thornhill, N.F.** (2008). *Diagnosis of process nonlinearities and valve stiction: data driven approaches*, Springer Science & Business Media.

[45] **Jelali, M., Huang, B.** (2010). *Detection and Diagnosis of Stiction in Control Loops: State of the Art and Advanced Methods*, Advances in Industrial Control, Springer-Verlag, London.

[46] **Hayes, M.** (1996). *Statistical digital signal processing and modeling*, John Wiley & Sons, `http://books.google.com.tr/books?id=N_VSAAAAMAAJ`.

[47] **Hagglund, T.** (1995). A control-loop performance monitor, *Control engineering practice*, ***3***, 1543–1551.

[48] **Forsman K., Stattin, A.** (1999). A new criterion for detecting oscillations in control loops, *Proceedings of European Control Conference*, Karlsruhe, Germany.

[49] **Miao, T., Seborg, D.E.** (1999). Automatic detection of excessively oscillatory feedback control loops, *Proceedings of the 1999 IEEE International Conference on Control Applications*, Kohala Coast-Island of Hawai'i, USA, pp.359–364.

[50] **Thornhill, N.F., Huang B., Zhang, H.** (2003). Detection of multiple oscillations in control loops, *Journal of Process Control*, ***13***, 91–100.

[51] **Matsuo, T., Tadakuma, I., Thornhill, N.F.** (2004). Diagnosis of a unit-wide disturbance caused by saturation in manipulated variable, *Proceedings of the IEEE Advanced Process Control Applications for Industry Workshop*, Vancouver, Canada, pp.1–9.

[52] **Helbig, A., Marquardt, W., Allgöwer, F.** (2000). Nonlinearity measures: definition, computation and applications, *Journal of Process Control*, ***10***(2-3), 113–123.

[53] **Guay, M.** (1996). Measurement of nonlinearity in chemical process control, *Ph.D. thesis*, Queen's University, Kingston, Ontario, Canada.

[54] **Subba Rao, T.S., Gabr, M.M.** (1980). A test for linearity and stationarity of time series, *Journal of Time Series Analysis*, ***1***(2), 145–158.

[55] **Hinich, M.** (1982). Testing for Gaussianity and linearity of a stationary time series, *Journal of Time Series Analysis*, ***3***(3), 169–176.

[56] **Choudhury, M.A.A.S., Shah, S.L., Thornhill, N.F.** (2004). Detection and diagnosis of system nonlinearities using higher order statistics, *Automatica*, ***40***, 1719–1728.

[57] **Theiler, J., Eubank, S., Longtin, A., Galdrikian, B., Farmer, J.D.** (1992). Testing for nonlinearity in time-series-The method of surrogate data, *Physica D*, ***58***, 77–94.

[58] **Kaplan, D.**, (1997). Frontiers of Blood Pressure and Heart Rate Analysis, volume 35, chapterNon-linearity and non-stationarity: the use of surrogate data in interpreting fluctuations, IOS Press, pp.15–28.

[59] **Thornhill, N.** (2005). Finding the source of nonlinearity in a process with plant-wide oscillation, *IEEE Transactions on Control Systems Technology*, ***13***(3), 434–443.

[60] **Horch, A.** (1999). A simple method for detection of stiction in control valves, *Control Engineering Practice*, ***7***(10), 1221–1231.

[61] **Singhal, A., Salsbury, T.I.** (2005). A simple method for detecting valve stiction in oscillating control loops, *Journal of Process Control*, ***15***(4), 371–382.

[62] **Salsbury, T.** (2006). Control performance assessment for building automation systems, *Proceedings of the IFAC Workshop on Energy Saving Control in Plants and Buildings*, volume 1, Bulgaria, pp.7–18.

[63] **Rossi, R., Scali, C.** (2005). A comparison of techniques for automatic detection of stiction: simulation and application to industrial data, *Journal of Process Control*, ***15***(5), 505–514.

[64] **He, Q.P., Wang, J., Pottmann, M., Qin, S.J.** (2007). A curve fitting method for detecting valve stiction in oscillating control loops, *Industrial & Engineering Chemistry Research*, ***46***(13), 4549–4560.

[65] **Choudhury, M.A.A.S., Thornhill, N.F., Shah, S.L., Shook, D.S.** (2006). Automatic detection and quantification of stiction in control valves, *Control Engineering Practice*, ***14***(12), 1395–1412.

[66] **Kano, M., Maruta, H., Kugemoto, H., Shimizu, K.** (2004). Practical model and detection algorithm for valve stiction, *Proceedings of the 7th IFAC-DYCOPS Symposium*, Boston, USA.

[67] **Yamashita, Y.** (2006). An automatic method for detection of valve stiction in process control loops, *Control Engineering Practice*, ***14***(5), 503–510.

[68] **Horch, A., Heiber, F.** (2004). On Evaluating Control Performance On Large Data Sets, ***Edited by Shah S.L. and MacGregor J.****, editor, Dynamics and Control of Process Systems, Proceedings of the 7th IFAC Symposium*, volume 2, Elsevier, Cambridge, Massachusetts, USA, pp.535–540.

APPENDICES

APPENDIX A.1 : MATLAB Code

```
Performance Indices (AR_ Least Square & FCOR algorithm)
%Harris-index Calculation
%_____________________________________
n=length(y);
%k=abs(lagdiff);
m=30;
k=10;
yst=detrend(er(n:-1:k+m,1),'constant');
y_ar=detrend(er,'constant');
X=zeros(n-m-k+1,m);
for i=1:(n-m-k-1)
    X(1,1)=y_ar(n);
    X(1,2:m)=y_ar(n-k-1:-1:n-k-m+1);
    X(i+1,:)=y_ar(n-k-i:-1:n-k-m-i+1);
    X(n-m-k+1,:)=y_ar(m:-1:1);
end
X;
A=transpose(X);
A1=inv(A*X);
A2=A1*A;
alpha=A2*yst;
%alpha
fprintf('alfa: %3.15f\n',alpha)
%minimum variance & variance
min_var=(1/(n-k-2*m+1))*transpose(yst-X*alpha)*(yst-X*
    alpha);
fprintf('minimum variance: %3.4f\n',min_var)
variance=(1/(n-k-m+1))*transpose(yst)*yst;
fprintf('variance: %3.4f\n',variance)
harris=min_var/variance;
fprintf('harris:  %3.4f\n',harris)

%FCOR algorithm
%_____________________________________
Ts=30;
modelar=ar(y_ar,m,'Ts',Ts);
yfiltered=filter(modelar.a,1,er);
```

```
noise=var(yfiltered);
fprintf('Noise Variance: %3.4f\n',noise)
[r3,lags]=xcorr(er,yfiltered,k-1,'coeff');
%m=(length(lags)-1)/2+1;
%n=length(lags);
fcorindex=transpose(r3)*r3
%konrol et
r3_yeni=sum(er.*yfiltered);
A=sum(er.^2);
B=sum(yfiltered.^2);
ro=(r3_yeni)/sqrt((A*B));
%FCOR=ro^2

%N4SID algorithm
%_____________________________________
subspacemodel=iddata(detrend(y,'constant'),detrend(u,'
    constant'),30);
modelsubspace=n4sid(subspacemodel,'best','N4Weight','CVA'
    ,'Focus','simulation');
impulsecoeff=impulse(modelsubspace);
%figure(3)
%stem(impulsecoeff)
sumimcoeff=sum(impulsecoeff.^2);
minvarsubspace=26.1959*sumimcoeff;
varact=mse(er);
harris_ss=minvarsubspace/varact

Oscillation Detection (ACF & Regularity & h (Oscillation
    Index))
%Power spectrum
%=======================================
[Pxx1,f]=periodogram(ce2,[],[],fs);%Filtrelenmis hali
figure(2)
semilogx(f,Pxx1/sum(Pxx1))
xlabel('Frequency f/fs','fontweight','bold','fontsize'
    ,12)
title('Power Spectra','fontweight','bold','fontsize',12)

figure(3)
[Pxx2,f1]=periodogram(ce1,[],[],fs); %Filtre edilmemis
    hali
semilogx(f1,Pxx2/sum(Pxx2))
xlabel('Frequency f/fs','fontweight','bold','fontsize'
    ,12)
title('Power Spectra','fontweight','bold','fontsize',12)

%ce2=ce1;
```

```
%Decay Ratio Approach of the Auto-covariance function
%=======================================
%ACF plot script
[osvec,lags]=xcov(ce2,round(N/4),'coeff');
v=osvec(round(N/4)+1:length(osvec));
figure(4)
plot(v(1:round(length(v)/2)))
xlabel('Lags','fontweight','bold','fontsize',12)
title('Auto-covariance function(ACF)','fontweight','bold'
    ,'fontsize',12)
hold on
plot(1:length(v(1:round(length(v)/2))),0,'.r')
for i=1:length(v)-1
    a(i)=v(i+1)-v(i);
end
a;

for i=1:length(v)-2
    if a(i+1)>0&a(i)<0
        Y1(i)=a(i+1);
    else if a(i+1)<0&a(i)>0
        Y2(i)=a(i+1);
        end
    end
end


for i=1:length(v)-100
    if Y1(i)>0
        t2(i)=i+1;
    end
    if Y2(i)<0
        t3(i)=i+1;
    end
end

A1=t2(t2>0);
p2=A1(1);
p4=A1(2);
B=t3(t3>0);
p3=B(1);
p1=1;
slopeb=(v(p1)-v(p3))/(p1-p3);
distanceb=abs(slopeb*p2*(-1)+v(p2)-v(p1)+slopeb*p1)/sqrt
    (1+slopeb^2);

slopea=(v(p2)-v(p4))/(p2-p4);
```

```
distancea=abs(slopea*p3*(-1)+v(p3)-v(p2)+slopea*p2)/sqrt
    (1+slopea^2);

decayratio=distancea/distanceb
%Forsman&Stattin_1999
%=========================================
%find zero crossings
k1=ce2(1:N-1);
k2=ce2(2:N);
tt=k1.*k2;
indx_one=find(tt<0);
indx_two=find(tt==0);
indx=sort([indx_one,indx_two]);
figure(5)
plot(1:N,ce2)
grid on
indx_1=indx+1;

%interpolasyon yap?lan yer(zero-crossingleri bulmak icin)
for s=1:length(indx_1)
   y1(s)=((0-ce2(indx(s)))/(ce2(indx_1(s))-ce2(indx(s))))
       *(indx_1(s)-indx(s))+indx(s);
end
y1';

f=1:length(ce2);

for m=1:length(y1)-1
  alan=find(y1(m)'<f&f<y1(m+1)');
  area(m)=trapz([0 ce2(alan(1:end))' 0]);
end
A=area(area>0);
B=area(area<0);
alf=0.5;gama=0.7;

for m=1:length(y1)-1
  if area(m)<0
        eps(m)=y1(m+1)-y1(m);
  else if area(m)>0
        delta(m)=y1(m+1)-y1(m);
      end
  end
end
eps1=eps(eps>0);
delta1=delta(delta>0);

for w=1:length(A)-1
     x(w)=A(w+1)/A(w);
```

```
    if x(w)>alf & x(w)<(1/alf)& (delta1(w+1)/delta1(w))>
       gama &(delta1(w+1)/delta1(w))<(1/gama)
        ha(w)=w;
    end
end
ha1=find(ha>0);

for q=1:length(B)-1
    z1(q)=B(q+1)/B(q);
    if z1(q)>alf&z1(q)<(1/alf)& (eps1(q+1)/eps1(q))>gama
       &(eps1(q+1)/eps1(q))<(1/gama)
        hb(q)=q;
    end
end
hb1=find(hb>0);

Forsman_st=(length(ha1)+length(hb1))/length(y1)

%Thornhill, 2003
%
   ------------------------------------------------------------

%[c,lags]=xcov(ce);
z=find(sign(osvec(1:end-1))~=sign(osvec(2:end)));
zero_crossing=lags(z);

%=================Thornhill Test Code====
clear osvec v;
% ACF zero crossing test (Thornhill)
n=length(ce);
osvec=xcov(ce,n,'coeff');
v=osvec(ceil(length(osvec)/2):length(osvec));
%fp1=v(1:round(n/4)-1);
%fp2=v(2:round(n/4));
fp1=v(1:end-1);
fp2=v(2:end);
fp1fp2=fp1.*fp2;
acfzcindex_one=find(fp1fp2<0);
acfzcindex_two=find(fp1fp2==0);
acfzcindex=sort([acfzcindex_one',acfzcindex_two']);

%    for i=1:length(acfzcindex)
%    if abs(v(acfzcindex(i)))>abs(v(acfzcindex(i)+1))
%        acfzcindexcorrected(i)=acfzcindex(i)+1;
%    else
%        acfzcindexcorrected(i)=acfzcindex(i);
%    end
```

```
acfzcindex_1=acfzcindex+1;

for s=1:length(acfzcindex_1)
    interpolindx(s)=((0-v(acfzcindex(s)))/(v(acfzcindex_1
       (s))-v(acfzcindex(s))))*(acfzcindex_1(s)-
       acfzcindex(s))+acfzcindex(s);
end

    if le(length(interpolindx),10)
        for i=1:length(interpolindx)-1
            deltaT(i)=interpolindx(i+1)-interpolindx(i);
        end
    else
        for i=1:10
            deltaT(i)=interpolindx(i+1)-interpolindx(i);
        end
    end


Tperiod=(2/length(deltaT))*sum(deltaT);
r_oscindex=(1/3)*(Tperiod/(2*std(deltaT)))

Bicoherence Analysis
close all
clear all
clc

ce=sp-y; er=ce;
% Data series with K segments
overlap=0.65;seglength=64;LX=seglength;
erol=buffer(er,seglength,floor(seglength*overlap),'
   nodelay');
if nnz(erol)<numel(erol);
    erol=erol(:,1:end-1);
end

%Substract the mean
    erol_new=detrend(erol,'constant');

%Hanning window
[m,n]=size(erol_new);
for k=1:m
    w(k,:)=0.5-0.5*cos(2*pi*(k-1)/(seglength-1));
    erol_1(k,:)=w(k,:).*erol_new(k,:);
end

%Calculate DFT of the segment
DFT_length=128;LS=DFT_length;
```

```
for ix=1:n
A=fft(erol_1,DFT_length);
Y=A(:,ix);
for k=1:seglength
    for l=1:seglength
        Bsp(k,l)=Y(k)*Y(l)*conj(Y(k+l));
        de1(k,l)=abs(Y(k)*Y(l))^2;
        de2(k,l)=abs(Y(k+l))^2;
    end
end
D1{ix}=de1;
D2{ix}=de2;
Bs{ix}=Bsp;
end

D1m = D1{1}; D2m = D2{1}; Bm = Bs{1};
for k = 2:length(Bs);
    D1m = D1m + D1{k};
    D2m = D2m + D2{k};
    Bm = Bm + Bs{k};
end
D1 = D1m/k; D2 = D2m/k; Bm = Bm/k;
numseg=length(erol);
%_____________________________________

bic2 = zeros(LX*2);
for k = 1:LX
    for l = 1:LX
        bic2(k+LX,l+LX) = abs(Bm(k,l))^2/(D1(k,l)*D2(k,l)
           +eps);
    end
end

for k = 1:LX*2
    for l = 1:LX*2
        if (k <= LX)&(l <= LX)
            bican(k,l) = bic2(2*LX-k+1,2*LX-l+1);
        elseif (k > LX)&(l <= LX)
            bican(k,l) = bic2(k,2*LX-l+1);
        elseif (k <= LX)&(l > LX)
                bican(k,l) = bic2(2*LX-k+1,l);
        elseif (k > LX)&l > bic2(k,l);
            bican(k,l) = bic2(k,l);
        end
    end
end
bicanpl = bican;
bican = bican(LX+1:LX+LS/2,LX+1:LX+LS/2);
```

```
waxis = linspace(0,0.5,length(bican)+1);
waxis = waxis(1:end-1);
limit = waxis(end)*(2/3);

k = 1;
while k < length(waxis)
    if waxis(k)>limit
        limit = k-1;
        k = Inf;
    else
        k = k + 1;
    end
end

for f1 = 1:limit
    for f2 = 1:length(waxis)
        if f2 == 1 | f2 >= f1;
            bican(f1,f2) = 0;
        end
    end
end

for f1 = limit:length(waxis)
    for f2 = 1:length(waxis)
        if f2 == 1 | f2 >= -2*f1 + length(waxis)*2
            bican(f1,f2) = 0;
        end
    end
end

cont = 1;
for f1 = 1:length(waxis)
    for f2 = 1:min([f1, -2*f1+length(Y)]);
        bicpermed(cont) = bican(f1,f2);
        cont = cont + 1;
    end
end

bic2m = mean(nonzeros(bicpermed));
bic2v = std(nonzeros(bicpermed));
bic2max = max(bicpermed);

surf(waxis,waxis,bican');
axis([0 0.5 0 0.5 0 1]);
    %set(hcc,'view',[145 15],'Alim',[0 1],...
    %    'Clim',[0 0.08]);
    view([145 15])
```

```
[c,rows] = max(bican');
[c,column] = max(max(bican'));
f1 = rows(column);
f2 = column;

output.f1 = waxis(f1);
output.f2 = waxis(f2);

K=numseg; calfa=5.99;
bicsign=bicpermed(bicpermed>calfa/(2*K));
NGI=(sum(bicsign)/length(bicsign))-calfa/(2*K*length(
    bicsign));
fprintf('NGI: %3.4f\n',NGI)
title('Squared bicoherence','fontweight','bold','fontsize
    ',12)
TNLI=sum(bicsign)

NLI=abs(bic2max-(bic2m+2*bic2v));

fprintf('NLI: %3.4f\n',NLI)


Surrogate Data

-       Generate Surrogate Data

function out = SD_MakeSurrogates(x,surrmethod,nsurrs,
    extrap)
% Ben Fulcher, 27/1/2011

bevocal = 0; % Display text information/commentary to
    screen

% INPUTS:
% number of surrogates to generate
if nargin < 3 || isempty(nsurrs)
    nsurrs = 1; % just create a single surrogate
end

% Any extra parameters (some methods require)
if nargin < 4
    extrap = [];
end


N = length(x); % length of the time series
out = zeros(N,nsurrs); % each column is a new surrogate
```

```
tic % time it

switch surrmethod
    case 'RP'
        % Random Phase Surrogates
        % Surrogates maintain linear correlations in the
            data, but any
        % nonlinear structure is destroyed by the phase
            randomization

        if bevocal
            fprintf(1,'Constructing␣%u␣surrogates␣using␣
                the␣Random␣Phase␣Method\n',nsurrs)
            fprintf(1,['Linear␣correlations␣are␣
                maintained␣but␣nonlinear␣structure␣will␣be
                ␣' ...
                        'destroyed␣by␣the␣phase␣
                            randomization\n'])
        end

        % lost a datapoint if odd
        if rem(N,2) == 0
          n2 = N/2;
        else
          n2 = (N-1)/2;
        end

        for surri = 1:nsurrs
            % (*) Compute Fourier Transform of x => z
            z = fft(x,2*n2);

            % (*) Randomize Phases
            zMag = abs(z); % magnitude
            zPhase = angle(z); % phase

            randphase = 2*pi*rand(n2-1,1); % compute
                random phases

            % ensure phi(1)=0, and all others are in
                [0,2*pi]
            % (not quite sure what the zPhase(n2+1) is
                there for)...
            % negative phases to ensure complex
                conjugates -- IFT will be
            % real.
            newPhase = [0; randphase; zPhase(n2+1); -
                flipud(randphase)];
```

```
        % zNew is like z, but with randomized phases:
        zNew = [zMag(1:n2+1)', flipud(zMag(2:n2))']'
            .* exp(newPhase .* 1i);

        % Transform back into the time domain
        xNew = real(ifft(zNew,N));
        out(:,surri) = xNew;
    end

case 'AAFT'
    if bevocal
        fprintf(1,['Constructing␣%u␣surrogates␣using␣
            the␣Amplitude␣Adjusted␣Fourier␣'...
                'Transform␣(AAFT)␣Method\n'],nsurrs)
        fprintf(1,['Linear␣correlations␣are␣
            maintained␣but␣nonlinear␣structure␣will␣be
            ␣destroyed␣' ...
                'by␣the␣phase␣randomization.␣
                    Amplitude␣Distribution␣is␣
                    approximately␣maintained\n'])
    end

    % Sort and rank order the data
    [xSorted, ix] = sort(x);
    [~, xRO] = sort(ix); % rank ordered permutation

    % lost a datapoint if odd
    if rem(N,2) == 0
      n2 = N/2;
    else
      n2 = (N-1)/2;
    end

    for surri = 1:nsurrs
        % Rand order white Gaussian-distributed noise
        nSort = sort(randn(N,1));
        y = nSort(xRO); % sorted Guassian white noise
            reordered as x

        % ------- Apply the RP method applied to y:
        % (*) Compute Fourier Transform of y => z
        z = fft(y,2*n2);

        % (*) Randomize Phases
        zMag = abs(z); % magnitude
        zPhase = angle(z); % phase
```

```
        randphase = 2*pi*rand(n2-1,1); % compute
            random phases

        % ensure phi(1)=0, and all others are in
            [0,2*pi]
        % (not quite sure what the zPhase(n2+1) is
            there for)...
        % negative phases to ensure complex
            conjugates -- IFT will be
        % real.
        newPhase = [0; randphase; zPhase(n2+1); -
            flipud(randphase)];


        % zNew is like z, but with randomized phases:
        zNew = [zMag(1:n2+1)', flipud(zMag(2:n2))']'
            .* exp(newPhase .* 1i);

        % Transform back into the time domain
        % phase-randomized version of random noise
            rank-ordered as x
        yRP = real(ifft(zNew,N));

        % ---------- rank order x with respect to yRP
       [~, ixyRP] = sort(yRP);
       [~, yRO] = sort(ixyRP);
       out(:,surri) = xSorted(yRO);
    end

case 'TFT'
    if bevocal
        fprintf(1,['Constructing␣%u␣surrogates␣using␣
            the␣Truncated␣Fourier␣'...
             'Transform␣(TFT)␣Method.\n'],nsurrs)
        fprintf(1,['Low␣Frequency␣phases␣are␣
            preserved,␣and␣high␣frequency␣phases␣will␣
            be␣'...
                'randomized.␣A␣way␣of␣dealing␣with␣
                   non-stationarity.\n'])
    end
    if isempty(extrap)
        fprintf(1,'You␣haven''t␣specified␣a␣cut-off␣
            frequency!!␣Setting␣N/8\n')
        fc = round(N/8);
    else
        fc = extrap; % extra input is the frequency
            cut-off
        if fc < 1
```

```
            fc = N*fc;
        end
    end

    % lost a datapoint if odd
    if rem(N,2) == 0
      n2 = N/2;
    else
      n2 = (N-1)/2;
    end

    for surri = 1:nsurrs
        % (*) Compute Fourier Transform of x => z
        z = fft(x,2*n2);

        % (*) Randomize Phases
        zMag = abs(z); % magnitude
        zPhase = angle(z); % phase

        randphase = pi*rand(n2-1,1); % compute random
            phases in (0,pi)
        randphase(1:fc) = zPhase(1:fc);

        % ensure phi(1)=0, and all others are in
            [0,2*pi]
        % (not quite sure what the zPhase(n2+1) is
            there for)...
        % negative phases to ensure complex
            conjugates -- IFT will be
        % real.
        newPhase = [0; randphase; zPhase(n2+1); -
            flipud(randphase)];


        % zNew is like z, but with randomized phases:
        zNew = [zMag(1:n2+1)' flipud(zMag(2:n2))']'
            .* exp(newPhase .* 1i);

        % Transform back into the time domain
        xNew = real(ifft(zNew,N));
        out(:,surri) = xNew;
    end

  otherwise
    error('Unknown surrogate generation method ''%s''
        ',surrmethod)
end
```

```
% Cute farewell message
if bevocal
    fprintf(1,'Generated␣%u␣%s␣surrogates␣in␣%s.\n',
       nsurrs,surrmethod,BF_thetime(toc,1))
end

end


-       Surrogate Analysis

clear all
clc
load 47TIC1511

%Filtering
erp=sp-y;
Ts=60;
n=length(erp);
%=================Thornhill Test Code====
clear osvec v;
% ACF zero crossing test (Thornhill)
osvec=xcov(erp,n-5,'coeff');
v=osvec(n-5+1:length(osvec));
%fp1=v(1:round(n/4)-1);
%fp2=v(2:round(n/4));
fp1=v(1:end-1);
fp2=v(2:end);
fp1fp2=fp1.*fp2;
acfzcindex=find(fp1fp2<0);

acfzcindex_1=acfzcindex+1;

for s=1:length(acfzcindex_1)
    interpolindx(s)=((0-v(acfzcindex(s)))/(v(acfzcindex_1
       (s))-v(acfzcindex(s))))*(acfzcindex_1(s)-
       acfzcindex(s))+acfzcindex(s);
end

    if le(length(interpolindx),10)
        for i=1:length(interpolindx)-1
            deltaT(i)=interpolindx(i+1)-interpolindx(i);
        end
    else
        for i=1:10
            deltaT(i)=interpolindx(i+1)-interpolindx(i);
        end
    end
```

```
Tperiod=(2/length(deltaT))*sum(deltaT)
r_oscindex=(1/3)*(Tperiod/2*std(deltaT));


%==========Thornhill Test Code Final==========
samplespercycle=Tperiod/Ts;
E=floor(samplespercycle)
%=============================================

%er=(detrend(nonlinearpure,'constant')/std(detrend(
    nonlinearpure,'constant')));
er=erp;

%Forming the embedded matrix
%E=11;
N=length(er);
Y=zeros(N-E+1,E);
for m=1:N-E+1
    Y(m,:)=er(m:E+m-1);
end

%Neighbour exclusion constraint&
Coef=zeros(N-E+1,N-E+1);
for i=1:N-E+1
    for j=1:N-E
        if abs(j-i)>E/2
            Coef(i,j)=j;
            dif(i,j)=sqrt(sum((Y(j,:)-Y(i,:)).^2));
        else
            Coef(i,j)=NaN;
            dif(i,j)=NaN;
        end
    end
end


[sortedvalues,sortIndex]=sort(dif,2);
nn=8;
for i=1:N-E
    jp(i,:)=sortIndex(i,1:nn);
end

%Squared of prediction errors
H=E;

for s=1:N-H
```

```
    total=0;
    for p=1:nn;
    total=er(jp(s,p)+H)+total;
    end
    prediction(1,s)=(1/nn)*(total);
    sqrddiff(1,s)=(er(s+H)-prediction(1,s)).^2;
end
gama_test=sum(sqrddiff(1,:));


%============Surrogate Data Test Index=======
for z=1:50;

    clear Ysurr Coef_surr;
    clear dif_surr jpsurr sortIndex_surr surrogatedata;

            surrogatedata=SD_MakeSurrogates(er,'AAFT',1);

Ysurr=zeros(N-E+1,E);
for m=1:N-E+1
    Ysurr(m,:)=surrogatedata(m:E+m-1);
end

%Neighbour exclusion constraint&
Coef_surr=zeros(N-E+1,N-E+1);
for i=1:N-E+1
    for j=1:N-E
        if abs(j-i)>E/2
            Coef_surr(i,j)=j;
            dif_surr(i,j)=sqrt(sum((Ysurr(j,:)-Ysurr(i,:)
                ).^2));
        else
            Coef_surr(i,j)=NaN;
            dif_surr(i,j)=NaN;
        end
    end
end


[sortedvalues_surr,sortIndex_surr]=sort(dif_surr,2);
nn=8;
for i=1:N-E
    jpsurr(i,:)=sortIndex_surr(i,1:nn);
end

%Squared of prediction errors

for s=1:N-H
```

```
        totalsurr=0;
        for p=1:nn;
        totalsurr=surrogatedata(jpsurr(s,p)+H)+totalsurr;
        end
        predictionsurr(1,s)=(1/nn)*(totalsurr);
        sqrddiffsurr(1,s)=(surrogatedata(s+H)-predictionsurr
            (1,s)).^2;
end
gama_surr(1,z)=sum(sqrddiffsurr(1,:));


        NPIindex=(mean(gama_surr)-gama_test)/(3*std(gama_surr
            ));
        fprintf('Current NonPredictibility:  %3.4f\n',
            NPIindex);
end

NPIindex=(mean(gama_surr)-gama_test)/(3*std(gama_surr));
fprintf('Final NonPredictibility:  %3.4f\n',NPIindex);


Stiction Analysis (Curve Fitting)
clear all
close all
clc
load 74FIC042

%Filtering
er=sp-y;
erf=sgolayfilt(er,3,11);
ce=detrend(erf,'constant');
%plot(1:length(detrend(er,'constant')),detrend(er,'
    constant'))
ce1=(ce-mean(ce))/std(ce);
f=[0 0.0007926/(1/60) 0.0018494/(1/60) 1];
a=[0 1 1 0];
b=firpm(20,f,a);
[h,w]=freqz(b,1);
plot(f,a,w/pi,abs(h))
Hd = dfilt.dffir(b);
ce2=filter(Hd,ce1);


%find zero crossings
N=length(ce);
k1=ce(1:N-1);
k2=ce(2:N);
tt=k1.*k2;
```

```
indx=find(tt<0);indx0=find(ce==0);
figure(2)
subplot(2,1,1)
plot(1:N,detrend(er,'constant'),'b','Linewidth',1.5)
hold on
plot(1:length(detrend(erf,'constant')),detrend(erf,'
    constant'),'g','Linewidth',1.5)
xlabel('Time(Samples)','fontweight','bold','fontsize',12)
ylabel('Control Error','fontweight','bold','fontsize',12)
title('Sinusoidal fitting','fontweight','bold','fontsize'
    ,12)
hold on
grid on
indx_1=indx+1;

%interpolasyon yap?lan yer(zero-crossingleri bulmak icin)
for s=1:length(indx_1)
   y1(s)=((0-ce(indx(s)))/(ce(indx_1(s))-ce(indx(s))))*(
      indx_1(s)-indx(s))+indx(s);
end
MinIdx=sort([indx0' y1]);

%Sinusoidal Fitting
for i=1:length(MinIdx)-1
xdata=[0:(MinIdx(i+1)-MinIdx(i))]';
ydata=ce(MinIdx(i):MinIdx(i+1));
w(i)=pi/(MinIdx(i+1)-MinIdx(i));
x0=[6,w(i)];
f=@(x,xdata)x(1)*sin(x(2)*xdata);
[x{i},resnorm(i)]=lsqcurvefit(f,x0,xdata,ydata);
gz=x{i}(1)*sin(x{i}(2)*xdata);
sinfit(i)=resnorm(i)/length(xdata);
plot(MinIdx(i):MinIdx(i+1),gz,'r','Marker','o')
end
MSEsin=mean(sinfit)

%Triangular Fitting
[Maxima, MaxIdx]=findpeaks(ce,'minpeakdistance',3);
DataInv=1.01*max(ce)-ce;
[Minima,Idx]=findpeaks(DataInv,'minpeakdistance',3);
Index_1=sort([MaxIdx Idx]);%Tum peakler s?raland?
%_____________________________________
for i=1:length(MinIdx)-1
    sx=ce(ceil(MinIdx(i)):floor(MinIdx(i+1)));
    [~,ipk]=max(abs(sx));
    Coef(i)=floor(MinIdx(i))+ipk;
end
Coef;
```

```
%_____________________________________
Index=sort([Coef MinIdx]);%Zero-crossing ve peakleri
    iceriyor.
%Zero-crossing once mi sonra m? ona bakt?k
if MinIdx(1)<Coef(1)
    %zero-crossingle ba?larsa
for i=1:2:length(Index)-1
    xdata_1=[Index(i) ceil(Index(i)):Index(i+1)];
    xdata_2=[Index(i+1):floor(Index(i+2)) Index(i+2)];
    ydata_1=[0 ce(ceil(Index(i)):Index(i+1))'];
    ydata_2=[ce(Index(i+1):floor(Index(i+2)))' 0];
p1=polyfit(xdata_1,ydata_1,1);
f1=polyval(p1,xdata_1);
p2=polyfit(xdata_2,ydata_2,1);
f2=polyval(p2,xdata_2);
subplot(2,1,2)
plot(1:N,ce,'Linewidth',1.5)
hold on
grid on
plot(xdata_1,f1,'r','Linewidth',1.2,'Marker','o')
xlabel('Time(Samples)','fontweight','bold','fontsize',12)
ylabel('Control␣Error','fontweight','bold','fontsize',12)
title('Triangular␣fitting','fontweight','bold','fontsize'
    ,12)
hold on
plot(xdata_2,f2,'r','Linewidth',1.2,'Marker','o')
f=[f1 f2]';
Y=[ydata_1 ydata_2]';
hata(i)=sum((f-Y).^2)/length(xdata_1);;
end
else if MinIdx(1)>Coef(1)
    %peak ile ba?larsa zero-crossing'e git
for i=2:2:length(Index)-2
    xdata_11=[Index(i) ceil(Index(i)):Index(i+1)];
    xdata_21=[Index(i+1):floor(Index(i+2)) Index(i+2)];
    ydata_11=[0 ce(ceil(Index(i)):Index(i+1))'];
    ydata_21=[ce(Index(i+1):floor(Index(i+2)))' 0];
p11=polyfit(xdata_11,ydata_11,1);
f11=polyval(p11,xdata_11);
p21=polyfit(xdata_21,ydata_21,1);
f21=polyval(p21,xdata_21);
subplot(2,1,2)
plot(1:N,ce,'Linewidth',1.5)
hold on
grid on
plot(xdata_11,f11,'r','Linewidth',1.2,'Marker','o')
xlabel('Time(Samples)','fontweight','bold','fontsize',14)
ylabel('Control␣Error','fontweight','bold','fontsize',14)
```

```
title('Triangular fitting','fontweight','bold','fontsize'
    ,14)
hold on
plot(xdata_21,f21,'r','Linewidth',1.2,'Marker','o')
f_new=[f11 f21]';
Y1=[ydata_11 ydata_21]';
hata(i)=sum((f_new-Y1).^2)/length(xdata_11);
end
    end
end

MSEtri=mean(nonzeros(hata'))
stc=MSEsin/(MSEsin+MSEtri)

Tuning Index

clc
%Estimated closed-loop response model
%_____________________________________________
clear all
close all
load 47FIC1507
sp=data(1:2:10000,2);
y=data(1:2:10000,1);
ce=y-sp;
u=data(1:2:10000,3);
yest=detrend(ce,'constant');
Ts=60;m=30;
modelar=ar(yest,m,'Ts',Ts)
e=resid(modelar,yest);
plot(e)
[c,lags]=xcorr(yest,e,30,'unbiased');
figure(2)
k=length(c);
plot(0:(k-1)/2+1,c((k-1)/2:k),'Linewidth',2)
xlabel('Samples','Fontsize',12)
ylabel('Impulse Response(IR)Coefficient')
x=0:(k-1)/2+1;
coef=c((k-1)/2:k);
%_____________________________
%Calculation of area
N=length(coef);
k1=coef(1:N-1);
k2=coef(2:N);
tt=k1.*k2;
indx_one=find(tt<0);
indx_two=find(tt==0);
indx=sort([indx_one,indx_two]);
```

```
indx_1=indx+1;

%interpolasyon yap?lan yer(zero-crossingleri bulmak icin)
for s=1:length(indx_1)
  y1(s)=((0-coef(indx(s)))/(coef(indx_1(s))-coef(indx(s))
    ))*(indx_1(s)-indx(s))+indx(s);
end
y1';

f=1:length(coef);

for m=1:length(y1)-1
 alan=find(y1(m)'<f&f<y1(m+1)');
 area(m)=trapz([0 coef(alan(1:end))' 0]);
end

if length(y1)==3
    tuning_index=1
else
    tuning_index=max(abs(area))/sum(abs(area))
end
```

CURRICULUM VITAE

Name Surname: Gizem Kuşoğlu

Place and Date of Birth: İstanbul 07/11/1989

Adress: Tüpraş İzmit Refinery Cooperation

E-Mail: gizemkusoglu@gmail.com

B.Sc.: Istanbul Technical University / Department of Chemical Engineering
Istanbul Technical University / Department of Industrial Engineering

M.Sc.:

Professional Experience and Rewards:

List of Publications and Patents:

PUBLICATIONS/PRESENTATIONS ON THE THESIS